ABSTRACT

Title of Thesis: THE STUDY OF ENERGY METABOLISM IN THE PERIPARTURIENT DAIRY COW: INVESTIGATING THE ROLE OF KETONES AND NAD+

Mariana da Silva, Master of Science, 2024.

Thesis Directed By: Ph.D. J. Eduardo Rico
Department of Animal and Avian Sciences.

Dairy cows typically experience increased energy demands during the transition from gestation to lactation, and a myriad of metabolic adaptations are set in place to facilitate this transition. This thesis integrates findings from two experiments exploring energy metabolism during this critical phase. In the first experiment, the effects of hyperketonemia on dairy cow health and productivity were investigated. Eight Holstein cows (19.62 ± 5.44 days postpartum) were intravenously infused with either Na-BHB (KET) or NaCl (CON) for 48 hours. The study aimed to assess the impact of elevated beta-hydroxybutyrate (BHB) levels on blood biomarkers and immune response. Despite no significant differences in dry matter intake or overall milk yield, KET cows exhibited lower milk yield post-immune challenge (LPS bolus) and higher plasma NEFA levels. While plasma glucose concentrations remained unchanged, but BHB concentrations were significantly higher in the KET group ($P < 0.001$). The second experiment focused on the role of Nicotinamide Adenine Dinucleotide (NAD) coenzymes in energy metabolism during the transition from gestation to lactation. Twenty-six peripartal dairy cows were enrolled in an observational study to examine the NAD metabolome in liver, blood, and

milk. Liver biopsies were performed 21 days before and 7 days after parturition, and blood samples were collected weekly. The study hypothesized that hepatic NAD levels deplete while blood and milk NAD pools increase postpartum, with a possible influence of residual feed intake (RFI). Measurements of plasma glucose, free fatty acids, BHB, and insulin, along with comprehensive NAD metabolome profiling using HPLC coupled to mass spectrometry, aimed to elucidate the relationship between NAD metabolism, metabolic biomarkers, and production performance. After calving, animals showed decreased glucose and insulin levels, and increased NEFA and BHB levels, with no significant group differences (P = 0.53). Oxidative stress markers (protein carbonyl, 8-OHdG) and total antioxidant capacity were measured on plasma. The DNA and protein oxidative stress markers remained unchanged relative to parturition, but the Low-RFI group tended to display higher antioxidant capacity (P = 0.08). NAD metabolites increased, and NAD precursor concentrations decreased in the liver. Nicotinamide Mononucleotide was higher in the High-RFI group (P = 0.04) and tended to decrease post-calving (P = 0.06). The liver NAD metabolome remained stable (P = 0.83). Both studies underscore the complexity of energy metabolism during the peripartum period in dairy cows. Collectively, our findings expand our understanding of novel aspects of energy metabolism, with potential implications for health, productivity, and disease resilience in dairy cows. Further research is essential to fully understand these mechanisms and improve management strategies for dairy cows during this critical period.

THE STUDY OF ENERGY METABOLISM IN THE PERIPARTURIENT DAIRY COW: INVESTIGATING THE ROLE OF KETONES AND NAD+

by

Mariana da Silva

Thesis submitted to the Faculty of the Graduate School of the
University of Maryland, College Park, in partial fulfillment
of the requirements for the degree of

Master of Science

2024

Advisory Committee:

Ph.D. J. Eduardo Rico, Chair

Ph.D. Richard Kohn

Ph.D. Zhengguo Xiao

Acknowledgements

I would like to express my gratitude to Dr. J. Eduardo Rico for his invaluable supervision during my master's degree program at the University of Maryland. I also extend my sincere thanks to my committee members, Dr. Zhengguo Xiao and Dr. Kohn, for their exceptional guidance and contributions throughout my studies.

Special thanks to the USDA-Beltsville farm crew, including Mike Kemp, Brad Appleby, and the dedicated caretakers, as well as the CRMEC farm manager Brian Schnebly and his team. Your assistance has been key in the success of my research.

I am also grateful to my research collaborators, Asha Miles and Ransom Baldwin, for their consistent support and guidance. Additionally, I appreciate the hard work and dedication of the undergraduate students, Neha Potphode, Margaret Hubbard and Isabel Ahn, who provided essential assistance both on the farm and in the lab.

Table of contents

List of Tables

List of Figures

List of Abbreviations

ADF	Acid detergent fiber
BCS	Body condition score
BDH1	3-Hydroxybutyrate dehydrogenase 1
BHB	Beta-hydroxybutyric acid
BW	Body weight
CPT	Carnitine palmitoyl transferase
CRP	C-reactive protein
CV	Coefficient of variation
DHR-123	Dihydrorhodamine 123
DIM	Days in milk
DMI	Dry matter intake
EDTA	Ethylenediaminetetraacetic acid
ER	Endoplasmic reticulum
FA	Fatty acid
FFA	Free fatty acid
FoxO1	Forkhead box protein 1
GLM	generalized linear model
GLUT2	Glucose transporter 2
GLUT4	Glucose transporter 4
HMGCS2	3-Hydroxy-3-methylglutaryl-CoA synthase 2
HPLC	High performance liquid chromatography
IL-1β	Interleukin 1-beta
IL-6	Interleukin 6
IL-10	Interleukin 10
IKK	I kappa B kinase beta
mTOR	Mammalian target of rapamycin
MUN	Milk urea nitrogen
NAD	Nicotinamide adenine dinucleotide
NADPH	Nicotinamide adenine dinucleotide phosphate
NEFA	Non-esterified fatty acid
NLRP3	NOD-like receptor protein 3
NMN	Nicotinamide mononucleotide

NMNAT	Nicotinamide mononucleotide adenylyltransferase
NNT	Nicotinamide nucleotide transhydrogenase
NDF	Neutral detergent fiber
NEB	Negative energy balance
NEFA	Non-esterified fatty acids
NFκB	Nuclear factor kappa B
NOX	NADPH oxidase
PARP	Poly (ADP-ribose) polymerase
PC	Protein carbonyl
PEPCK	Phosphoenolpyruvate carboxykinase
RFI	Residual feed intake
ROS	Reactive oxygen species
SCOT	Succinyl-CoA-3-oxaloacid CoA transferase
SCS	Somatic cell score
SEM	Standard error of the mean
SD	Standard deviation
SREBP	Sterol regulatory element binding protein
TAC	Total antioxidant capacity
TAG	Triglycerides
TLR4	Toll-like receptor 4
TNF-α	Tumor necrosis factor alfa
TMR	Total mixed ration
VFA	Volatile fatty acid
8-OHdG	8-hydroxydeoxyguanosine

Chapter 1

INTRODUCTION

1.1 Energy metabolism in the dairy cow

One of the most challenging and vulnerable moments in a dairy cow's life is the transition from gestation to lactation. During this time, a myriad of homeorhetic adaptations occur to support the demands of the growing fetus and the lactating mother (Bauman & Curie, 1980). Modern dairy cows experience dramatic demands of energy metabolism to support lactation, and some of the changes that take place at the start of lactation include increased glucose demands, heightened lipolytic activity (*i.e.*, increase in blood free fatty acids; FFA) and hepatic ketone production (*e.g.*, beta-hydroxybutyrate; BHB). The threshold blood concentration of BHB that characterizes hyperketonemia is typically 1.2mmol/L, being associated with increased risk of culling and diagnose of peripartal diseases (Seifi *et al.*, 2011). Cows experiencing adaptive difficulties to the onset of lactation may experience metabolic stress, metabolic disorders, and heightened disease propensity (*e.g.*, metritis; displaced abomasum; Ospina *et al.*, 2010).

The effects of ketone bodies on health have been a case of study for many years. An increased availability of ketone bodies is considered beneficial for multiple conditions in mammals, such as inflammatory diseases (*e.g.*, Gout; Goldberg *et al.*, 2017) and obesity-related cardiovascular disease (Dashti *et al.*, 2003). We know that in conditions such as epilepsy, fasting (*i.e.*, the induction of hyperketonemia) is a treatment utilized by at least one hundred years, and has been spread into general practice across the world throughout to this day (Höhn *et al.*, 2019). In the dairy cow, ketosis (*i.e.*, blood BHB >1.2mmol/L, for the subclinical level)

is a condition that carries the stigma of being associated with infectious diseases, as well as with reduced productivity and fertility (Duffield *et al.,* 2009; Rutherford *et al.,* 2016). Nonetheless, multiple studies have shown that it is possible for an animal to have circulating ketone blood levels >1.2mmol/L, and still display a health and production-positive phenotype, with increased milk yield and fat content (Rathbun *et al.,* 2017; Van holder *et al.,* 2015).

Ketones originated from the breakdown of fatty acids, through the condensation of Acetoacetate-CoA and Acetyl-CoA by the action of the hepatic enzyme HMGCS2, yielding BHB/Acetoacetate, which in turn is dependent on the ratio of NAD+/NADH (Puchalska & Crawford, 2017). This metabolite can be transported to the extrahepatic mitochondria where it may be oxidized to Acetyl-CoA, which then enters the TCA cycle, and ultimately yields ATP through the electron transport chain and ATP-synthase. Importantly, NADH acts as an electron donor that creates the membrane potential that drives the synthesis of ATP.

Nicotinamide Adenine Dinucleotide (NAD) coenzymes are central catalysts of metabolism, and play vital roles in energy metabolism within eukaryotic cells. The NAD system is present in virtually all cellular processes, and a depletion in its intracellular levels is associated with the progression of aging in mammals, as well as with a number of pathologies, ranging from heart failure to cancer (Navas & Carnero, 2021). Although unknown in dairy cows, limited data in other mammals, like rodents indicates that a depletion of the hepatic NAD metabolome (NAD cofactors and associated metabolites) occurs at the onset of lactation (Ear *et al.,* 2019).

These two molecules, NAD+ and BHB have been rediscovered by science in recent years, and novel roles have been elucidated. Beta-hydroxybutyrate, through the receptor GPR109A, acts as a signal controlling the acetylation and deacetylation of histones that control the expression of genes involved in antioxidative stress response (glutathione peroxidase, catalase and other reactive oxygen species scavenging mechanisms) and lipid

metabolism (Shimazu *et al.*, 2013; Lee *et al.*, 2020). This epigenetic modification is mediated by sirtuins (1-7), which are NAD+ dependent. Sirtuins act as posttranslational modifiers and PARPs act in DNA repair, both exerting anti-cancer and anti-aging properties. Together, this utilization of NAD+ not as a redox agent, but as a substrate, reveals the amplitude of potential this molecule has (Navas & Carnero, 2021).

Ketone bodies also have demonstrated anti-inflammatory properties, deactivating the Nod-like receptor protein 3 (NLRP3) inflammasome in macrophages and neutrophils (Goldberg *et al.*, 2017; Youm *et al.*, 2015). This ultimately leads to lower transcription of pro-inflammatory markers, like pro-interleukin 1-beta (pro-IL-1β), interleukin 6 (IL-6), tumor necrosis factor alpha (TNF-α), and increases the transcription of immune suppressor ones, like interleukin 10 (IL-10; Swartz *et al.*, 2019). In cases where animals experience chronic inflammation, such as during obesity, BHB posits itself as a therapeutic option. Importantly, if dry cows reach parturition with a BCS >3.5, they are at higher risk for the development of metabolic disorders, like clinical ketosis (Roche *et al.*, 2009). However, under an acute immune challenge (*e.g.*, endotoxemia), where the immune system should be recruited quickly to fight the imminent infection, hyperketonemia might potentially have deleterious effects. Regarding immune performance, BHB concentrations above 1.0 mmol/L reduce phagocytosis *in vitro*, and impair the generation of hydrogen peroxide (Hoeben *et al.*, 1997), thus inhibiting partially the generation of oxidative burst.

Energy related disorders are a concern in periparturient dairy cows, and mitigation of their consequences is a major priority for Dairy farmers. Ketosis alone is estimated to cost the dairy industry US$ 289 per case (average total; McArt *et al.*, 2015). On the other hand, NAD+ is a metabolite that only recently has been explored in ruminants, most of the work being done with precursors (*i.e.*, Niacin; Yuan *et al.*, 2012), but relevant physiological values have not been established. A more nuanced understanding of energy metabolism and the roles of ketones

in the pathogenesis of peripartal disease is urgently needed, particularly in regard to its effects on immune function. An improved understanding of these gaps may lead to targeted management approaches on the herd level (*e.g.*, nutritional) and more accurate diagnoses of disease onset.

Chapter 2

LITERATURE REVIEW

2.1 Ketone biology

2.1.1 Glucose metabolism

The transition from the dry period to lactation represent a metabolic and immunological challenge to the modern dairy cow. To support the sudden increase in energy demand, the body coordinates physiological changes in the metabolism of body tissues to allow a greater partitioning of nutrients to lactogenesis (Bauman and Currie, 1980). Lipid and glucose metabolism adapt allowing this homeorhetic process, but dysregulation and the onset of clinical conditions take place in cases the animal is unable to balance production and body demands.

Unlike other non-herbivorous mammals, ruminants ingest fibrous carbohydrates that are non-digestible by mammalian enzymes. These are mostly fermented by rumen microbes into various short-chain fatty acids (acetate and propionate being the two most abundant ones), that will ultimately serve as lipogenic and glucogenic precursors (Aschenbach *et al.,* 2010). The pancreas exhibits a greater response to propionate compared to glucose, which highlights the crucial role of circulating propionate in insulin secretion (Manns and Boda, 1967). Soluble carbohydrates are even more fermentable than fiber, which contributes to the low amount of free glucose to be absorbed, and contributes to the VFA pool (Bergman, 1990). At the onset of lactation, 80% of glucose turnover is diverted to the mammary gland, and to support that, rates of gluconeogenesis in the liver are increased and glycogen is mobilized (Bauman and Currie, 1980).

The liver is recognized as a key site for ceramide production and a significant source

of circulating ceramides, which are linked to systemic insulin resistance and decreased pancreatic insulin secretion (Rico *et al.,* 2019; Watt *et al.,* 2012; Boon *et al.,* 2013; Holland and Summers, 2008). Saturated fatty acids (SFA) can disrupt insulin action by leading to reduced pancreatic insulin secretion and causing peripheral insulin resistance. These detrimental effects are mainly caused by the buildup of ceramides, sphingolipids that accumulate during obesity and impair cellular insulin signaling and secretion (Rico *et al.,* 2019; Sjoholm, 1995; Kleppe, *et al.,* 2003; Bikman and Summers, 2011).

Additionally, a transient state of insulin resistance occurs, decreasing the peripheral tissues utilization of glucose as a fuel and increasing the oxidation of lipids and amino acids. The mechanism behind insulin insensitivity includes a few factors, like peripartal sources of inflammation (Chirivi *et al.,* 2022) and decreased expression of cell metabolic regulators, like sirtuin 1 (Liang *et al.,* 2009). Moreover, the negative energy balance causes an increased mobilization of fatty acids from the adipose tissue stores, which is then reflected in increased plasma concentrations of non-esterified fatty acids (NEFA). Lipolysis is inturn enhanced by a transient increase in adipose tissue sensitivity to catecholamines, and concomitant reduction of lipid synthesis, allowing the adipose tissue metabolism to change from lipogenic to lipolytic (McNamara, 1991). Besides acting as a fuel in tissues such as the skeletal muscle, NEFA can also be used for milk fat synthesis or be processed by the liver (15-20%) to yield ketones (*i.e.*, partial oxidation) or ATP and CO_2 (*i.e.*, complete oxidation).

In dairy cows, the major glucose source is gluconeogenesis from propionate (Wiltrout and Satter, 1972). Propionate is produced by ruminal bacteria from carbohydrates derived from the diet. In liver slices from biopsies at -21, 1 and 21 days relative to parturition, the capacity to convert propionate to CO2 was 127 and 83% of prepartum values on day 1 and 21, respectively. The capacity of the liver to convert propionate to glucose postpartum was 126% (1 day) and 85% (21 days) of prepartum values (Overton *et al.,* 2015). This suggests an

increased efficiency in propionate utilization for gluconeogenesis after parturition. In calf hepatocytes treated with 1-5mM of sodium propionate, there was an upregulation in the expression of transcription factors that control hepatic gluconeogenic genes. These include forkhead box O1, peroxisome proliferator-activated receptor gamma coactivator 1-alpha (PGC-1α, linked to mitochondrial biogenesis and regulation of cellular energy metabolism (Liang & Ward, 2006)), and hepatocyte nuclear factor 4 (HNF4, a key regulator of hepatic differentiation and cell proliferation (Walesky & Apte, 2015)). These changes are likely due to propionate enhancing mammalian target of rapamycin complex 1 (mTORC1) activity and inhibiting mTORC2, thereby boosting gluconeogenesis. Exposure to palmitate resulted in the opposite effect, with decreased gluconeogenesis by inhibiting mTORC1 and activating mTORC2 (Wang *et al.*, 2023).

In addition, gluconeogenic amino acids such as L-lactate and alanine serve as glucose precursors, more importantly after parturition (Larsen and Kristensen, 2013). Pyruvate Carboxylase is responsible for the carboxylation of pyruvate to oxaloacetate, which in turn replenishes the availability of this metabolite in the tricarboxylic acid (TCA) cycle. Phosphoenolpyruvate carboxykinase (PEPCK) is the rate-limiting enzyme for gluconeogenesis, and it is found in the cytosolic and mitochondrial forms. It converts oxaloacetate into phosphoenolpyruvate and regulates the TCA cycle flux. When intravenously infusing [U-14C]-labeled amino acids in sheep, Reilly and Ford (1971) found that dietary protein intake positively correlates with glucose production, suggesting that the supply of amino acids seems to be an important factor for their utilization in gluconeogenesis.

Glycogen content in the liver decreased postpartum relative to -21 days before parturition (Overton *et al.*, 2015). It was 26.9 and 25.5% of the prepartum value on days 1 and 21. The stores of glycogen in the liver are limited and its mobilization happens physiologically during the peripartum, and cows that had a higher glycogen content postpartum had lower

conversion of palmitate to triglycerides. In contrast, no differences in the oxidation of palmitate to CO2 were observed between -21 and 1, but at 21 days after parturition, it was 84% of the prepartum values. The capacity of conversion of palmitate to esterified products by the liver was 148 and 139% of the prepartum value at days 1 and 21, respectively. (Overton *et al.*, 2015).

2.1.2 Negative Energy Balance and Fatty Acid Catabolism

The transition period refers to the critical days between the end of gestation and the beginning of lactation, and is commonly defined as 3 weeks before and 3 weeks after parturition (Grummer *et al.*, 1995). This period is a moment when important metabolic and immunologic changes take place. By the end of gestation, the gravid uterus and fetus require about 0.82 Mcal of energy, 117 g of protein, 10.3 g of calcium, 5.4 g of phosphorus, and 0.2 g of magnesium (Bell *et al.*, 1995; House *et al.*, 1993). Right after parturition, colostrum production significantly exceeds the nutrient demands of late gestation. To produce 10kg of colostrum on the first day of lactation, 11 Mcal of energy, 140 g of protein, 23 g of calcium, 9 g of phosphorus, and 1 g of magnesium are required (Goff & Horst, 1997). Since the energy demands of lactation cannot be met by diet alone during the first weeks after parturition, lipid mobilization of energy stores from adipose tissues are typically deployed. This state of negative energy balance (NEB) is characterized by elevated fatty acids in circulation, hypoglycemia, and insulin resistance. In addition to that, the demand of modern cows to produce milk is significantly higher nowadays than it was 70 years ago. A 3.8-fold increase from 1950 to 2010 has been observed, going from 2,400 to 9,200 kg of milk per year (Knaus, 2009). The goals of economic efficiency and optimal dairy cow health are often in conflict. Restricting the gap between nutrient and energy supply and demand helps cows adapt better and avoid dysfunctional processes during the transition period. The high incidence of health issues in

cows during this period underscores the vulnerability of many production systems (Sundrum, 2015).

In hepatocytes, NEFA might be processed in three manners: complete oxidation, providing energy for the liver; partial oxidation, utilizing acetyl-CoA from β-oxidation to produce ketone bodies (acetone, acetoacetic acid, and beta-hydroxybutyrate [BHB]); or reconversion into triacylglycerols (TAG) and transport back to the adipose tissue as VLDL (Drackley, 1999; Drackley *et al.*, 2001). However, ruminants have a limited export capacity of TAG, causing fat accumulation in the liver (hepatic steatosis). With increased fatty acid load within hepatocytes, mitochondrial oxidative capacity becomes impaired, with reduced disposal of fats and ketogenesis rates. As a result, the whole liver function is affected due to oxidative stress, with generation of reactive oxygen species (ROS), cell death, and chronic inflammation (Puchalska and Crawford, 2017).

2.1.3 Ketogenesis

During negative energy balance states, with a shorter pool of oxaloacetate for the TCA and increased availability of fatty acids, the hepatic mitochondrion import fatty acids through the carnitine palmitoyltransferase (CPT-1) for β-oxidation, yielding ATP and acetyl-CoA. Oxaloacetate originates from pyruvate in the glycolytic process. If glucose levels drop significantly (such as during fasting or due to low insulin around parturition), oxaloacetate is primarily used in gluconeogenesis rather than condensed with acetyl-CoA for the TCA cycle. Consequently, acetyl-CoA is redirected toward producing ketone bodies (Laffel *et al.*, 1999). Two molecules of acetyl-coa are brought together by the mitochondrial thiolase (also known as acetyl coenzyme A acetyltransferase (ACAT)), to acetoacetyl-CoA. This is the substrate to hydroxy methylglutaryl-CoA synthase (HMGCS2) to form hydroxy methylglutaryl-CoA.

Then, HMG-CoA lyase breaks down this molecule into acetoacetate and acetyl-CoA. Part of the acetoacetate becomes acetone, but the large majority is converted into BHB by BHB-dehydrogenase (BDH1), then transported out of the liver mitochondria through the monocarboxylate transporter 7, a proton coupled transporter located in the plasma membrane (MCT-7, encoded by SLC16A6; Hugo *et al.*, 2012) and released into the circulation for uptake by the peripheral tissues (Puchalska and Crawford, 2017).

Beta-oxidation of fatty acids is a significant source of metabolic energy, especially in conditions of elevated demand for energy, such as the beginning of lactation. For the catabolism of saturated fatty acids (*e.g.*, palmitate (16:0) and stearate (18:0)), first acyl-Coa dehydrogenase (specific to lipid length, include long-chain (LCAD), medium-chain (MCAD), and short-chain acyl CoA dehydrogenases (SCAD)) catalyze the formation of a trans double bond between the alpha and beta carbon in the molecule, removing two electrons and yielding one molecule of FAD(2H). In sequence, enoyl CoA hydratase hydrates this double bond, adding a hydroxyl group and a proton to the molecule. The enzyme beta-hydroxyl acyl CoA dehydrogenase removes the electrons and protons previously added, producing one molecule of NADH. The last step is the breakdown of the alpha and beta carbon bond by the enzyme beta keto-thiolase, generating one molecule of acetyl-CoA and a fatty acid molecule that is two carbons shorter in length. Overall, mitochondrial β-oxidation yields 4 ATP equivalents in the form of one FAD(2H) and one NADH, in addition to one molecule of acetyl-CoA (Talley & Mohiuddin, 2020). Additional enzymes are required for unsaturated lipids and different molecular structures.

In addition to the liver, other tissues are capable of extrahepatic ketogenesis. In dairy cows, the rumen is also considered a main ketogenic organ (Rico & Barrientos-Blanco, 2024; Bergman, 1971), and the hindgut fermentation might also contribute to the circulating ketone pool (Abeyta *et al.*, 2023). Astrocytes, besides being ketogenic cells, also might have the

survival/death decision of neural cells controlled by their partitioning of fatty acids between ketogenesis and *de novo* ceramide synthesis (Guzmán & Blázquez, 2001). In conditions of diabetic nephropathy, the kidney presents ketogenic activity upregulating HMGCS2, the main enzyme responsible for ketogenesis (Zhang *et al.,* 2011). In the newborn gut, the breakdown of long-chain fatty acids results in ketone formation. Interestingly, gluconeogenesis is also active in the intestinal mucosa of newborns, which might indicate the gut mucosa in infancy behaves to some extent like the liver (Hahn & Taller, 1987).

Insulin is the primary regulator for ketogenesis, and low insulin states promote the formation of ketones. Insulin dephosphorylates of hormone-sensitive lipase, lowering its activity, and activates lipogenesis via acetyl CoA carboxylase, downregulating ketogenesis. It also decreases the uptake of NEFA into the mitochondria due to the higher activation of acetyl-CoA carboxylase, through which malonyl CoA is increased, blocking the import of NEFA into the mitochondria (Laffel *et al.,* 1999). In addition, it inhibits the HMG-CoA synthase activity, resulting in lower in total ketones in circulation. Glucagon, on the other hand, stimulates hormone sensitive lipase and HMG-CoA synthase by phosphorylation, upregulating ketogenesis. The phosphorylation of acetyl-CoA carboxylase by glucagon reduces the production of malonyl CoA and increases fatty acid uptake by the mitochondria, increasing ketogenesis due to the heightened amount of substrate available.

2.1.4 Ketolysis

Ketone bodies can be utilized by a broad range of tissues, including the heart, skeletal muscle, and the brain (Puchalska & Crawford, 2017). Ketones are an important source of energy for extrahepatic tissues in states of low glucose, especially for the brain, which is not capable of utilizing fatty acids as a fuel. To initiate the oxidation of ketones, they are first

transported into the cells through one of the monocarboxylate transporters. In the neural system alone, three isoforms of the membrane transporter MCT are expressed: MCT1, MCT2 and MCT4, with specific cellular and regional brain distribution (Pierre & Pellerin, 2005). BHB suffers oxidation to AcAc by the activity of the enzyme BDH1, which is converted to acetoacetyl-CoA by succinyl CoA-oxoacid transferase (SCOT), being then cleaved to form acetyl-CoA by the enzyme methylacetoacetyl CoA thiolase (MAT) (Laffel, 1999). Acetyl-CoA is then used in the TCA cycle, ultimately generating ATP through the electron transport chain.

Furthermore, the oxidation of ketone bodies to generate ATP reduces less molecules of NAD+ than the oxidation of carbohydrates (Elamin *et al.*, 2020), allowing the diversion of this metabolite to its function as a substrate for repairing enzymes like sirtuins and poly (ADP-ribose) polymerases (PARPS), instead of being used in redox reactions. In dairy cows, mRNA levels of PARP1 decrease significantly between 42 and 14 days before parturition, as a possible consequence of decreased energy availability (Buhler *et al.*, 2018).

2.1.5 Metabolic and immunologic adaptations to the peripartum

Even though BHB levels have been used to evaluate the degree of maladaptation in the transition period, it is the change in body condition score that predicts an animal susceptibility to peripartal diseases (Rathbun *et al.*, 2017), which is better represented by plasmatic NEFA concentration. Analyzing the whole picture, it is difficult to distinguish the effects of these biomarkers, especially since they are interrelated. It is known that NEFA cause a pro-inflammatory response via TLR4 (Zhang, 2018), and that mature neutrophils rely primarily on glucose to fulfill its energy requirements, diverting it from production and physiological use (Bradford *et al.*, 2015). This complicates even more the negative energy balance, and its relation to insulin resistance and altered adipose tissue metabolism are important components

of the phenomenon of metabolic or sterile inflammation in dairy cows, which has recently received scientific attention (LeBlanc, 2020). BHB appears as a possible modulator of systemic inflammation through unclear mechanisms, but with anti-inflammatory properties reported in leukocytes.

The increase in serum NEFA concentrations caused by excessive body fat mobilization is associated with the development of displaced abomasum, clinical ketosis, retained placenta, and metritis (Ospina, 2010). In the immunological field, NEFA have been associated with an increase in pro-inflammatory cytokines synthesis (Zhanga, 2018) and lower oxidative burst capacity (Pascottini, 2021). Ster et al. (2012) mixed neutrophils from mid-lactation cows with a mixture of NEFA at 0,0.1, 0.25, 0.5, or 0.75 mmol/l to mimic concentrations in early postpartum cows. They observed a dose-dependent reduction in oxidative burst function, with significant impairment at the two higher concentrations. They also demonstrated inhibition of proliferation of peripheral blood mononuclear cells (PMBC) with NEFA as low as 0.13 mmol/l. Another explanation for how NEFA are capable of inducing an inflammatory response is that NEFA are ligands for TLR4, capable of inducing intracellular signaling and initiating nuclear factor kappa B (NF-κB) cascades. In detail, the transcription factor NF-κB is sequestered in the cytoplasm by binding to its inhibitor IκBα, whose phosphorylation is dependent on IKKβ activity. In response to stimuli, the NF-κB subunit p65 separates from IκBα and translocates into the nucleus where NF-κB can regulate the transcription of several inflammatory cytokine genes, such as TNF-α, IL-6, and IL1β (Zhanga, 2018).

Concerning BHB, different associations have been established. Van Holder (2015) found that cows with subclinical ketosis (BHB 1.2-2.9 mmol/L) or clinical ketosis (BHB≥3.0 mmol/L) actually had a higher milk yield and fat percentage than non-ketotic cows. Considering the isolated effects of a serum concentration of BHB up to 1.2 mmol/L, research has shown that supplementing Sodium Butyrate at 1.1% of diet DM increases both the content

and yield of milk fat regardless of dietary starch content, without reducing dry matter intake (DMI) (Izumi, 2019). In fact, the authors reported that supplemented cows were more feed efficient than control cows.

Nevertheless, one of the proposed mechanisms for impaired immune function in cows during the peripartum is the inhibition of the mechanistic Target of Rapamycin (mTOR) (Sipka *et al.,* 2022). The mammalian target of rapamycin (mTOR) coordinates cell growth and metabolism with environmental inputs from nutrients and growth factors (Saxton & Sabatini, 2017). Its inhibition can decrease phagocytic capacity in macrophages and dendritic cells and extend the pro-inflammatory response. Ketogenic diets cause inhibition of mTOR in the liver and brain cells of mice (McDaniel *et al.,* 2012), suggesting a possible indirect effect of BHB on immune function through mTOR.

Neutrophils phagocytic capacity is high during the periparturient period, but it slightly decreases after calving (Kehrli *et al.,* 1989). The total number of leukocytes and percentage of neutrophils peak at parturition, and sharply decrease after that. A possible explanation might be related to the increased corticosterol levels at calving (Guidry *et al.,* 1976), since cortisol levels raise from 2.7 ng/ml 4 days before parturition to 11.1 ng/ml on the calving day, and circulating neutrophils increased from 3.363 per mm3 two days before calving to 5.889 per mm3 two days after calving. The average yeast ingested per neutrophil decreased during the second week postpartum, potentially offsetting the rise in circulating neutrophils.

Zarrin *et al.,* (2017) evaluated the effects of hyperketonemia (4h IV infusion) before and after parturition regarding glucose and insulin. The most remarkable effect is that after 1.5h, the infusion of BHB caused decrease of plasma glucose concentrations relative to preinfusion levels both before and after parturition and increased plasma insulin concentrations before but not after partum, possibly through inhibition of lipolysis due to the energetic surplus.

This immediate source of extra nutrients requires adjustments in fuel homeostasis, and a possible effect of BHB reducing gluconeogenesis is suggested.

It is evident that the metabolic status influences the immune response when an animal is subjected to a challenge. What is proposed is that glucose is the discriminating factor, not BHB. Gross et al. (2020) found faster recovery of milk yield and DMI in animals with a higher concentration of plasmatic glucose when challenged in one of the quarters with LPS. Besides, these animals had lower SCC, activity of lactate dehydrogenase, serum albumin, and IgG present in milk, whose decline is associated with recovery of mammary gland health, as they are indicators of the barrier integrity. During an inflammatory response, insulin resistance and cortisol release allow the diversion of glucose to the immune system, and in case of low supplies, the immune function becomes impaired. However, in healthy mid-lactation cows with induced hyperketonemia (BHB IV infusion maintaining levels above 1.7mmol/L for 56 hours) an intramammary LPS challenge showed similar results. Besides increased IL-10 and 8, they also had higher serum amyloid A and Haptoglobin mammary tissue compared to control animals. This is in agreement with the aforementioned study, in which ketotic animals had a delayed recovery. Besides, as BHB decreases neutrophil recruitment, the immune system probably compensated upregulating IL-8 mRNA abundance.

The absence of mitochondria in red blood cells (RBCs) prevents them from utilizing ketone bodies as a fuel source. Hence, it was hypothesized that ketotic cows might exhibit hematological alterations. Lower values of red cell distribution width and higher values of mean corpuscular volume, mean corpuscular hemoglobin were reported in cows naturally ketotic. RDW, MCV and MCH are observed in human patients with liver damage, which can be a common mechanism in cows. Besides, these animals had lower counts of white blood cell and albumin (Ha et al. 2022). Specifically, the lower count of monocytes reported by this study

might be influenced by an hepatocyte signaling to the bone marrow, as it was already reported in humans (Jordan *et al.,* 2019).

Increased parity is associated with higher incidence of all peripartal diseases (Lean *et al.,* 2023). Clinical ketosis, especially prevalent in parities over three, often coincided with or preceded other diseases and may enhance productive potential. This phenomenon may be attributed to older animals mobilizing more lipids early postpartum to supply peripheral tissues, evidenced by variations in glucose, NEFA, and BHB levels. Pasture-fed herds exhibit significantly lower odds of subclinical ketosis compared to intensive farming systems. Moreover, higher parities are associated with hypocalcemia, as evidenced by decreased blood concentrations of calcium and phosphorus (Lean *et al.,* 2023).

2.1.6 Endotoxemia

Lipopolysaccharide (LPS, endotoxin) is the main component of the outer leaflet of Gram-negative bacteria and possesses strong immunostimulatory properties (Heine *et al.,* 2001). Besides being the primary component of sepsis, it also plays a role in Parkinson's disease through neurotoxicity and brain inflammation, likely due to gut permeability to LPS originated from the local microbiota (Brown *et al.,* 2023) and with type 2 diabetes, since abdominal subcutaneous adipocytes secrete TNF-α and IL-6 in response to LPS, causing a low-grade chronic inflammation, leading to insulin resistance (Creely *et al.,* 2007).

The endotoxin model is likely the most commonly used model of systemic inflammation, involving the intravenous administration of purified LPS (endotoxin) from *Escherichia coli* or other Gram-negative bacteria to healthy individuals (Andreasen *et al.,* 2008). Lipopolysaccharides bind to the soluble LPS-binding protein, which promotes binding to CD14 and MD-2, membrane-associated proteins, and to co-receptors like the TLR4. Activated TLR recruit their specific repertoire of the Toll-Interleukin1 receptor (TIR) adapters

such as the myeloid differentiation protein (MyD88), Mal (MyD88-associated protein Mal), TIR domain containing adaptor molecule 1 (TRIF), or TRIF-related adaptor molecule (TRAM), resulting in the recruitment and activation of the IL-1-receptor-associated kinase (IRAKs) and TNF-receptor-associated factor-6 (TRAF6). This cascade will lead to the activation of NF-κB essential modulator (NEMO), degrading the inhibitor of NFκB (IκB) and allowing NFκB to translocate to the nucleus, activating gene transcription (O'Neill *et al.*, 2009).

In addition, TLR4 activated by the endotoxin cause the increased transcription of the NOD-like receptor pyrin-domain containing 3 (NLRP3) inflammasome and IL-1-β through the NFκB pathway. The NLRP3 inflammasome is cytosolic, and responsible for sensing danger and pathogen-associated molecular patters (DAMPs and PAMPs). Priming licenses the NLRP3 by deubiquitylation, and a second signal is necessary for activation (*e.g.*, potassium efflux, relocalization of the inflammasome to the mitochondria, release of mitochondrial DNA or ROS to the cytosol). Apoptosis-associated speck-like protein containing a caspase activation (ASC) and recruitment domain (CARD) are nucleated through polymerization by the activated inflammasome into prion-like filaments using Pyrin-Pyrin interactions (PYD-PYD). On top of those filaments, pro-caspase-1 forms its own filaments through CARD-CARD interactions, allowing pro-caspase-1 to be auto-activated. Caspase-1 cleaves pro-IL-1-β and pro-IL-18 into their active forms, stimulating inflammation (Guo *et al.*, 2015). Exogenous ketone supplementation was found to not affect LPS-induced activation of caspase-1 in human monocytes, but plasma IL-1-β tended to be lower than the baseline 60 minutes after LPS administration (Neudorf *et al.*, 2020).

Dairy cows are exposed different sources of LPS throughout their life. In animals presenting subacute ruminal acidosis (SARA) and fed a high-grain concentrate, there is a decrease of the rumen pH, along with increased presence of LPS in the cecum, feces and rumen

and the initiation of an acute phase response, probably due to the translocation of LPS from the digestive tract into circulation (Plaizier *et al.,* 2012). Animals with SARA exhibit elevated blood glucose and lactate levels, along with lower β-hydroxybutyrate (BHBA) and NEFA compared with healthy animals. Following a LPS challenge, serum cortisol concentrations increase, and calcium concentrations decrease, with NEFA concentration becoming similar between healthy cows and cows suffering from SARA (Aditya *et al.,* 2018). Ruminal dysbiosis, with increased presence of *Proteobacteria* causes a systemic inflammation that is associated with the higher incidence of mastitis by impairing host anti-inflammatory enzymes (Zhao *et al.,* 2022). Intermittently induced endotoxemia decreases feed intake and milk production in dairy cows, and it is associated with greater incidence of left displaced abomasum (LDA) and retained placenta (RP; Zebeli *et al.,* 2018).

In bacterial infections, ketones might act as energy substrates to meet the demands of effective T cells. Ketolysis activates T Cell function against *Staphylococcus aureus* infection by fueling the tricarboxylic acid (TCA) cycle and affecting histone acetylation (Cai *et al.,* 2024). In addition, ketogenic diets increase CD8+ T effector cell cytokine production, cytolytic activity, and boost their respiratory capacity, with ketolysis being consider a metabolic and epigenetic driver of optimal CD8+ T cell effector responses. Furthermore, these cells preferentially used ketones over glucose to fuel the tricarboxylic acid (TCA) cycle in vitro and *in vivo* (Luda *et al.,* 2023). In dairy cows with subclinical endometritis, BHB and NEFA concentrations were higher than in healthy animals, but in animals presenting purulent vaginal discharge, these metabolite's concentrations were not different (Pascottini & LeBlanc, 2020).

The effects of ketone metabolism on viral infections are still unclear. The tuning down of the immunological cellular responses by BHB might be harmful if interferes with the early immune response, but beneficial in pathological activation, as it is the case of acute respiratory distress syndrome (ARDS). Viruses like Influenza and SARS-coronavirus activate the NLRP3

inflammasome, partially through the protein viroporin, which encodes a channel that increases the intracellular concentrations of sodium and calcium and reduced potassium, triggering the inflammasome. Blocking the ion channel and the inflammasome activation might alleviate ARDS and increase survival. On the other hand, BHB interacts with heterogeneous nuclear ribonucleoproteins (hnRNP), which might increase viral replication (Stubbs *et al.,* 2020).

2.2 The Nicotinamide Adenine Dinucleotide (NAD) metabolome

2.2.1 NAD+

An increase in oxygen requirements caused by the increased metabolism to support lactation causes an increased production of reactive oxygen species. Free radicals can exceed the antioxidant capacity, leading to oxidative stress. Therefore, failure to adequately control oxidative stress can result in an increased incidence of health disorders. Nicotinamide Adenine Dinucleotide (NAD) and its coenzymes are central mediators of all metabolic processes. Conditions of metabolic stress also dysregulate the NAD metabolome, and some mammalian species benefit from NAD precursors supplementation (Ear *et al.,* 2019).

NAD is present in almost all cell metabolic processes as a cofactor, including glycolysis, gluconeogenesis, fatty acid oxidation and synthesis, amino acid catabolism, and others (Navas & Carnero, 2021), and exists as an electron donor (NADH) or acceptor (NAD+). Increasing intracellular NAD+/NADH ratio is associated with a number of health benefits, ranging from protection to metabolic diseases to decreased age-related physiological impairment. Reduced NADH levels can be accomplished by caloric restriction. In yeast, NADH has shown to competitively inhibit Sir2, and a depletion of NADH is associated with increased lifespan (Lin *et al.,* 2004). In healthy brain tissue, the intracellular NAD+

concentrations are around 0.3 mM, while NADH were 0.06 mM, with a total NAD amount of 0.37 mM and a ratio of NAD+/NADH of 4.8. As aging progresses, the total NAD and NAD+ amounts decrease and the NADH concentration increases intracellularly (Zhu *et al.*, 2015). The nucleotide pool varies according to cell type and organelle. In the cytosol and nucleus, the ratio of NAD+/NADH is 800:1, while in the mitochondria it is 7:1 (Anderson *et al.*, 2017). In cardiomyocytes, NAD+ precursor supplementation was capable of increasing the intracellular NAD+ by more than 2-fold, but the mitochondrial redox state was only affected transiently since it is tightly regulated (Wu *et al.*, 2021).

Increasing the levels can be accomplished by reducing NAD+ consumption by CD38, changing the metabolic preference for fuels that benefit the ratio (like ketone bodies), or by consumption of precursors like nicotinamide riboside (NR) and nicotinamide. Notably, cow's milk is a source of both these molecules (Trammel *et al.*, 2016). NAD+ can be synthesized by three main pathways: de novo, which uses as substrate the amino acid tryptophan; Salvage, which uses Nicotinamide; and Preiss-Handler, which synthesizes it through Nicotinic acid (Sauve and Yang, 2016). Nicotinamide mononucleotide (NMN) and NR are processed through the salvage pathway, which is facilitated through the action of kinases. The phosphorylation of NR is accomplished by NR kinases 1 and 2, which are rate-limiting enzymes for NAD+ synthesis from NR (Ratajczak *et al.*, 2016). The overexpression of this enzyme is linked with increased hepatic NAD+ levels, decreased liver triglyceride content, improved insulin sensitivity, and glucose tolerance. This is due to increased expression of genes involved in β-oxidation (Cpt1a, Acox1) and reduced lipogenic genes (Fasn, Acaca). Thus, it becomes evident the role of NRK in attenuating fatty liver disorder and metabolic syndrome (Fan *et al.*, 2018).

NADH is produced mainly during glycolysis (through the action of glyceraldehyde-3-phosphate dehydrogenase), TCA cycle (isocitrate dehydrogenase, oxoglutarate dehydrogenase, and malate dehydrogenase), and the pyruvate dehydrogenase complex (Sauve and Yang, 2016).

NADH enters the electron transport chain in mitochondria and through Complex I, it is oxidized to NAD+. The majority of ATP produced happens through the ATP synthase pump. When the ratio of NADH/NAD+ is high, catabolism and energy production and oxidative reactions slow down (Titov *et al.*, 2016).

Moreover, NAD+ levels are affected by substrate availability and impact energy metabolism independently of the electron transport chain integrity. When the NAD+ is restored within the cell by an exogenous NADH oxidase, the effects caused by ETC inhibition are reversed, allowing the restoration of metabolic and proliferative processes that are impaired by mitochondrial inhibition. Gluconeogenesis in hepatocytes using pyruvate as a substrate is not affected by restoration of cytosolic NAD+ levels and is inhibited by mitochondrial restoration, but when lactate is used as a substrate, gluconeogenesis increases both with the restoration of cytosolic and mitochondrial NAD+ levels, but mostly with mitochondrial. Additionally, the ratio of BHB/acetoacetate is decreased with increased NAD+/NADH ratio. Pyruvate dehydrogenase, which is the complex that converts pyruvate into Acetyl-CoA has its activity decreased by phosphorylation. Under increased mitochondrial NAD+/NADH ratios, the complex was almost completely dephosphorylated (Titov *et al.*, 2016). This evidence provides some clues as to how NAD+ availability influences energy metabolism and substrate oxidation.

The cytosolic and mitochondrial NAD+ pools are regulated and maintained separately, but are interrelated by shuttle mechanisms like the malate-aspartate and the isocitrate α-ketoglutarate. When consumption of NADH by the mitochondria is accelerated, the malate-aspartate shuttle is responsible for exchanging NADH from the cytosol to the mitochondria, rebalancing the redox NAD+/NADH ratio (Hu *et al.*, 2021). Cytosolic isocitrate dehydrogenase (IDH) converts NADP+ into NADPH when converting isocitrate to α-ketoglutarate, which is shuttled to the mitochondria where it is converted back to isocitrate in a reaction that oxidizes NADH. This transfer of NADPH between cytosol and mitochondria is accomplished by the

isocitrate/α-ketoglutarate shuttle (Sazanov & Jackson, 1994). Nonetheless, a recently identified membrane transporter (SLC25A51) is capable of exchanging NAD molecules between the cytosol and the mitochondria, suggesting that part of the pool is pre-formed before reaching the interior even though mitochondrial NMNAT3 forms NAD from NMN inside of it (Ziegler *et al.,* 2021).

Nicotinamide Adenine Dinucleotide Phosphate (NADP) is synthesized from NAD+ by NAD kinase, an enzyme essential for cell survival. It uses ATP to transfer a phosphate group to the 2'-hydroxyl group of the adenosine ribose moiety of NAD. NADH can also be used as substrate, yielding NADPH, which provides reducing equivalents, having a central role in oxidative defense mechanisms (Agledal *et al.,* 2010), in addition to being key in lipid synthesis. The reduced form of NADP is also involved in the detoxification process mediated by cytochrome P-450 (it facilitates the breakdown by transferring electrons to convert insoluble organic molecules to hydrophilic ones), in the biosynthesis of fatty acids and amino acids, in the oxidative defense and in the generation of the oxidative burst in immune cells.

To protect the areas of production of highly reactive oxygen species (ROS), like the mitochondria, the cells have evolved antioxidant machinery. Oxidative phosphorylation uses the oxidation of NADH or FADH to generate the electrochemical gradient that generates the potential energy that ultimately generates ATP, and it is responsible for most of the ROS (Balaban *et al.,* 2005). Superoxide dismutase (SOD) exists both in the mitochondria (MnSOD) and the cytosol (SOD1) and catalyzes the conversion of superoxide radicals (O2-) into hydrogen peroxide (H2O2), which then become oxygen and water through the action of catalases, or react with glutathione peroxidase to form oxidized glutathione and water. NADPH supplies hydride ions to form reduced glutathione from the oxidized form, as it is a cofactor to glutathione reductase. Glutathione's role is to remove hydroperoxides generated physiologically, and it does so through 3 enzymatic reactions of the NADP-glutathione system.

Tert-butyl hydroperoxide is degraded through the oxidation of glutathione (GSH), and the early rate is determined by GSH initial concentration and the activity of GSH peroxidase, which reduces hydrogen peroxide to water, while the late rate is determined by the electron supply by NADP or GSH (Kurosawa *et al.,* 1990). A similar process catalyzed by NADPH happens with thioredoxin peroxidase, oxidizing reduced thioredoxin to form water and oxidized thioredoxin (Balaban *et al.,* 2005). Importantly, an increase in NADPH due to increased catabolism (either through increased activity of pyruvate dehydrogenase complex or increased flow of acetyl-CoA from β-oxidation to the TCA cycle) is associated with endoplasmic reticulum (ER) stress. NADPH is generated through three isozymes in the TCA in the liver: cytosolic isocitrate dehydrogenase (IDH1), mitochondrial IDH2, and cytosolic malic enzyme (ME1), and under diminished expression of these enzymes, the ratio of GSSH (oxidized glutathione) to GSH (reduced) is elevated, probably due to lower NADPH production. This results in alleviation of ER stress, restoring its oxidative protein maturation capacity and promoting ER homeostasis (Gansemer *et al.,* 2020).

This antioxidant system can be inactivated by its own substrates in cases of high oxidative stress. Glutathione peroxidase is inactivated by hydroxyl radicals, but not by superoxide anions, while catalase is inhibited by both of these but not by organic peroxides and SOD is inactivated only by hydrogen peroxide (Pigeolet *et al.,* 1990). If this system is overwhelmed with increased free radical production, autocatalysis takes place, and the cell dies (Kannan & Jain, 2000). Under consumption of a high-fat, high-sugar diet, mice present upregulation of the gp91phox subunit of NADPH oxidase and downregulation of the main antioxidant enzymes (SOD, catalase, glutathione peroxidase, and heme oxygenase). This, along with increased plasma malondialdehyde (a lipid peroxidation product marker of oxidative stress) characterize the origin of increased free radicals seen in models of metabolic syndrome (Roberts *et al.,* 2006).

Although the generation of ROS in most cells characterize as a damaging byproduct of metabolism, in phagocytes they are the core for generating oxidative burst. When macrophages are stimulated with LPS *in vitro*, after 1h is possible to see a decrease in NAD+ levels. To compensate, they upregulate NAMPT, suggesting that the main pathway used by immune cells to maintain the intracellular NAD+ pool during a challenge is the salvage pathway, which has as substrate NAM synthesized by the hepatocytes. To express a pro-inflammatory response, they release pro-inflammatory cytokines and decrease SIRT3 expression, besides decreasing QPRT activity. Inhibition of QPRT leads to the accumulation of succinate, which decreases mitochondrial respiration and increases ROS (Billingham and Chandel, 2019).

Even though we know about the importance of NAD(P)H to physiological biochemical reactions for decades, there are still many functions being unraveled as scientists investigate further. As a major redox homeostasis indicator within the cell, it serves as a target for sensors and regulatory mechanisms that will determine the energy status and all the consequences that come with it. With a wide range of physiological roles, it becomes evident the significance of the metabolite in maintaining health, and as an opportunity for the development of preventive and therapeutic opportunities.

2.2.2 NAD and coenzymes during parturition

In mice, NAD and NADP mammary tissue contents are both low during gestation, and increasingly raise after parturition and during the first 30 days of lactation, remaining elevated until the beginning of mammary involution (McLean, 1958). In support, changes in the activities of enzymes responsible for the biosynthesis of nicotinamide nucleotides occur (Greenbaum & Pinder, 1968). NAD pyrophosphatase catalyzes the nucleotidyl transfer from ATP to NMN to form NAD and pyrophosphate (Paulik *et al.*, 1991). Its expression is low in

early pregnancy (10 days into gestation) but increases throughout mid-lactation and especially after parturition in mice. It reaches maximum activity 5 days into lactation and remains high until the first two days of mammary involution. Nicotinamide mononucleotide adenylyltransferase (NMNAT) catalyzes the chemical reaction of NMN and ATP, generating diphosphate and NAD+. It is already high during mid-pregnancy, and only raises by 2-2.5-fold at parturition, with the maximum activity at 5 days of lactation, and decreasing throughout the lactation, slowly declining during mammary involution. NAD kinase phosphorylates NAD+, producing NADP. The activity of this enzyme is low during the first 10 days of pregnancy, but it rises during the second half of it. It raises by two-fold at parturition, and remains high for 10 days, increasing significantly during the second half of lactation and decreasing during early mammary involution (Greenbaum & Pinder, 1968). The biosynthesis of these nucleotides is important not only for the metabolism of the mammary gland itself, but also for the production of fat, in which NADP plays a special role (McLean, 1958).

After parturition, the liver redistributes its NAD metabolome to meet the new energy requirements of the organs, in special the newly secreting mammary gland. It exports NAD metabolites into circulation, thereby reducing their hepatic content. In agreement with the idea of a postpartum disruption of energy homeostasis, the supplementation of NR to mice and rats resulted in increased NAD+ metabolites in liver blood, and mammary, increased circulating levels of prolactin, enhanced mammary size, and increased the biosynthesis of milk components (protein, fat, and lactose) and milk yield, with higher levels of brain-derived neurotrophic factor (BDNF) (Ear *et al.,* 2019). Pups of mothers that received the NAD+ supplement were larger at weaning and had better glycemic control.

2.2.3 NAD Precursors and administration routes

Niacin, or Nicotinic Acid, is a B vitamin, and a precursor of Nicotinamide Adenine Dinucleotide (NAD) and coenzymes. Niacin may not only have a role in NAD generation, but also in regulating lipolysis, BHB, NEFA, glucose and insulin concentrations, milk yield and composition, and immune function (Ringseis *et al*., 2019). In recent years, NR and NMN have been studied for their efficacy in increasing the intracellular NAD+ pool. Oral supplementation with either compound results in their oxidation by the liver, which subsequently secretes NAM to be distributed to peripheral tissues. NAMPT is the enzyme responsible for producing NMN from NAM, and is the limiting factor to form NAD+ from NAM, which might explain the lower efficiency to increase NAD levels in oral supplementation compared to IV infusions. (Liu *et al.*, 2018).

Nonetheless, when infused intravenously, NR reaches tissues intact and is more effective at increasing the NAD+ pool compared to NMN. The proposed mechanism is that NR, being a small molecule, is capable of crossing cell membranes efficiently. When infusing NAD+ itself intravenously in humans, (Grant *et al.,* 2019), plasmatic NAD+ levels did not increase until after 2h of infusion, suggesting that it was uptaken/metabolized immediately by the peripheral tissues. Still, the levels were maintained elevated until at least 2h after the end of infusion. They also found increased NMN levels, which they associate with ectoenzymes involved in the conversion from NAD+ to NMN (which can cross the membrane). Based on the above evidence, the IV infusion of NR is the most efficient way of increasing the cellular NAD+ pool, with an order of efficacy as follows: NR>NMN>NAD+, and may be associated with the size of the molecule.

Considering the mitochondrial pool of NAD+, a recently identified membrane transporter, SLC25A51, facilitates the exchange of NAD molecules between the cytosol and the mitochondria, suggesting that part of the pool is pre-formed before reaching the interior

even though mitochondrial NMNAT3 forms NAD from NMN inside of it (Ziegler *et al.*, 2021). It has been suggested that the NAD+ pool of different organelles interacts and regulates the amount in each part of the cell, and not necessarily the precursor has to reach the interior intact, because of the existence of NAD+ transporters.

Nicotinamide Adenine Dinucleotide (NAD) can also be generated through the catabolism of tryptophan in the kynurenine pathway. Evidence indicates that NAD has immunoregulatory properties. It is capable of, for instance, regulating cytokines production by peripheral blood lymphocytes and monocytes (increased IL-10) and triggering innate and adaptive immune responses in the absence of antigen through the NAD+/tryptophan signaling pathway (Biefer *et al.*, 2017).

2.2.4 NAD Precursors and administration routes in ruminants

The composition of the diet seems to influence the effects of nicotinic acid (NA). Drackley et al. (1998) supplemented NA and dietary fat (whole soybeans and liquid animal fat) during an entire lactation (from week 4 to 43 postpartum) and evaluated the effects in milk production and plasma metabolic biomarkers. In control cows, the addition of NA decreased dry matter intake (DMI), but in fat-supplemented animals, it increased DMI, specifically in early lactation. Milk yield was increased in 3,5% for NA supplemented cows during this period too (4 to 25 weeks). In agreement with that, in control animals receiving NA, it increased NEFA in plasma and decreased body condition score. But in animals receiving a combination of fat and NA, it decreased NEFA and increased fat yield. Casein and crude protein content were decreased by Nicotinic Acid independently of the diet.

Similarly, when Morey et al. (2011) fed a high dose of encapsulated niacin (24 g/d of

encapsulated niacin; 9.6 g/d of bioavailable nicotinic acid) from 21 days pre to 21 days postpartum, the results showed decreased postpartum plasma NEFA concentration in all parity animals but also decreased prepartum DMI in 4 kg/d for multiparous treated animals. They also found an increase in plasma nicotinamide at -7 and 21, decreased prepartum glucose concentration, and lower levels of liver triglyceride (primiparous cows). No effects were observed on BHB, insulin, BCS, weight, energy balance, or milk or milk component production.

In comparison with other NAD precursors, such as Nicotinamide, NA was more efficient in increasing its own concentrations in plasma, being the only form found in the body fluids analyzed (ruminal and duodenal fluid, and plasma). Campbell et al. (1994) supplemented either Nicotinic Acid (12g/d), Nicotinamide (12g/d), or a combination of both (6g/d of each) in mid-lactation cows with ruminal and duodenal cannulas. After 1h of supplementation, ruminal samples showed that Nicotinamide was converted to Nicotinic Acid and other forms. However, cows receiving Nicotinamide had the highest concentration in the duodenum, which could be explained as the excess of niacin not utilized by the ruminal microorganisms (or absorbed) being able to reach the initial intestinal tract. Productive and metabolic parameters were unaffected.

The transition from the dry period to lactation is one of the most metabolically demanding phases in a dairy cow's life cycle. Though not clearly established if transitioning cows suffer from NAD pool depletions, it has been reported that cows with mild fatty liver have a reduced expression of Sirtuin 1 mRNA and protein levels, which facilitates hepatic fatty acid synthesis and inhibits fatty acid oxidation and lipid transport. In the salvage pathway, Nampt generates NMN, which is conjugated to ATP and converted to NAD by Nmnat. Intracellular Nampt is acetylated in the cytoplasm during normal nutrient status but is deacetylated by SIRT1 in food deprivation; NR protects mitochondrial dysfunction of NAFLD

through NAD elevation and SIRT1 activation. SIRT1 deacetylation of Nampt increases secretion and enzymatic activity; SIRT1 is sensitive to intracellular redox ratios and protects from oxidative stress increasing the activity of catalase (Okabe *et al.,* 2019).

Low SIRT1 expression caused by hepatic steatosis causes a reduction of PPARα, CPT1 and 2 (key enzymes in the process of transferring fatty acids into the mitochondria for β-oxidation) impairing fat oxidation, and increased SREBP-1 (lipid synthesis). This dysregulation of lipid metabolism leads to chronic hepatic inflammation, insulin resistance, and liver damage (Li *et al.,* 2020). In this context, studies involving niacin supplements (nicotinic acid, whether rumen-protected or unprotected at high doses) have been undertaken. Yuan (2012) results show reduced somatic cell score, milk fat, energy, and yield. This reduction mechanistically improved energy balance, lowering plasma NEFA concentrations at 1, 7 and 14 days post-partum. Interestingly, no effects on BHB were observed.

NAD levels quantification in erythrocyte lysates using the colorimetric ELISA method, revealing that animals receiving niacin supplementation showed increased NAD levels, which were positively associated with glucose, insulin, and triglyceride levels, and inversely correlated with BHB levels (Petrovic *et al.,* 2022). The activation of the receptor GPR109A by the nicotinic acid reduces lipolysis, improving energy balance. Nicotinamide supplementation to transitioning cows led to improved gluconeogenesis, as NAD is involved in the conversion of lactate to pyruvate and malate to oxaloacetate. This resulted in higher serum glucose concentrations, lower fatty acid and triglyceride levels, elevated glutathione levels, and reduced reactive oxygen species (Wei *et al.,* 2018).

Niacin can block fatty acid mobilization and reduce milk energy output postpartum, reducing negative energy balance in the critical period of the initial weeks of lactation. Even though inhibition of lipolysis initially led to reduced fat and energy yield, by the third week,

the energy-corrected milk yield of cows supplemented Niacin was the same as control cows (Yuan *et al.*, 2012), suggesting that niacin could have the potential to help cows overcome the beginning of lactation to achieve their full potential later.

Furthermore, NAD+ levels increase oocyte quality and improve fertility in mice, which can be another justification for supplementing NAD precursors in the peripartum period (Bertoldo *et al.*, 2021).

2.2.5 Epigenetic influence of BHB and NAD, impact on transcriptional factors and sirtuins

Epigenetics encompasses modifications in gene expression without altering the DNA sequence, with molecules like BHB serving as epigenetic modifiers. Through post-translational modifications (PTMs), BHB influences the expression of genes related to metabolism and inflammation. It serves as a modification substrate for histone β-hydroxybutyrylation, methylation, acetylation and DNA methylation. Transcriptional factors belonging to the Forkhead box (Fox) family are characterized by a conserved DNA-binding domain, play crucial roles in regulating energy metabolism, differentiation, apoptosis, cellular proliferation, and stress response (Osil & Obsilova, 2008; Zhang *et al.*, 2021). AMPK can directly phosphorylate FoXO1 at 6 distinct amino acids positions. In C. elegans, this AMPK-driven phosphorylation of FoXO1 promotes FoxO-dependent transcriptional activity and is associated with positive effects on lifespan extension (Greer *et al.*, 2007; Zhang *et al.*, 2021). AMPK is an energy sensor activated in states of energy deficit, increasing lipid oxidation and glucose uptake (Long & Zierath, 2006). PPAR-α is a main regulator of the lipid metabolism, and its methylation state is a biomarker of NAFLD development (Theys *et al.*, 2022). Activation of PPAR-α contributes to energy homeostasis by reducing triglyceride levels, while PPAR-γ

activation enhances insulin sensitivity and glucose metabolism (Tyagi *et al.,* 2011).

As BHB reduces three times less molecules of NAD to generate ATP compared to glucose, this benefits the NAD+/NADH ratio (Elamin *et al.,* 2020). This will activate sirtuins, especially sirtuins 1 and 3, that are NAD+ dependent. Sirtuins are class III histone deacetylases (HDACs) that depend on NAD+ to deacetylate protein targets and regulate several cellular processes. In addition to sirtuins, NAD+ also serves as a substrate for NAD-consuming enzymes like poly (ADP-ribose) polymerases (PARPs), which act in DNA repair. Supplementation of NAD+ or NMN resulting in increased intracellular and extracellular NAD+ levels improve PARP-dependent DNA repair regardless of CD73 activity, an ectoenzyme that regulates the intracellular NAD+ levels and is associated with tumor resistance (Wilk *et al.,* 2020).

NAD+ regulates the activities of sirtuins, epigenetic modifiers involved in various biological functions that act by the deacetylating proteins. There are 7 different sirtuins, the first three being the most important in regulating oxidative metabolism and lipid biosynthesis. SIRT1 regulates energy metabolism, insulin sensitivity, inflammation, and oxidative stress, and its main targets are peroxisome proliferator-activated receptors (PPAR), forkhead box O transcription factors (FOXOs), and nuclear factor κB (Nf-κB). By deacetylating FOXOs at multiple lysine residues and, thus, increasing its expression, SIRT1 allows adiponectin gene transcription, which increases insulin sensitivity (Qiao & Shao, 2006). In addition to that, SIRT1 deacetylation of Nf-κB is associated with decreased transcription of pro-inflammatory genes. In SIRT1 knockout mice, the hyperacetylation of Nf-κB increased its binding to gene promoters and led to an adipocyte phenotype of reduced insulin action and increased inflammation (Yoshizaki *et al.,* 2008). NAD+ is also a substrate for PPAR1, to which it donates its ADP-ribose moiety for protein substrates, aiding in DNA repair (Navas and Carnero, 2021).

In dairy cows, low SIRT1 expression caused by hepatic steatosis causes a reduction of PPARα, CPT1 and 2 (key enzymes in the process of transferring fatty acids into the mitochondria for β-oxidation) impairing fat oxidation, increases SREBP-1 (lipid synthesis), and causes dysregulation of lipid metabolism that leads to chronic hepatic inflammation, insulin resistance, and liver damage (Li, 2020).

SIRT2 is mostly found in the cytosol and is involved in regulating hepatic metabolism. Lack of SIRT2 results in increased glycogen accumulation, increased ALT and AST (indicators of hepatocyte damage), reduced hepatic fat accumulation (by downregulating transporters needed for fatty acid uptake, like GLUT2, FATP2 and FATP5), increased liver fibrosis and senescence (Park *et al.*, 2021). Phosphoenolpyruvate carboxykinase (PEPCK1) is the rate-limiting enzyme for gluconeogenesis, and SIRT2 is capable of deacetylating it, thus increasing its activity. It is proposed that SIRT2 senses NAD+ levels, and influences glucose production to supply the needs of the brain and other vital organs (Jian *et al.*, 2011). This evidence clarifies the role of SIRT2 in regulating lipogenesis and gluconeogenesis.

SIRT3 regulates fatty acid oxidation during fasting and ATP production, and it is upregulated during fasting in liver and brown adipose tissue (Hirshey *et al.*, 2010). Protein hyperacetylation caused by the absence of SIRT3 causes exacerbation of liver triglyceride accumulation. When comparing the liver of knockout mice (*Sirt3*-/-) with mice expressing normal SIRT3, it was observed that the enzyme long-chain acyl-coenzyme A dehydrogenase (LCAD) is hyperacetylated at lysine 42, causing reduced activity and impaired oxidation of long chain fatty acids, ultimately leading to their accumulation in plasma. Also, it was shown incomplete fatty acid oxidation using palmitate as substrate under increasing lipid concentrations, which is highly associated with hepatic steatosis and metabolic syndrome. SIRT3 is, therefore, involved in hepatocyte homeostasis, and its overexpression is associated with reduced triglyceride accumulation, increased mitochondrial oxygen consumption, and

increased fasting BHB production (Osborne *et al.,* 2022). The overall better functioning mitochondrial oxidative mechanism in animals displaying this enzyme is linked with higher ATP concentrations and ketone body production (Hirshey *et al.,* 2010). A possible mechanism through which SIRT3 regulates the activity of HMGCS2, the rate-limiting enzyme for β-hydroxybutyrate synthesis, is by deacetylating the lysine residues 310, 447 and 473, increasing its activity during fasting (Shimazu *et al.,* 2010).

Sirtuin 4 localized in the mitochondrial matrix, and its roles on health and disease are still largely uncomprehended. SIRT4 has demonstrated capacity of protecting against LPS-induced pathogenesis in bacterial infections, and to act as a viral restriction factor, protecting against both DNA and RNA viruses (Betsinger & Cristea, 2019). SIRT5 is a desuccinylase, and it regulates HMCGS2 both *in vivo* and *in vitro*. Loss of the activity of SIRT5 downregulates ketogenesis and causes the accumulation of medium and long-chain acylcarnitines *in vivo* (Rardin *et al.,* 2013). SIRT6 is expressed in the nucleus, and it is a histone deacetylase that maintains adequate chromatin regulation in situations such as telomere and genome stabilization, gene expression and DNA repair (Tennen & Chua, 2011). SIRT7 is also nuclear and plays a role in repairing DNA double strand breaks, being recruited by PARP1 to sites of DNA damage. SIRT7 targets acetylated lysine in the N-terminal tail of histone H3 (H3K18Ac), regulating the recruitment of the damage response factor 53BP1 to the break and affecting efficiency of non-homologous end joining (NHEJ) (Vazquez *et al.,* 2016). The decline of the expression and activity of SIRT7 disrupts metabolic homeostasis, accelerates aging, and heightens the risk of various age-related pathologies. These include cardiovascular and neurodegenerative diseases, pulmonary and renal disorders, inflammatory diseases, and cancer (Raza *et al.,* 2023).

2.3 Immune response

2.3.1 Modulation of the immune response by BHB and NAD

Divergent perspectives exist regarding the effects of ketones on immunological function. Hoeben et al. (1997) isolated neutrophils from high-producing cows and performed assays to assess oxidative burst function in samples with BHB added at concentrations ranging from 0.01 to 2.5 mmol/l, and found impairment of generation of hydrogen peroxide with BHB ≥ 1.0 mmol/l, suggesting that BHB induces an inhibitory effect on neutrophils' respiratory burst activity. Other researchers found no association between BHB levels and the count or function of neutrophils (Pascottini *et al.*, 2021).

Beta-hydroxybutyrate concentrations between 1.2 and 10 mmol/L are capable of increasing chemotaxis ability through activation of the HCA2 receptor in heifer's neutrophils (Carretta *et al.*, 2020). This same receptor, also known as GPR109A, is not required for blocking the NLRP3 inflammasome (Youm, 2015), which controls the activation of caspase-1 and the release of the pro-inflammatory cytokines IL-1β and IL-18 in macrophages, suggesting that BHB role in mediating inflammation may be related to multiple signaling pathways. The use of Selenium to mitigate the expression of the NLRP3 inflammasome in bovine mammary epithelial cells decreased ROS, ASC, caspase-1, Pro-IL-1β, and IL-1β, promoting the resolution of inflammation caused by S. aureus. This shared mechanism suggests that BHB may also possess the potential to resolve inflammation. Regarding chemotaxis, even though Suriyasathaporn et al. (1999) found that it was reduced in cows with naturally elevated BHB in blood (> 1.6 mmol/l), when these same neutrophils were incubated with BHB, acetoacetate or acetone (or a combination), only BHB did not impaired chemotaxis, suggesting a major role of the other ketone bodies. Neutrophils circulating in the blood and milk of dairy cows represent a heterogeneous population. A subset of these neutrophils express MHC II molecules, typically

associated with antigen-presenting cells—a role not traditionally attributed to neutrophils. This subset is considered microbicidal, exhibiting higher phagocytic capacity and greater production of reactive oxygen species compared to MHC II-negative neutrophils (Rambault *et al.*, 2023). In addition, endocytosis of antibody-antigen complexes mediated by FCγR is capable of converting neutrophils into neutrophil-derived cells with properties of dendritic cells, which are capable of antigen cross-presentation, activating T cells and representing an opportunity for immunotherapy by inducing CD8+ T cell anti-tumor immunity (Mysore *et al.*, 2021).

Low BHB concentrations *in vitro* (0.5-1mM) are capable of attenuating the NLRP3 inflammasome activation, suggesting that an imbalance between AcAc and BHB is linked to inflammatory conditions (Onizawa, 2022). On the other hand, research indicates that BHB impairs macrophage and neutrophil functions, increases NLRP3 inflammasome activity, and reduces immune cell adhesion, migration, and phagocytosis (Song *et al.*, 2022; Dong *et al.*, 2022). In contrast, BHB downregulates the inflammasome in other species (Youm *et al.*, 2015). T-cells exposed to 5mM D-BHB show elevated cytokine levels and a shift towards mitochondrial oxidative phosphorylation, enhancing T-cell activation and memory formation. Additionally, a very low carbohydrate diet *in vivo* boosts genes related to T-cell activation and effector function, increases Th2 cell subsets, and enhances T-cell immune capacity (Hirschberger *et al.*, 2021).

Carretta et al. (2023) incubated PMN from Holstein Heifers with HCAR-2 agonists (Niacin and BHB) and found that these ligands induced the generation of NETs (neutrophil extracellular trap, extracellular structures made out of chromatin and with the function of trapping and killing pathogens) and triggered the release of the enzyme MMP-9 (matrix metalloproteinase 9, an immune cell recruiter). Even though the aforementioned effects are beneficial against infections, an amplified activation could cause inflammatory diseases. None of the ligands induced apoptosis or affected cell surface expression of CD11b/CD47, which are

involved in endothelial adhesion and migration of neutrophils.

When human macrophages are stimulated with LPS in vitro, after 1h is possible to see a decrease in NAD+ levels. To compensate, they upregulate NAMPT, suggesting that the main pathway used by immune cells to maintain the intracellular NAD+ pool during a challenge is the salvage pathway, which has as substrate NAM synthetized by the hepatocytes. To express an anti-inflammatory response, they release pro-inflammatory cytokines and decrease SIRT3 expression, besides decreasing QPRT activity. Inhibition of QPRT leads to accumulation of succinate, which decreases mitochondrial respiration and increases ROS production (Billingham and Chandel, 2019).

In dairy cows supplemented with rumen-protected niacin (79 mg of rumen-protected NA/kg of body weight daily) during the transition period (21 days before calving until 3 weeks postpartum), hepatic transcript profiling indicates an exacerbation of the systemic inflammation-like condition (Ringseis *et al.,* 2019). Liver biopsies collected 7 days postpartum revealed down-regulated mRNA associated with cellular metabolic processes, lipid catabolism, and molecular biosynthetic processes. Conversely, up-regulated mRNA was related to leukocyte differentiation, hematopoiesis, immune system development, regulation and activation, and acute inflammatory response (*e.g.,* Haptoglobin increased 2-fold, serum amyloid P component). The supplementation of niacin may induce a stress response in the liver, upregulating genes such as ATF3 and E2F4, which are involved in inflammation regulation and the amplification of the acute phase response. This response involves increased production of positive acute phase proteins (*e.g.*, Haptoglobin, APCS), which contribute to restoring tissue homeostasis during early inflammation, injury, or infection, alongside reduced levels of negative acute phase proteins such as apolipoproteins, RBP, transferrin, and albumin, suggesting a prioritization of immune function over anabolic processes. No differences were observed in feed intake, milk yield, milk protein yields, or TAG levels in liver or serum.

However, a reduction in milk fat percentage and yield was observed.

Buhler et al. (2018) incubated PMN cells from second lactation cows (84 DIM) with 4 μg/mL of NA or NAM and found increased production of reactive oxygen species (ROS) and phagocytic capacity. Even though NA is expected to reduce ROS accumulation and resulting oxidative stress, it is possible that the initial increase (30 and 180 minutes after incubation) is part of initial signaling to induce anti-oxidative processes. This would be an explanation for the increased phagocytic capacity that is dependent on this ROS signaling mechanism.

Chapter 3

INVESTIGATING THE ROLE OF KETONES DURING EARLY LACTATION IN DAIRY COWS

Abstract

At the onset of lactation, dairy cows experience increased energy demands, which triggers heightened lipolysis and hepatic ketone synthesis (*e.g.*, beta-hydroxybutyrate; BHB). Currently, peripartal hyperketonemia (*i.e.*, blood BHB ≤ 1.2 mmol/L; sub-clinical ketosis) carries the stigma of being associated with impaired health, and reduced productivity, and fertility. Nonetheless, this dogma is contradicted by recent observations showing neutral or positive associations between these parameters. Furthermore, ketones may exert beneficial effects in animals experiencing diseases associated with chronic inflammation. To evaluate the effects of hyperketonemia during early postpartum, eight Holstein cows (19.62 ± 5.44 days postpartum; 3.75 ± 1.9 lactations) were allocated to i.v. infusions containing 2.5 M solutions of either Na-BHB (n = 4; **KET**) or NaCl (n = 4; **CON**). Cows (enrolled in two blocks; n = 4 per block) were randomly assigned to treatments in a longitudinal cohort study with 48-hour infusion periods. At 36 hours of each experimental period, cows received an i.v. lipopolysaccharide (**LPS**) bolus (30 ng/kg of BW of *E. coli* O55:B5). Cows were milked twice daily. Blood was sampled at h 0, 2, 5, 7, 10, 12, 24, 32, and 48 relative to the start of infusion, and at h 0, 1, 2, 3, 6, and 12, relative to the start of the LPS challenge. Data were analyzed under a mixed model with the fixed effects of block, treatment, and time, and their interactions. We did not detect any significant differences in DMI (P = 0.40) or milk yield (P = 0.15) between the groups, however, daily milk yield was lower in KET relative to CON after the LPS challenge (P = 0.01). No treatment differences were detected in plasma glucose (P = 0.38) either before or after the immune challenge. Plasma NEFA were different (P = 0.05) between the groups throughout most time points, with KET being higher than CON, overall. Plasma and

blood BHB were higher in KET relative to CON ($P< 0.01$) prior to the LPS challenge and tended to be different after ($P= 0.06$). We did not detect any significant differences in insulin ($P = 0.37$), TNF-α ($P = 0.51$), IL-1-β ($P = 0.91$) or IL-10 ($P = 0.31$) between the groups before or after the LPS challenge.

3.1 Introduction

During early lactation, dairy cows experience a negative energy balance as their energy expenditure surpasses their intake from feed. To meet the increased energy demands of the lactating mammary gland and maintain basal metabolic functions, cows undergo homeorhetic adaptations (Bauman & Curie, 1980). These adaptations include enhanced lipolysis in adipose tissue and insulin resistance (Bell & Bauman, 1997). β-hydroxybutyrate (BHB), a byproduct of fatty acid catabolism, acts as a cellular fuel for organs such as the brain, heart, and skeletal muscle (Puchalska & Crawford, 2017), thereby sparing glucose for the mammary gland. Hyperketonemia, characterized by a circulating BHB concentration above 1.2 mmol/L, has been associated with adverse health outcomes, such as metritis and displaced abomasum (Ospina *et al.,* 2010), infectious diseases, reduced productivity and fertility (Duffield *et al.,* 2009; Rutherford *et al.,* 2016), costing the dairy industry an average of $289 per case (McArt *et al.,* 2015).

Despite the negative associations drawn in previous literature, some studies have reported that animals can have circulating ketone blood levels greater than 1.2 mmol/l and still exhibit a normal health and production phenotype, in some cases characterized by increased milk yield and milk fat content (Rathbun *et al.,* 2017; Van Holder *et al.,* 2015). This discrepancy might be due to the confounding effects of concurrently elevated metabolites, such as circulating NEFA, which are known pro-inflammatory substances (Shi *et al.,* 2015). Ceramides, a type of sphingolipid that can be derived from circulating NEFA, is associated with the pathogenesis of insulin resistance in mammals, including Dairy cows (Holland and Summers, 2008; McFadden and Rico, 2019). Conversely, an increased availability of ketone bodies is considered beneficial for various conditions in mammals, such as inflammatory diseases (*e.g.*, gout; Goldberg *et al.,* 2017) and obesity-related cardiovascular disease (Dashti *et al.,* 2003).

Endotoxemia, defined as the presence of lipopolysaccharides (LPS) in the bloodstream, is often associated with ketosis in dairy cows. A study by Chirivi et al. (2023) found that 72.2% of cows with naturally occurring beta-hydroxybutyrate (BHB) levels above 1.2 mmol/L also exhibited endotoxemia and had higher levels of circulating bacterial DNA compared to clinically healthy animals. This immune system stimulation triggers the release of pro-inflammatory cytokines. Interestingly, ketones might reduce the transcription of pro-inflammatory markers such as pro-interleukin 1-beta (pro-IL-1β), interleukin 6 (IL-6), and tumor necrosis factor-alpha (TNF-α), while increasing the transcription of anti-inflammatory markers like interleukin 10 (IL-10; Swartz *et al.,* 2019). Additionally, ketone bodies can deactivate the Nod-like receptor protein 3 (NLRP3) inflammasome in macrophages and neutrophils during chronic inflammatory conditions such as gout (Goldberg *et al.,* 2017; Youm *et al.,* 2015). Regarding innate immune function, BHB concentrations above 1.0 mmol/L reduce phagocytosis and impair the generation of hydrogen peroxide, partially inhibiting the oxidative burst (Hoeben *et al.,* 1997). At concentrations above 1.2 mmol/L, BHB increases chemotaxis through the activation of the HCA2 receptor (Carretta *et al.,* 2020) and induces neutrophil extracellular trap (NET) formation (Carretta *et al.,* 2023). Furthermore, in vitro studies have shown that high BHB levels impair migration by causing directional deviation and altered cell morphology, including longer tails due to impaired contraction, and inhibit apoptosis, leading to impaired resolution of inflammation (Song *et al.,* 2022).

The objective of the current study is to determine the effects of hyperketonemia, in the absence of concurrent exacerbated lipolysis, on energy metabolism, health performance, milk production, and immune function prior to and during endotoxemia in early lactation dairy cows.

3.2 Materials and methods

3.2.1 Design and treatments

Experimental procedures were approved by the Institutional Animal Care and Use Committee (IACUC) at the University of Maryland. Eight early lactation, multiparous Holstein cows, averaging 19.62 ± 5.44 DIM (mean ± SD) from the Central Maryland Research and Education Center (CMREC), were used in a longitudinal randomized controlled trial. All animals received a common diet. Animals were moved into the tied stall barn 5 weeks before the beginning of the experiment to guarantee optimal adaptation to the housing and experimental feeding conditions. Cows (n=4 per treatment; total observations=8) were randomly allocated to 2 treatments over 2 experimental periods. The animals were divided into two groups: 1) Normo-ketonemic control (i.v. saline solution injection (NaCl); negative control; n = 4); 2) Hyperketokemic (i.v. 2.5M BHB-Na solution; n =4). In all cases, the infusion period lasted 48 h. The BHB-Na solution was prepared by mixing 315.2g of BHB salt per total volume of 1.0 L of distilled water to achieve 2.5M. The NaCl solution was prepared by mixing 146.1g of NaCl per total volume of 1.0 L of distilled water to achieve 2.5M. Both solutions were stirred, pH corrected to 7.4, filtered with a 20µm mesh paper filter, and autoclaved at 121°C for 1h. The solutions were stored in 20 L sterile Nalgene jugs at 8°C until the trial started. A lipopolysaccharide (LPS) challenge was administered 36 from the start of the induction period (*E. coli* O55:B5 (Sigma Aldrich, St. Louis, MO). LPS was dissolved in sterile 0.9% saline solution to a stock solution of 2 mg/mL 6 hours previous to be used, and stored at 4°C. All doses were prepared in single syringes at a concentration of 0.085 µg/kg of BW. This solution was infused in a single bolus dose through the jugular catheter. After the bolus infusion, 5mL of 0.9% saline solution was used to flush the catheter and 1mL of 1:1000 heparin was applied.

Jugular catheters were fitted within 24 h prior to treatment start. Blood samples were collected at -72, -48, -24, 0, 2, 5, 7, 10, 12, 18, 24, 32 and 48 h relative to initiation of induction treatment, and 0, 1, 2, 3, 6 and 12 h, relative to LPS challenge. The day before the infusions started, cows were contralateral-jugular catheterized. One catheter was used for the continuous infusion and the second was for blood sampling. Cows were restrained in a chute and haltered to be immobilized. The area was clipped and cleaned with 70% ethanol once. Wearing sterile gloves, the jugular vein was occluded, and the catheter was introduced, being secured with a 18G Luer-Lok™ needle adapter (Exel International Inc, Tysons Boulevard, VA). Flux was tested by drawing 1 mL of blood to confirm correct placement. The catheter was flushed with 5 mL of 0.9% saline solution (Dechra Veterinary, Overland Park, KS) and 2 mL of 1:10 heparinized saline solution (100 U/mL, Sagent, Schaumburg, IL) to avoid clotting. The catheter was capped with an injectable plug Luer-Lok™cap (Exel International Inc, Tysons Boulevard, VA). The external section of the catheter was fixed to the cow's skin with 3M elastic adhesive tape (3M, Saint Paul, MN) and glued with Tag Cement (W.J. Ruscoe Company, Akron, OH). Installed catheters were secured by wrapping them with flexible self-adhering tape around the neck. This procedure was repeated with the contralateral jugular vein. Cows were continuously infused using Abbott XL Plump pumps (Abbott Laboratories, Chicago, IL) with an adapted cassette connected with a stainless-steel tip barbed adaptor Bulkhead Fitting 6,5 mm (Fischer Scientific, Hampton, NH). An adaptor was designed to connect an EPO sterilized silicon tube line placed inside the Nalgene jug filled with the solutions. In the beginning blood samples were taken every 15 min during the first hour of infusion and KET cow's infusion rates were regulated targeting the BHB levels of 1.6 mmol/L. Control infusion rates were paired with KET average rates to maintain osmolar concentrations. After hour 2, blood BHB concentration was tested every hour. To collect blood, 3 mL were extracted and discarded to remove the heparin contained in the catheter. After sample collection, to avoid clotting the catheter line was flushed

with 5 mL of 0.9% saline solution (Dechra Veterinary, Overland Park, KS) and filled with 1 mL of 1:1000 heparinized 0.9% saline solution (solution 10 U/mL; Sagent, Schaumburg, IL).

To monitor blood BHB levels, blood was collected (1 mL) from the catheter at regular intervals, and BHB was measured using a ketone strip handheld meter (Precision Xtra, Abbott Laboratories, Abbott Park, IL)**.** Health status was evaluated hourly during the LPS challenge, by monitoring respiration rates and body temperatures, as well as by assessing general attitude, attention towards the surroundings, head position, ear position, facial expression, response to approach, back position, standing posture, lying position, panting, and shivering through a pain score (PS) following the methods described by Gleerup *et al.* (2015). To calculate pain scores, all individual scores were transformed to categorical binary data using a pain score of 3 as the cut-off point as highest expression of pain. Diets were based on corn silage and alfalfa-silage as the main forage components and corn grain as the major concentrate component.

3.2.2 Data and sample collection

Throughout the experiment, cows were housed in individual tie stalls. Cows were fed 115% of the expected intake at 0600 h daily. Feed intake and orts were recorded and adjusted daily. Water was available ad libitum in each stall and stalls were bedded with sawdust and cleaned twice per day. Cows were milked twice daily, and milk yield was recorded at each milking throughout the experiment. BW of cows was 667.91 ± 51.12 kg and milk yield (46.5 ± 4.56 kg/d) was not different between the groups at the beginning of the experiment ($P = 0.19$ and $P = 0.07$, respectively).

Response variables were averaged for 3 days of the covariate period (-72, -48 and -24h relative to the beginning of infusion) and for the 3 days of each treatment period. Diet

ingredients and orts were sampled daily during the covariate and treatment periods for each period. Milk was sampled at each milking during the covariate and treatment periods twice daily. One sample was taken from each cow at each milking. The aliquot was collected in a sealed tube with preservative (Bronopol Tablet; Lancaster DHIA, Manheim, PA) and stored at 4o C for milk component analysis. Blood was collected by coccygeal venipuncture into two evacuated tubes; one contained potassium EDTA as an anticoagulant and the other contained sodium heparin as an anticoagulant. Blood was stored on ice until centrifugation at 2,000 x g for 15 min at 4 °C (within 30 min of sample collection). Plasma samples were stored at -80 °C for further analyses. Body weights were measured on the last day of the covariate period. BCS was determined by two trained investigators on a 5-point scale (Wildman *et al.*, 1982) on the same day body weights were measured.

3.2.3 Sample analysis

Plasma samples were analyzed in duplicate using commercial kits to determine the plasma concentrations of glucose (Wako Chemicals, Richmond, VA; inter-assay CV: 3%, NEFA (NEFA-HR kit, Wako Chemicals USA, Richmond, VA; inter-assay CV: 3%), BHBA (Wako Chemicals, Richmond, VA; inter-assay CV: 2%) using enzymatic colorimetric procedures. Insulin (Mercodia, Uppsala, Sweden; inter-assay CV: 3%), C reactive protein (CRP; MyBioSource, San Diego, CA, inter-assay CV: 6%), tumor necrotic alpha (TNFα; MyBioSource, San Diego, CA, inter-assay CV: 7%), and IL-1β (Fisher Scientific, inter-assay CV: 3%), interleukin 10 (IL-10; Antibodies Online, Limerick, PA; inter-assay CV: 5%), were quantified using bovine-specific ELISA. Spectrophotometric measurements were conducted using a SpectraMax Plus 384 Microplate Reader (Molecular Devices, San Jose, CA).

Individual milk samples were analyzed for fat, true protein, lactose concentration, SCC and MUN by mid-infrared spectroscopy by the Lancaster DHIA lab (Manheim, PA). Samples of the TMR were taken daily and stored at -20°C. A compilation of samples was prepared and shipped to a commercial laboratory to be analyzed (Cumberland Valley Analytical Services, CVAS, Waynesboro, PA). Feed intake and milk production and composition were monitored for 3 consecutive days prior to treatment administration to establish baselines values, during the 48-h treatment period, and during 1 week following the end of treatment; the latter in order to assess carryover effects.

3.2.4 Cell isolation and flow cytometry

Heparin anti-coagulated jugular whole blood (20 mL per cow) was collected and processed within 2 hours. Blood from each cow was diluted 1:1 with 1×DPBS (pH 7.3) (ThermoFisher Scienticif, Gibco™) for neutrophil isolation. Diluted blood was carefully layered down the side of 50 mL Falcon tubes containing 10 mL of Ficoll-paque PLUS. Tubes were centrifuged for 30 min at 4 °C at 700 × *g* with break off. After centrifugation, the top layer was discarded (mononuclear cell fraction), and blood was transferred into new tubes. Deionized water was added (90% of RBC volume) for hypotonic lysis and mixed for 30 seconds to lyse the red blood cells. 10×PBS (10% of RBC volume) was added to each tube to restore isotonicity. Tubes were centrifuged at 500 × *g* for 10 min at 4°C, and the supernatant was discarded to isolate the white cell pellet. The pellet was resuspended with 1 mL of Hanks' Balanced Salt Solution (HBSS without Ca2+ and Mg2+, Thermo Scientific™), and 5mL of ACK lysis buffer was added to proceed with a hypertonic lysis, being pipetted up and down for 2 to 3 minutes. Immediately after, 20 mL of HBSS were added to restore isotonicity, then tubes were centrifuged at 900 × *g* for 10 min at 4°C, supernatant was discarded, and cells were resuspended with 1 mL HBSS.

Isolated neutrophils were adjusted to a concentration of 10^6 cells/ml and an aliquot of 100 µL transferred to polystyrene round-bottom 12 x 75 mm BD Falcon tubes (n. 352052) for cell staining and subsequent functionality assays. Neutrophils were blocked with Fc blocking buffer diluted in FACS buffer at 1:50 ratio for 20 minutes, centrifuged at 1500 rpm for 5 min at 4°C, then incubated with the primary monoclonal antibody CH138A, a bovine granulocyte marker (Monoclonal Antibody Center, WSU College of Veterinary Medicine, Pullman, WA), at 10 µg/ml for 1 hour at 4 °C. Cells were then washed 3 times by centrifugation at 1500 rpm for 5 minutes and resuspend them in 200 µl of ice cold FACS buffer (PBS, 1% BSA, 10% FBS), then incubated with the secondary Alexa Fluor-647 labeled antibody for 30 minutes, after which the functionality assays took place. Cytospin preparations allowed fixation of neutrophils into a glass slide, where they were stained with Diff-Quick (Dade Behring, Marburg, Germany). A differential count of 200 cells was performed using standard morphological criteria, indicating a yield of 86% neutrophils ± 4% (mean ± SEM) and 96 ± 1% live cells (mean ± SEM) by Trypan blue exclusion.

Neutrophil respiratory burst was assessed according to manufacturer's instruction (Abcam, ab236210). Isolated neutrophils were incubated with dihydrorhodamine 123 (DHR-123) assay reagent for 15 min at 37°C, followed by stimulation with phorbol myristate acetate (PMA, 200 nM) for 45 min at 37°C. DHR-123 is converted to the fluorescent compound rhodamine 123 by reactive species produced by activated neutrophils.

Phagocytosis was assessed using IgG Phagocytosis Assay kit (IgG FITC) (Cayman Chemical, Ann Arbor, MI) following the manufacturer's instructions. Freshly isolated neutrophils were incubated in RPMI medium with 1:100 dilution of rabbit IgG coated, FITC labeled latex beads for 2 h. Trypan blue solution was added to quench surface-bound IgG complex. Cells were then gently washed with assay buffer twice and FITC uptake was measured by flow cytometry.

Flow cytometry was performed on a FACSCanto II. FCS (flow cytometry standard format) 3.0 data file was used to export data that was analyzed using FlowJo (Windows version 10.10). Compensation controls were created for each fluorochrome. Forward and side scatter gates were used to discriminate doublets and debris (FSC-A, FSC-H, SSC-A × SSC-H). Matched unstained samples were used as controls. Only viable cells were included for the studies. Samples were fixed with 1% paraformaldehyde. The median fluorescent intensity (MFI) of neutrophils was measured at 530 nm, as well as the number of positive cells (staining for CH138A and Alexa Fluor-647 and producing ROS, detected by DHR-123 or FITC).

3.2.5 Statistical analysis

All data for plasma and milk variables were analyzed as repeated measures over time relative to infusion under the MIXED procedure of SAS (SAS Institute Inc, version 9.3). The statistical model included the random effect of cow nested within treatment and the fixed effects of time relative to infusions, treatment, treatment × time, and their interaction. The most appropriate covariance structure for the repeated-measures analysis was selected for each variable after evaluating 7 different covariance structures (variance components, first-order autoregressive, heterogeneous first-order autoregressive, and compound symmetry), and the structure with the smallest Akaike's information criterion coefficient was selected for analysis. Modeling of the covariance structure allowed the identification of patterns that best describe relationships between the repeated measures in the model. Initial milk yield and composition and baseline physiological measures were used as covariates. Preplanned orthogonal contrasts compared all treatments against the normo-ketonemic control. Residuals were assessed for normality and outliers (PROC UNIVARIATE). To improve residual distribution a transformation to the log scale was made on variables in need for it. Studentized residual values

considered outliers and removed from the analysis (typically 1 per response variable). The method of Kenward-Roger was used for calculation of denominator degrees of freedom. Main effects were declared significant at $P \leq 0.05$, and tendencies were declared at $P \leq 0.10$. Interactions were declared significant at $P \leq 0.10$, and tendencies were declared at $P \leq 0.15$. All data was expressed as least square means and standard error of the means, unless otherwise specified.

3.3 Results

3.3.1 Production responses

3.3.1.1 DMI and feed composition

Dry matter intake (DMI) was unaffected by induced hyperketonemia both before and after the LPS challenge. Before the LPS challenge, DMI was 52.06 ± 1.19 kg/day for the hyperketonemic group and 53.52 ± 1.19 kg/day for the Control group ($P = 0.40$) (Figure 3.1, A). The chemical composition of diet analysis is represented in Table 1.

Table 1. Chemical composition of diets.

Ingredient	Amount
Dry Matter (%)	49.25
Crude Protein (% DM)	15.7
ADF (% DM)	21.05
aNDF (% DM)	30.25
Lignin (% DM)	3.35
Crude Fat (% DM)	5.07

Ash (% DM)	9.07

Diet mix was composed of crude protein 15.7%, NDF 0.9%, crude fat, 5.07%, ash 9.07%, Calcium 1.0%, Phosphorus 0.32%, Magnesium 0.34%, Potassium 1.3%, Sodium 0.95%, Iron 598 ppm, Manganese 77 ppm, Zinc 83.5 ppm, Copper 27.5 ppm.

3.3.1.2 Milk Production

Milk production did not differ significantly between the hyperketonemic and control groups (46.61 ± 0.57 kg/day vs. 47.95 ± 0.57 kg/day, $P = 0.15$), except on the day following the LPS challenge, when hyperketonemic animals exhibited lower milk production ($P = 0.02$) (Figure 3.1, B).

Hyperketonemia did not significantly impact overall milk composition. Specifically, milk fat concentrations were 3.93 ± 0.23% in the hyperketonemic group and 3.87 ± 0.23% in the control group, with no significant differences observed ($P = 0.88$) (Figure 3.1, C). Milk protein concentrations were also similar between the groups, with the hyperketonemic group showing 3.03 ± 0.11% and the control group 3.04 ± 0.11% ($P = 0.96$) (Figure 3.1, D). Milk lactose concentrations did not differ significantly between the hyperketonemic (4.90 ± 0.01%) and control (4.88 ± 0.01%) groups ($P = 0.48$) (Figure 3.1, E). Additionally, milk urea nitrogen (MUN) concentrations were 9.99 ± 0.62% in the hyperketonemic group and 8.58 ± 0.62% in the control group, with no significant difference observed ($P = 0.13$) (Figure 3.1, F). There were no significant differences in somatic cell count (SCC) concentrations between the hyperketonemic (23.5568 ± 1.76 units) and control (19.0682 ± 1.76 units) groups overall ($P = 0.14$) (Figure 3.1, G). However, on the second day of infusion, the hyperketonemic group exhibited significantly higher SCC compared to controls ($P < 0.05$).

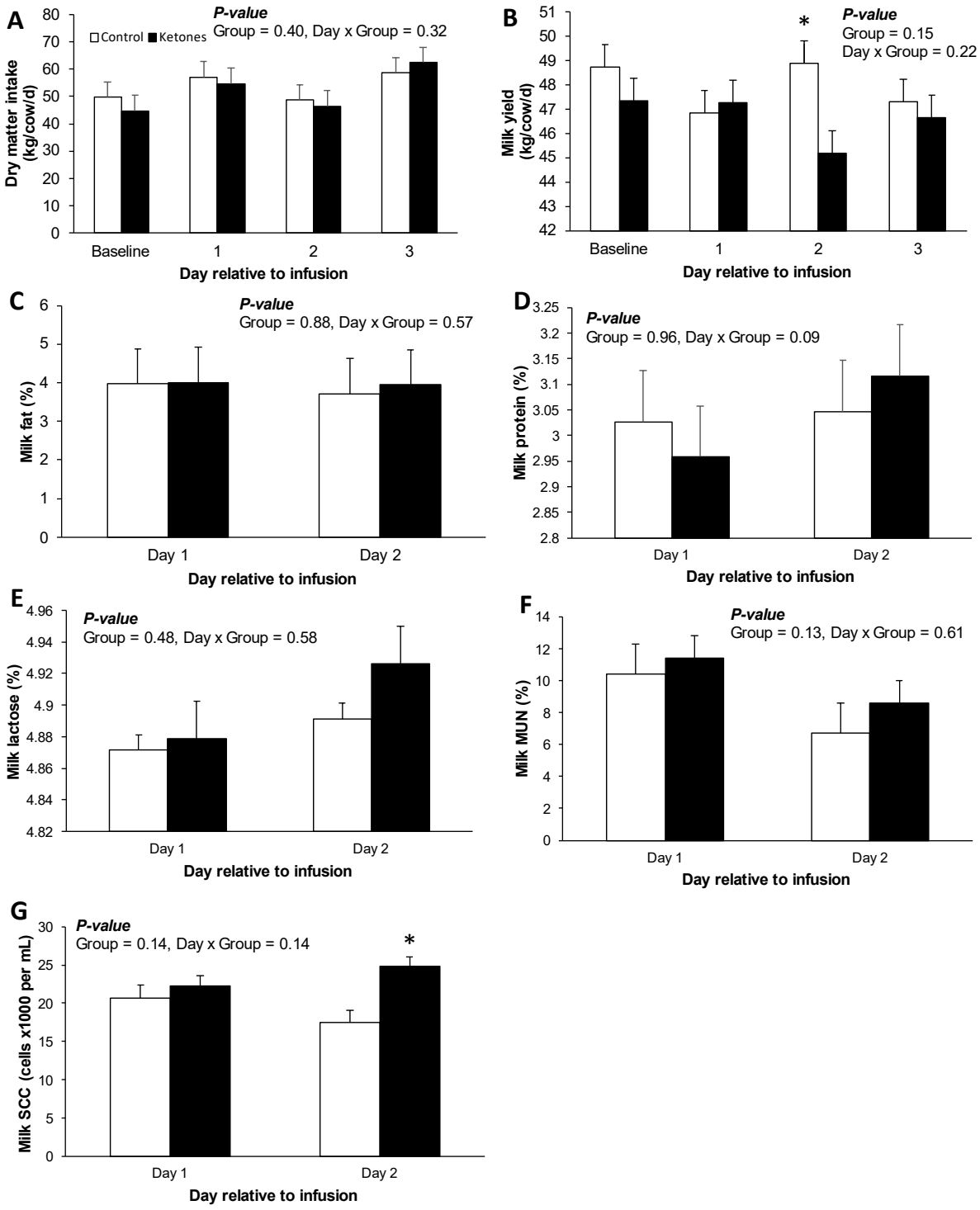

Figure 3.1. Production parameters of hyperketonemic and normoketonemic early lactation dairy cows. **(A)** Dry matter intake (kg/day) **(B)** Milk yield (kg/day) **(C)** Milk fat (%) **(D)** Milk protein (%) **(E)** Milk lactose (%) **(F)** Milk MUN (%) **(G)** Milk SCC (cells (x1000) per ml of milk). Data are represented as least squares means and their standard errors. *, $P < 0.05$; +, $P < 0.10$.

3.3.2 Plasma Metabolites and Hormones

3.3.2.1 Plasma BHB Concentrations

Whole blood BHB concentrations were measured using a ketone meter. We detected significant differences between the groups, with the hyperketonemic group averaging 1.66 ± 0.09 mmol/L, and the control group 0.5250 ± 0.18 mmol/L ($P < 0.001$) (Figure 3.2, B). Infusion rates are depicted on Figure 3.2, A.

Plasma BHB concentrations were significantly higher in the ketone group due to the BHB solution injection. Prior to the LPS challenge, the mean plasma BHB concentration for animals receiving the ketone infusion was 689.59 ± 51.79 µmol/L, compared to 407.22 ± 51.68 µmol/L for animals receiving the saline infusion, showing a significant difference ($P = 0.001$) (Figure 3.2, C). Following the induction of endotoxemia, BHB levels in the ketone group decreased at 2, 3, and 6 hours post-LPS challenge. Specifically, in the hyperketonemic animals, the mean BHB concentration post-LPS was 763.56 ± 116.47 µmol/L, whereas in the saline-infused animals, it was 425.52 ± 116.47 µmol/L ($P = 0.08$) (Figure 3.2, D).

3.3.2.2 Non-Esterified Fatty Acids (NEFA)

There were no significant differences in NEFA concentrations between the hyperketonemic and control groups prior to LPS stimulation (353.01 ± 12.67 mmol/L vs. 262.13 ± 12.64 mmol/L, $P = 0.17$) (Figure 3.2, E). However, after the LPS challenge, plasma NEFA levels were significantly higher in the hyperketonemic group compared to the control group (412.95 ± 12.79 mmol/L vs. 212.09 ± 12.76 mmol/L, $P = 0.01$) (Figure 3.2, F). NEFA concentrations tended to be higher in the hyperketonemic group 10 and 12 hours after the beginning of the infusion ($P = 0.07$). Additionally, NEFA levels were significantly different

between the groups at all time points after LPS stimulation ($P < 0.05$), except for the first hour post-stimulation, where no significant difference was observed ($P = 0.17$).

3.3.2.3 Plasma Glucose Concentrations

The intravenous infusion of BHB did not significantly affect plasma glucose concentrations in the hyperketonemic compared to the control group. Before the LPS challenge, plasma glucose concentration was 43.48 ± 1.87 mmol/L in the hyperketonemic group and 46.01 ± 1.87 mmol/L in the control group ($P = 0.37$) (Figure 3.2, G). Following the LPS challenge, plasma glucose concentration was 42.82 ± 1.70 mmol/L in the hyperketonemic group and 42.24 ± 1.70 mmol/L in the control group ($P = 0.81$) (Figure 3.2, H). The beginning of the infusion resulted in a decrease in plasma glucose concentrations in both groups. Endotoxemia induced by the LPS challenge led to an increase in glucose levels, peaking at 2 and 3 hours post-challenge.

3.3.2.4 Plasma Insulin Concentrations

Plasma insulin concentrations did not differ significantly between the groups before or after the LPS challenge (0.1357 ± 0.01 µg/L hyperketonemic versus 0.1537 ± 0.01 µg/L Control, $P = 0.37$) (Figure 3.2, I). The nadir for both groups was at 0 and 24 hours of infusion and the zenith at 10 hour of infusion and 6-hour post-LPS challenge. Insulin concentrations remained high following LPS challenge until 48 hours of infusion.

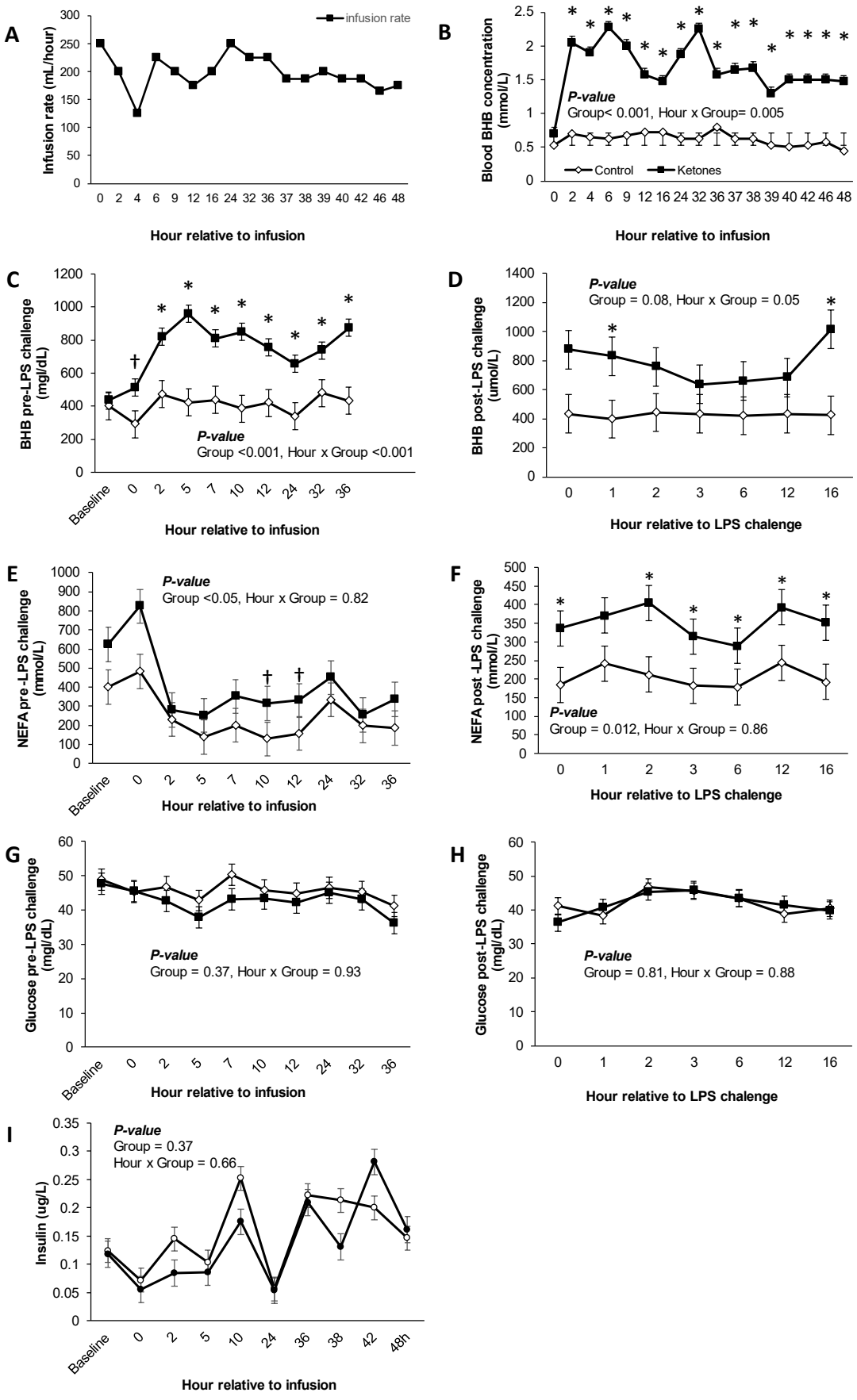

Figure 3.2. Plasma concentration of metabolic blood biomarkers in hyperketonemic and

normoketonemic early lactation dairy cows. **(A)** Infusion rates (ml/hour) **(B)** Blood BHB concentrations (mmol/L) **(C)** Plasma BHB pre-LPS (mmol/L) **(D)** Plasma BHB post-LPS (mmol/L) **(E)** NEFA pre-LPS (mmol/L) **(F)** NEFA post-LPS (mmol/L) **(G)** Glucose pre-LPS (mg/dL) **(H)** Glucose post-LPS (mg/dL) **(I)** Insulin (ug/L). Data are represented as least squares means and their standard errors. *, $P < 0.05$; +, $P < 0.10$.

3.3.3 Immune responses

3.3.3.1 Plasma TNF-α Concentrations

There were no discernible differences in plasma tumor necrosis factor-alpha (TNFα) levels concentrations between the hyperketonemic and control groups (138.64 ± 35.83 pg/ml vs. 173.38 ± 35.83 pg/ml, $P = 0.51$). Plasma TNF-α concentrations peaked following LPS injection, reaching the highest levels 3 hours post-LPS. Before the LPS challenge, levels of TNF-α were 52.8641 ± 78.38 pg/ml in the hyperketonemic group and 73.5580 ± 78.38 pg/ml in the Control group, rising to 485.01 ± 78.38 in the ketones group and 389.61 ± 78.38 pg/ml in the control group 3 hours post-LPS challenge (Figure 3.3, A).

3.3.3.2 Plasma IL-10 Concentrations

There were no discernible differences in IL-10 plasma levels between the hyperketonemic and control groups (38.1121 ± 1.65 pg/ml vs. 35.207 ±1.91 pg/ml, $P = 0.31$). The zenith for IL-10 plasma concentrations was 1 hour post-LPS challenge, with 41.5825 ± 2.66 pg/mL hyperketonemic versus 38.4056 ± 3.08 pg/mL Control, not significantly different between the groups ($P = 0.44$). There was a tendency ($P = 0.07$) for the Ketone group to have a higher IL-10 concentration at 0h of LPS, and an observation close to a tendency ($P = 0.14$) at 12 h of infusion (Figure 3.3, B).

3.3.3.3 Plasma CRP Concentrations

Plasma C-reactive protein (CRP) levels were similar between the hyperketonemic and control groups (68.5785 ± 3.39 ng/ml vs. 71.7243 ± 3.84 ng/ml, $P = 0.57$). At the moment of LPS challenge (36 hours of infusion), plasma CRP levels were 66.7377 ± 5.55 ng/ml in the hyperketonemic group and 69.3652 ± 5.58 ng/ml in the control group ($P = 0.42$). At 16 hours post LPS challenge, CRP levels raised to 75.0739 ± 4.83 ng/ml in the hyperketonemic group and 75.8057 ± 5.58 ng/ml in the control group ($P = 0.92$) (Figure 3.3, C).

3.3.3.2 Plasma IL-1β Concentrations

There were no discernible differences in IL-1β plasma levels between the hyperketonemic and control groups (0.6555 ± 0.04 pg/ml vs. 0.6512 ± 0.04 pg/ml, $P = 0.31$). The zenith for IL-1β plasma concentrations was 3 hours post-LPS challenge, with 0.7924 ± 0.08 pg/mL hyperketonemic versus 0.8162 ± 0.08 pg/mL Control, not significantly different between the groups ($P = 0.84$) (Figure 3.3, D).

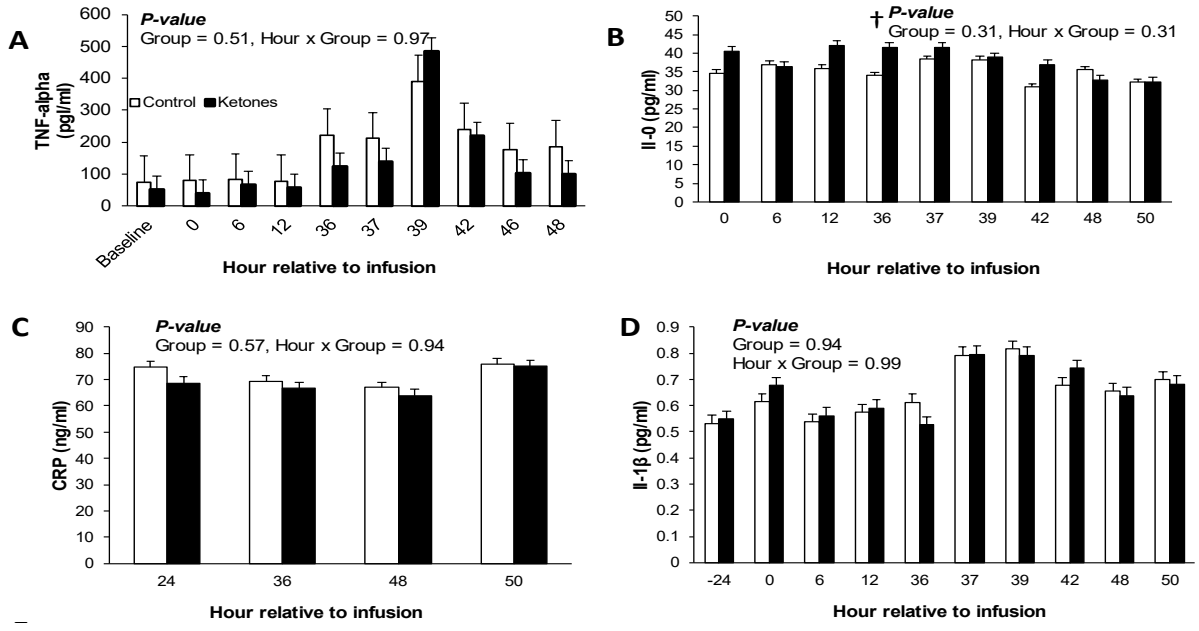

Figure 3.3. Plasma concentration of inflammatory biomarkers in hyperketonemic and normoketonemic early lactation dairy cows. **(A)** TNF-α (pg/ml) **(B)** IL-10 (pg/ml) **(C)** CRP (ng/ml) **(D)** IL-1β (pg/ml). Data are represented as least squares means and their standard errors. *, $P < 0.05$; +, $P < 0.10$.

3.3.3.4 Oxidative burst and Phagocytosis in neutrophils

Flow cytometry analysis was conducted to evaluate the oxidative burst of neutrophils using Alexa Fluor-647-labeled IgM antibodies and DHR-123 with PMA stimulation, and to assess phagocytic activity using the same antibody with FITC-labeled phagocytosed particles. The dot plot provides a detailed representation of the fluorescence intensity for both Alexa Fluor-647 and DHR-123 (Figure 3.5, A), or Alexa Fluor-647 and IgG-FITC (Figure 3.5, B). The x-axis represents the fluorescence intensity of Alexa Fluor-647 (anti-neutrophil antibody), while the y-axis represents the fluorescence intensity of IgG-FITC (phagocytosed particles) or DHR-123 (oxidative burst).

Neutrophils were identified based on their forward and side scatter properties, which distinguish them from other cell types in the sample. The gating strategy effectively isolated the neutrophil population for subsequent analysis and excluded cell debris (Figure 3.5, C). Single cells are represented in Figure 3.5, D.

Results are shown as overlaid histograms, representing the distribution of DHR-123 fluorescence in the neutrophil population, or IgG-FITC fluorescence (figures 3.5, E and 3.5, F). The red line represents the hyperketonemic group, while the blue line represents the control group. Unstained cells are represented by the grey line.

The median fluorescence intensity (MFI) of the neutrophil population summarizes the overall respiratory burst activity (40039 ± 6149 in the hyperketonemic group and 25012 ± 1883 in the control group, $P = 0.17$) (Figure 3.5, G) and phagocytic activity of neutrophils (4477 ±

1111 in the hyperketonemic group and 4418 ± 2085 in the control group, $P = 0.48$) (Figure 3.5, H). The percentage of DHR-123 positive neutrophils is shown in figure 3.5, I (83% in the hyperketonemic group and 80.97% in the control group, $P = 0.42$), and the percentage of IgG-FITC positive neutrophils is shown in figure 3.5, J (15.29% in the hyperketonemic group and 21.07% in the control group, $P = 0.34$).

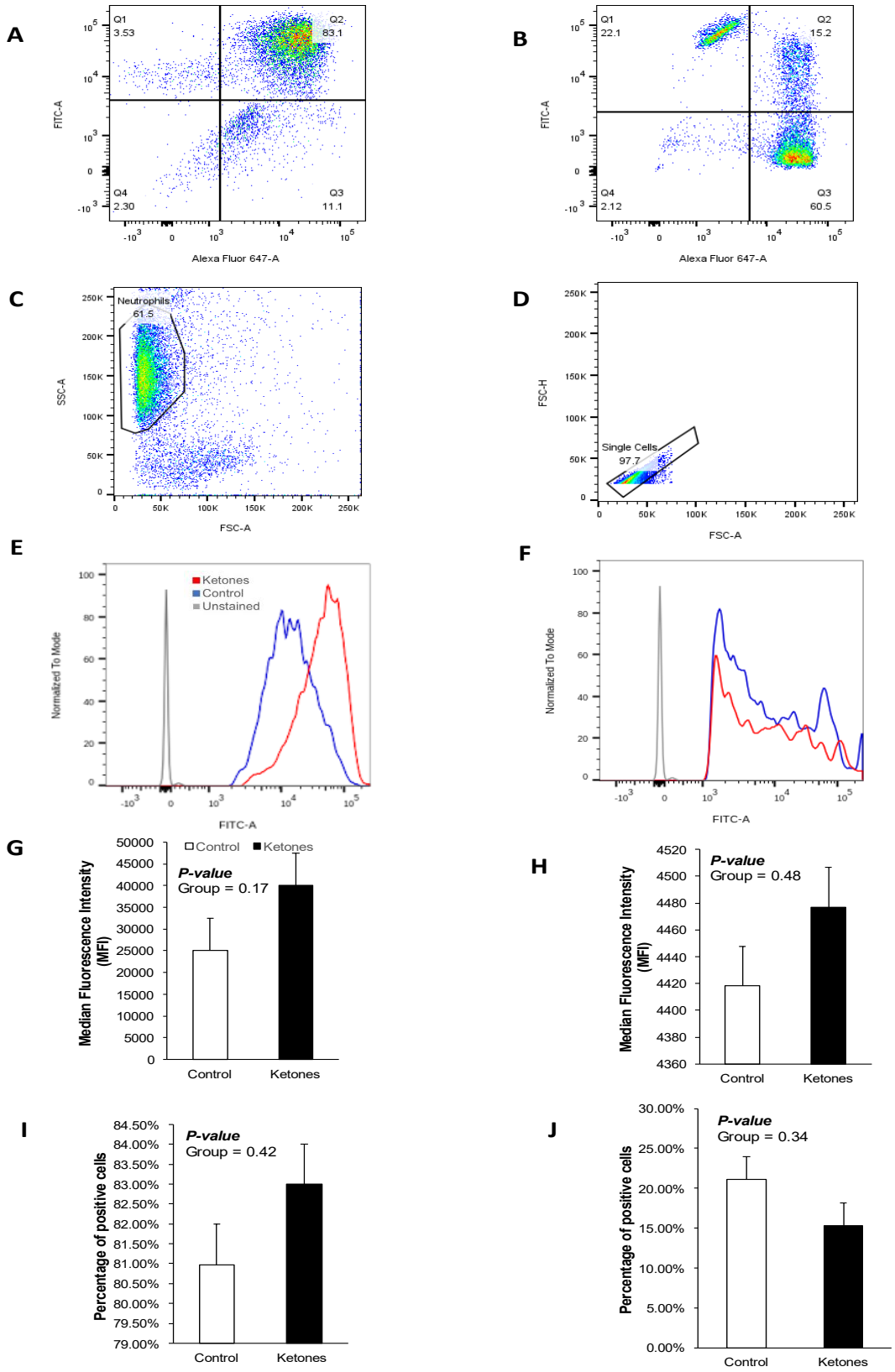

Figure 3.4. Neutrophil's phagocytic capacity and oxidative burst in hyperketonemic and normoketonemic early lactation dairy cows. **(A)** Representative flow cytometry dot plot showing neutrophils from normoketonemic and hyperketonemic dairy cows in the oxidative burst assay **(B)** Dot plot showing neutrophils in the phagocytosis assay **(C)** Neutrophil gating

based on forward and side scatter **(D)** Single cells **(E)** Histogram displaying DHR-123 levels under oxidative burst assay **(F)** Histogram displaying IgG-FITC levels in neutrophils under phagocytosis assay **(G)** Quantification of green fluorescence expression as median fluorescence intensity (MFI) in the oxidative burst assay **(H)** Quantification of green fluorescence expression as median fluorescence intensity (MFI) in the phagocytosis assay **(I)** Percentage of positive cells in the oxidative burst assay **(J)** Percentage of positive cells in the phagocytosis assay. Data are represented as least squares means. *, $P < 0.05$; +, $P < 0.10$ (n= 6).

3.3.4 Health Status

Rectal temperatures showed no significant differences between the hyperketonemic and control groups, with values of 102.95 ± 0.38°F and 102.68 ± 0.38°F, respectively ($P = 0.63$). Before the LPS challenge (at 0 hours), lower temperatures were recorded (101.17 ± 0.49°F for the hyperketonemic group vs. 101.15 ± 0.49°F for the control group, $P = 0.97$). Higher temperatures were observed 3 hours post-LPS challenge (104.07 ± 0.49°F for the hyperketonemic group vs. 103.55 ± 0.49°F for the control group, $P = 0.46$), with no significant differences between the groups (Figure 3.5, A).

Respiration rates (RR) also did not differ significantly between the hyperketonemic and control groups (31.57 ± 3.27 vs. 33.87 ± 3.30 respirations per minute, $P = 0.63$). Prior to the LPS challenge (0 hours), lower respiration rates were recorded (25.50 ± 4.51 for the hyperketonemic group vs. 30.50 ± 4.51 for the control group, $P = 0.44$). Six hours post-LPS challenge, higher respiration rates were noted (35.50 ± 4.51 vs. 36.00 ± 4.51 respirations per minute, $P = 0.93$), again with no significant differences between the groups (Figure 3.5, B).

Pain scores did not show significant differences between the hyperketonemic and control groups (2.58 ± 0.55 vs. 3.5 ± 0.55, $P = 0.28$). Prior to the LPS challenge, both groups had a pain score of 0 ($P = 1.0$). However, one hour post-LPS challenge, a significant difference was observed, with higher pain scores in the control group (4.00 ± 0.90) compared to the

hyperketonemic group (1.25 ± 0.90, $P = 0.04$). The highest pain scores were recorded 4 hours post-LPS challenge (5.75 ± 0.90 for the hyperketonemic group vs. 5.00 ± 0.90 for the control group, $P = 0.56$), with no significant differences between the groups (Figure 3.5, C).

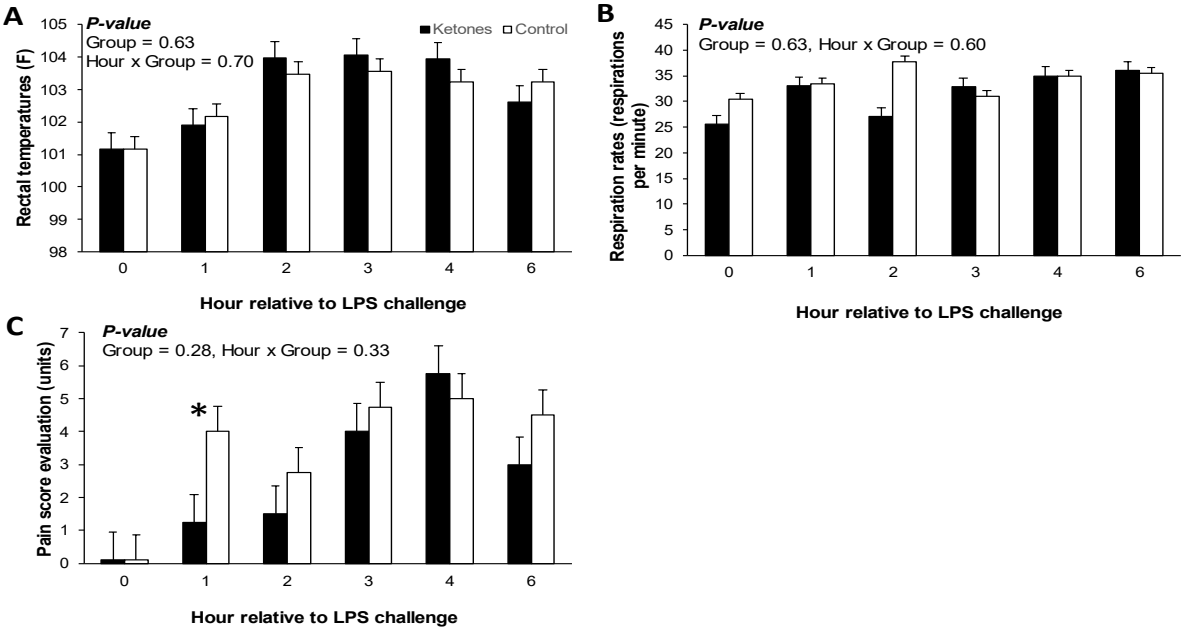

Figure 3.5. Health evaluation in hyperketonemic and normoketonemic early lactation dairy cows during the LPS challenge. **(A)** Rectal temperatures (°F) **(B)** Respiration rates (respirations per minute) **(C)** Pain score evaluation. Data are represented as least squares means and their standard errors. *, $P < 0.05$; +, $P < 0.10$.

3.4 Discussion

The initiation of ketone infusion led to a rapid and sustained hyperketonemia, with BHB levels reaching 1.66 mmol/L. Following the LPS challenge, a decrease in BHB levels was observed. This reduction can be partially attributed to the increased renal plasma flow induced by LPS stimulation, as reported by Schaller et al. (2007), which might enhance urinary elimination of BHB. Additionally, at a dose of 20 UI/kg, LPS impairs the vascular response to catecholamines and induces vasodilation, partly due to the increased production of free radicals, which is alleviated by the intravenous infusion of antioxidants such as N-

acetylcysteine. An alternative explanation for the observed decrease in BHB levels is the increased consumption of ketones by extrahepatic tissues. These tissues may utilize ketones as an energy source, conserving glucose for the activated immune system and lactating mammary gland.

Although previous studies, such as those by Zarrin et al. (2017), have noted a decrease in glucose levels during the early hours of ketone infusion, it is important to consider that glucose is a tightly regulated metabolite, particularly during parturition. The 48-hour infusion period, during which hyperketonemia was maintained at physiological levels, may not have been long enough to detect significant changes in glucose levels. The observed increase in circulating NEFA in the hyperketonemic group could be due to the appetite-suppressant effect of BHB, likely mediated by reduced secretion of ghrelin (Vestergaard *et al.*, 2021). However, no significant changes in dry matter intake (DMI) were detected, possibly due to the limited statistical power available to analyze this parameter.

Low plasma insulin concentration during early lactation is associated with higher milk yield in the long term. Cows with low plasma insulin (<0.49 ng/ml) group on the day of parturition, 3 and 10 after had higher NEFA concentrations, fat-corrected milk, and energy-corrected milk compared with cows with higher circulating insulin (>0.49 ng/ml) (Zinicola & Bicalho, 2019). Insulin follows a circadian pattern, with nadir concentrations occurring between midnight and 6 a.m. (before the first morning meal) and increasing throughout the day to peak after the afternoon meal. This pattern was observed in both groups. Additionally, early lactation cows experience a marked reduction in insulin production by the pancreas and increased insulin resistance in tissues such as adipose tissue and muscle (Bell & Bauman, 1997), aiming to spare glucose for the newly secreting mammary gland. This explains the lower insulin levels observed in our early lactation cows (0.1357 ± 0.01 µg/L hyperketonemic versus 0.1537 ± 0.01 µg/L Control) compared to heifers or mid-lactation animals.

Regarding cytokine production, no significant differences were observed between the groups. IL-10 is an anti-inflammatory cytokine that suppresses the production of pro-inflammatory cytokines and might offer protection against the effects of endotoxemia, the liver being the primary source of it after LPS stimulation. In mice, IL-10 levels peak concurrently with TNF-α at 1.5 hours post-LPS challenge, decrease at 6 hours, and rise again between 8 and 12 hours at a 5 mg/kg dose. Endogenous TNF-α down-regulates early and up-regulates late LPS-induced IL-10 synthesis *in vivo* (Barsig *et al.*, 1995). In individuals with obesity receiving an oral ketone supplement, plasma IL-10 levels averaged 0.315 pg/ml, compared to 0.300 pg/ml in the placebo group (Neudorf, 2020). These findings are consistent with our results in dairy cows. In whole blood stimulated in vitro with LPS, IL-10 secretion was 1.06 pg/ml in the absence of BHB. With increasing BHB concentrations, IL-10 secretion progressively increased, reaching 1.92 pg/ml with 2 mM BHB and 4.47 pg/ml with 5 mM BHB.

No significant differences were detected in TNF-α secretion between the groups, despite claims that BHB can reduce its secretion under chronic inflammatory conditions (Castro *et al.*, 2024). Without an LPS challenge, plasma circulating TNF-α is similar between individuals in physiological levels of ketosis (1.5 mmol/L, 1.99 pg/ml) and the ones receiving placebo (1.76 pg/ml; Neudorf, 2020), which supports our findings indicating lack of significant differences between hyperketonemic and normoketonemic animals.

Milk production was not different between the groups, except on the day following the LPS challenge. This observation suggests that hyperketonemia does not adversely affect milk production under normal conditions. However, during acute health challenges such as endotoxemia, the anti-inflammatory properties of BHB might modulate the immune response in a way that could impair productive outcomes. This indicates that while BHB is generally not detrimental, its effects under stress conditions requires further investigation to understand its impact on milk production during immune challenges.

A comparison of the mammary glands of ketotic and non-ketotic cows revealed that cows with subclinical (BHB >1.2 mM and <3 mM) or clinical ketosis (BHB >3 mM) exhibited lower milk yield and protein content in milk, decreased dry matter intake and glucose serum concentrations, and greater contents of H2O2 and malondialdehyde (MDA) in mammary gland tissue (Sun, 2021), which are associated with the effects of metabolic stress on free radical production and levels of lipid peroxidation product. Moreover, ketotic cows had lower activities of superoxide dismutase (SOD), glutathione peroxidase (GSH-Px), and catalase (CAT) in mammary gland tissue, those being related to the degree of oxidative stress. They also had greater expression of mRNA of pro-inflammatory cytokines (TNFA, IL6, and IL1B), greater activity of caspase-1 (result of upregulated NLRP3); higher IKKβ activity and ratio of p-IκBα to IκBα (not different between control and SCK; promoted the transcription of proinflammatory cytokines); greater protein abundance of Bax, caspase 3, and caspase 9 (apoptosis-related).

It is important to acknowledge that the cows utilized in this experiment were "naturally" ketotic around day 8 postpartum and exhibited higher serum fatty acid concentrations compared to the control group. This condition, combined with the negative energy balance typical of the postpartum period, serves as a more valuable indicator of inflammation, oxidative stress, and dysfunction than BHB concentration alone. Additionally, Acetoacetate levels were not measured, despite their typical increase in ketotic cows. Acetoacetate is a known trigger of NLRP3 inflammasome activation in bovine mononuclear cells (Onizawa, 2022) and could have significantly contributed to the pro-inflammatory results found. In addition to that, low concentrations of BHB (0,5-1mM) attenuate the activation of the NLRP3 inflammasome. The secretion of IL-1β caused by acetoacetate, and an imbalance of AcAc and BHB is more likely to be linked to inflammatory conditions.

Several experiments were conducted aiming to assess the isolated effect of BHB on

immune cells. These studies utilized macrophages or neutrophils from healthy cows and incubated them with BHB *in vitro*. One study found impaired migration, characterized by directional deviation and altered morphology (longer tails due to impaired contraction) (Song *et al.,* 2022). Another study reported inhibition of apoptosis, leading to impaired resolution of inflammation (Song *et al.,* 2022). Additionally, a different study observed increased NLRP3 inflammasome activity, along with decreased adhesion, migration, and phagocytosis (Dong *et al.,* 2022). This is in contradiction to what is reported in other species, it is known that BHB downregulated this inflammasome (Youm *et al.,* 2015)

In vitro, T-cells stimulated with 5mM of metabolically active D-BHB for 48 hours had higher transcriptional and protein levels of CD4+ T-cell cytokines interleukin IL-2, IL-4, IL-8, and IL-22. In addition, interferon γ (IFNγ), perforin 1, granzyme B, cytotoxic T lymphocyte-associated antigen 4 (CTLA4), and tumor necrosis factor alpha (TNFα) protein levels were higher in cells cultured with BHB. Regarding metabolism, T cells exposed to BHB show a shift towards mitochondrial oxidative phosphorylation (OXPHOS), with higher basal and maximal respiratory rates, mitochondrial ATP production, and spare respiratory capacity. BHB also increased ROS formation, which are required as a second messenger for T-cell activation, directing T cells to memory cells formation. *In vivo,* it was demonstrated that individuals on a very low carbohydrate diet (with BHB serum levels of 1-1.5mM) have higher transcription of genes related to T-cell activation, effector function, T-cell receptor signaling strength (Nur77), and memory cell development. In addition, the ketogenic diet caused an increase of the Th2 transcription factor GATA3, elevating the Th2 cell subset, and elevated IFNγ, GZMB, and CTLA4 cytokine levels in T1 CD8+ T cells and significantly increased cell lysis activity, leading to enhanced T-cell immune capacity (Hirschberger *et al.,* 2021).

3.5 Conclusion

In conclusion, our study highlights the metabolic and immunological responses of dairy cows to early postpartum hyperketonemia and endotoxemia. While no significant differences in DMI or overall milk yield were observed between the hyperketonemic and control groups, the hyperketonemic group exhibited a significant decrease in daily milk yield following the LPS challenge. Interestingly, plasma NEFA levels were higher in the group receiving the ketone infusion compared with the group receiving the saline infusion. Metabolic biomarkers related to carbohydrate metabolism (glucose and insulin) did not present significant differences in plasma. Key inflammatory markers (TNF-α, IL-1-β, IL-10) were higher in circulation following the LPS challenge, but did not differ between the groups. Neutrophil oxidative burst and phagocytic capacity was not affected by treatment. Future research should focus on managing hyperketonemia to optimize dairy cow health and productivity, potentially leading to more tailored practices for the dairy industry. Studies should also examine its long-term effects under stress and the impact of targeted nutritional or pharmacological interventions. These insights could enhance cow resilience and improve farm profitability. Our findings challenge the dogma of hyperketonemia's exclusively negative impacts, suggesting that its effects may be context-dependent.

Chapter 4

CHARACTERIZING THE NAD+ METABOLOME OF DAIRY COWS DURING THE TRANSITION FROM GESTATION TO LACTATION

Abstract

One of the most challenging and vulnerable moments in a dairy cow's life cycle is the transition from gestation to lactation. During this time, a myriad of homeorhetic adaptations occur to support the demands of the growing fetus and the lactating mother. Modern dairy cows experience dramatic demands of energy metabolism to support lactation, which is associated to metabolic stress, increased incidence of metabolic disorders (*e.g.*, ketosis) and heightened disease propensity (*e.g.*, infectious diseases; fatty liver). **N**icotinamide **A**denine **D**inucleotide (**NAD**) coenzymes are central catalysts of metabolism, and play vital roles in energy metabolism within eukaryotic cells. The NAD system is present in virtually all cellular processes, and a depletion in its intracellular levels has recently been associated with the progression of aging in mammals, as well as with a number of pathologies, ranging from heart failure to cancer. Although unknown in dairy cows, limited data in rodents indicates that a depletion of the hepatic NAD metabolome (NAD cofactors and associated metabolites) occurs at the onset of lactation. Because of its central role as a nutrient hub for several body tissues, as well as its central role in energy transduction, the liver constitutes a major target for the study of dairy cow energetics during function and dysfunction. Based on the above, we speculate that dairy cows transitioning from gestation to lactation will experience depletion of the hepatic, with concurrent elevations in the NAD pools of blood and milk postpartum. To evaluate our hypotheses, peripartal dairy cows (n=24) were enrolled in a longitudinal study spanning the transition period, and assessed the NAD metabolome in liver, blood, and milk, and its association with metabolic biomarkers and production performance.

Liver biopsies were performed 21 days before parturition and 7 days postpartum, and blood samples will be collected at d -30, -21, -14, -7, 0, 7, 14, and 21 relative to parturition. After calving, the animals exhibited decreased glucose and insulin levels, along with increased non-esterified fatty acids (NEFA) and beta-hydroxybutyrate (BHB) levels, not significantly different between the groups (P = 0.53). Despite these metabolic shifts, oxidative stress markers remained largely unchanged post-calving, with the Low-RFI group tending to have higher total antioxidant capacity 21 days after parturition (P = 0.08). HPLC coupled to mass spectrometry was utilized to comprehensively characterize the NAD metabolome in liver, blood, and milk. Our results indicate an increase in NAD metabolites and a decrease in NAD precursor concentrations in the liver post-calving. Nicotinamide Mononucleotide was significantly impacted by Residual Feed Intake (RFI), with lower levels in less efficient animals (P = 0.04) and a tendency to decrease post-calving (P = 0.06). The liver NAD metabolome remained stable after parturition and did not differ significantly between the groups (P = 0.83).

4.1 Introduction

Nicotinamide Adenine Dinucleotide (NAD) coenzymes are central catalysts of metabolism, and play vital roles in energy metabolism within eukaryotic cells. A depletion in their intracellular levels is associated with several pathologies in mammals, including heart failure, cancer, and the progression of aging (Navas & Carnero, 2021). The postpartum is a moment of metabolic stress in dairy cows (Drackley, 1999). Although most cows can withstand the metabolic challenges associated with the initiation of lactation, the fragility of the system is highlighted by the fact that roughly 1 in 2 cows typically succumb to some health complication during this period (Jordan & Fourdraine, 1993). Studies indicate that the NAD+ metabolites may influence energy metabolism in critical periods of life, such as the transition from gestation to lactation.

Although unknown in dairy cows, limited data in rodents indicates that a depletion of the hepatic NAD metabolome (NAD cofactors and associated metabolites) occurs at the onset of lactation (Ear *et al.,* 2019). NAD and NADP mammary tissue contents increase after parturition, a changed that is facilitated by increased activity of enzymes responsible for the biosynthesis of nicotinamide nucleotides (McLean, 1958). In agreement with the idea of a postpartum disruption of energy homeostasis, the supplementation of NR to mice and rats resulted in increased NAD+ metabolites in liver blood, and mammary, increased circulating levels of prolactin, enhanced mammary size, and increased biosynthesis of milk components (protein, fat, and lactose) and milk yield (Ear *et al.,* 2019).

NAD+ is present in most cellular metabolic reactions as a cofactor, including glycolysis, gluconeogenesis, fatty acids oxidation and synthesis, amino acids catabolism, and many others (Navas & Carnero, 2021). In addition, it serves as a substrate for repairing enzymes like sirtuins, that act as posttranslational modifiers, and PARPS, that act in DNA repair, both regulating cancer and aging progression (Pazzaglia & Pioli, 2020; Mangerich &

Burkle, 2012). Beta-hydroxybutyrate, through the receptor GPR109A, controls the acetylation and deacetylation of histones that control the expression of genes involved in antioxidative stress response and lipid metabolism (Shimazu *et al.,* 2013; Lee *et al.,* 2020). This epigenetic modification is mediated by sirtuins (1-7), which are NAD+ dependent. Moreover, the oxidation of ketone bodies to generate ATP reduces fewer molecules of NAD+ than the oxidation of carbohydrates (Elamin *et al.,* 2020), allowing the diversion of this metabolite to its function as a substrate instead of being used in redox reactions. Furthermore, NADH acts as an electron donor that creates the membrane potential that drives the synthesis of ATP. Together, this evidence reveals the amplitude of roles this molecule has (Navas & Carnero, 2021).

Residual feed intake (RFI) is a metric used to evaluate feed efficiency in dairy cows. It is calculated as the difference between an individual cow's actual feed (or energy) intake and the intake expected based on its energy needs according to its life stage (Connor, 2015). A positive RFI value indicates that the cow consumes more feed than expected, signaling inefficiency, while a negative RFI value suggests that the cow consumes less than expected, indicating greater efficiency (Connor *et al*., 2019). It is closely linked to energy metabolism, as it provides insights into how efficiently an animal converts feed into energy based on its physiological needs. Because of its central role as a nutrient hub for several body tissues, as well as its pivotal function in energy transduction, the liver constitutes a major target for the study of dairy cow energetics during normal function. In this context, potential disruptions in the hepatic NAD+ metabolome may determine the metabolic robustness of dairy cows entering lactation. In turn, the maintenance of NAD+ homeostasis may influence the ability of cows to sustain elevated milk production and their susceptibility to developing metabolic disorders (*i.e.*, dysfunction).

The ratio of NAD+/NADH is 800:1 in the cytosol and nucleus, while in the

mitochondria it is 7:1 (Anderson *et al.*, 2017). An increased NADPH concentration due to heightened catabolism is associated with endoplasmic reticulum (ER) stress, however, lower NADPH concentrations result in an elevated ratio of GSSH (oxidized glutathione) to GSH (reduced) (Gansemer *et al.*, 2020). Failure to adequately control oxidative stress can result in an increased incidence of health disorders. Free radicals generated due to the increase in oxygen requirements caused by the increased metabolism of early lactation can exceed the antioxidant capacity, leading to oxidative stress. To prevent that, cells have evolved antioxidant machinery. NADPH supplies hydride ions to form reduced glutathione from the oxidized form, as it is a cofactor to glutathione reductase, and catalyzes thioredoxin peroxidase, oxidizing reduced thioredoxin to form water and oxidized thioredoxin (Balaban *et al.*, 2005).

The objective of the current study is to determine if dairy cows transitioning from gestation to lactation will experience a depletion of the hepatic NAD metabolome, with concurrent elevations in the NAD pools of blood and milk postpartum. In addition, data collected about blood metabolic biomarkers (insulin, glucose, NEFA, BHB) and oxidative stress markers (protein carbonyl, 8OHdG, total antioxidant capacity) should elucidate how these variables correlate with the physiological adaptations to parturition and lactation.

4.2 Materials and methods

4.2.1 Design and treatments

Experimental procedures were approved by the Institutional Animal Care and Use Committee (IACUC) at the United States Department of Agriculture (USDA, Beltsville). Twenty-six multiparous Holstein cows from the Beltsville Agricultural Research Center (BARC, USDA ARS) were followed from late gestation (30 days before parturition) to early

lactation (21 days after calving). The animals were enrolled in a longitudinal observational study and received a common diet. Cows were categorized into two groups: 1) Low-RFI (residual feed intake), representing highly efficient animals (RFI coefficient <1; n =13); and 2) High-RFI, representing less efficient animals (RFI coefficient >1; n =13).

Liver biopsies were performed at d -21 and at d 7 postpartum, when near-maximal blood free fatty acids (FFA) and increased liver lipid accumulation are anticipated (Davis *et al.*, 2019). Liver biopsies were collected following Hughes (1962) procedure, being collected from the 10th intercostal space. Banamine® was administered intravenously at 1ml/100 lb of BW. The biopsy site was clipped and rinsed using water and a brush from the caudal to the ventral area. The incision area was prepared using alternating betadine surgical scrub 3 times, starting from the center of the surgical site to the outside of the prepared area in a circular manner. The area was then rinsed following the previous procedure using 70% ethanol. Lidocaine (12 mL; PHOENIX, St Josepth, MO) was subcutaneously administered at the center of the incision site. After 5 min, a 0.5-cm incision was made through the skin with a scalpel. Using a custom trocar, approximately 1g of liver tissue was collected and snap-frozen in liquid nitrogen immediately after collection. Biopsy sites were cleaned with hydrogen peroxide, stapled, and sprayed with antiseptic (Alushield®, Neogen). Staples were removed 10 days after the biopsies. All samples were stored at -80°C.

Blood samples were collected at d -30 (enrollment), and -21, -14, -7, 0, 7, 14, and 21, relative to parturition. Blood was collected by coccygeal venipuncture into two evacuated tubes containing potassium EDTA as an anticoagulant. Blood was stored on ice until centrifugation at 2,000 x g for 15 min at 4°C (within 30 min of sample collection). Plasma samples were stored at -80°C for further analyses. Whole blood was mixed with 5 μM Immucillin and stored at -80°C for metabolomic analysis. Blood and liver samples were analyzed for components of the NAD+ metabolome using a targeted, quantitative assay of the

NAD+ metabolome with the use of HPLC coupled to mass spectrometry (Trammell & Brenner, 2019).

Plasma samples were analyzed in duplicate using commercial kits to determine the plasma concentrations of glucose (Wako Chemicals, Richmond, VA; inter-assay CV: 3%, NEFA (NEFA-HR kit, Wako Chemicals USA, Richmond, VA; inter-assay CV: 4%), BHB (Wako Chemicals, Richmond, VA; inter-assay CV: 2%), and total antioxidant capacity (TAC; Cell Biolabs, San Diego, CA; inter-assay CV: 3%) using enzymatic colorimetric procedures. Insulin (Mercodia, Uppsala, Sweden; inter-assay CV: 4%), protein carbonyl (Cell Biolabs, San Diego, CA; inter-assay CV: 4%), and 8-OHdG (Cell Biolabs, San Diego, CA; inter-assay CV: 6%) were quantified using ELISA following manufacturer's instructions. Spectrophotometric measurements were conducted using a SpectraMax Plus 384 Microplate Reader (Molecular Devices, San Jose, CA).

4.2.2 Statistical analysis

All data for blood, liver and milk variables were analyzed as repeated measures over time relative to parturition under the MIXED procedure of SAS (SAS Institute Inc, version 9.3). The statistical model included the random effect of cow and the fixed effects of time relative to parturition. The most appropriate covariance structure for the repeated-measures analysis was selected for each variable after evaluating different covariance structures (variance components, first-order autoregressive, heterogeneous first-order autoregressive, compound symmetry, and unstructured), and the structure with the smallest Akaike's information criterion coefficient was selected for analysis. Modeling of the covariance structure allowed the identification of patterns that best describe relationships between the repeated measures in the model. Residuals were assessed for normality and outliers (PROC UNIVARIATE). To improve residual distribution a transformation to the log scale was made

on variables in need for it. Studentized residual values considered outliers and removed from the analysis. The method of Kenward-Roger was used for calculation of denominator degrees of freedom. Pearson correlation analysis were performed to analyze the association between metabolites and milk production. Main effects were declared significant at $P \leq 0.05$, and tendencies were declared at $P \leq 0.10$. Interactions were declared significant at $P \leq 0.10$, and tendencies were declared at $P \leq 0.15$. All data was expressed as least square means and standard error of the means, unless otherwise specified.

4.3 Results

4.3.1 Milk production

Table 2 presents the detailed composition of the milk samples analyzed in this study. The components measured include milk yield (lb/day), % of protein, % of fat, fat-corrected milk, energy-corrected milk, somatic cell score and somatic cell count. Samples were collected with a 7-day interval following parturition.

Table 2. Milk composition of selected cows from the USDA-Beltsville dairy herd.

Component	7 days postpartum	14 days postpartum	21 days postpartum
Milk yield	75.86	98.42	113.14
% Fat	3.98	5.3	4.94
# Fat	3	5.206	5.53
% Pro	3.52	3.02	2.82
# Pro	2.664	2.876	3.184
FCM	81.38	126.98	138.54
ECM	82.76	120.22	131.46
SCC	45.8	96.8	31
SCS	1.96	2.738	1.09

FCM: Fat-corrected milk, ECM: Energy-corrected milk, SCS: Somatic cell score, SCC: Somatic cell count (n= 5 per timepoint).

4.3.2 Plasma Metabolites and Hormones

4.3.2.1 Plasma Glucose Concentrations

The Low-RFI group did not show a significant difference in plasma glucose concentrations compared to the High-RFI group, with values of 57.34 ± 1.44 mg/dL for Low-RFI and 54.62 ± 1.82 mg/dL for High-RFI ($P = 0.25$). A significant effect of the day on plasma glucose concentration was detected ($P < 0.001$), with a decrease observed after parturition in both groups. On day 7 before parturition, plasma glucose concentrations were 60.43 ± 3.02 mg/dL for the Low-RFI group and 53.50 ± 3.74 mg/dL for the High-RFI group ($P = 0.15$). By day 14 after parturition, plasma glucose levels had decreased to 49.63 ± 2.64 mg/dL in the Low-RFI group and to 45.17 ± 3.70 mg/dL in the High-RFI group, with no significant difference between the treatments ($P = 0.32$) (Figure 4.1, A).

4.3.2.2 Plasma Insulin Concentrations

Plasma insulin concentrations did not show significant differences between the groups before or after parturition, with values of 0.2760 ± 0.024 µg/L for the Low-RFI group and 0.2913 ± 0.029 µg/L for the High-RFI group ($P = 0.69$). The highest insulin levels were observed before parturition. On day 14 prior to calving, plasma insulin concentrations were 0.5586 ± 0.06 µg/L for the Low-RFI group and 0.4632 ± 0.05 µg/L for the High-RFI group ($P = 0.69$). The lowest levels were recorded after parturition, with concentrations of 0.092 ± 0.04 µg/L for the Low-RFI group and 0.06 ± 0.06 µg/L for the High-RFI group on day 7 ($P = 0.72$). A significant effect of the day relative to parturition was detected ($P < 0.001$) (Figure 4.1, B).

4.3.2.3 Plasma BHB Concentrations

No significant differences in plasma BHB concentrations were detected between the groups, with concentrations of 561.47 ± 51.86 µmol/L for the Low-RFI group and 613.48 ± 65.57 µmol/L for the High-RFI group (P = 0.53). The highest levels of plasma BHB were observed after parturition. On day 14 after calving, plasma BHB concentrations were 838.17 ± 96.22 µmol/L for the Low-RFI group and 1302.69 ± 134.75 µmol/L for the High-RFI group, showing a significant difference between the groups, with the High-RFI group having higher ketone levels (P = 0.005). The lowest plasma BHB levels were recorded before parturition, with concentrations of 377.99 ± 109.87 µmol/L for the Low-RFI group and 364.15 ± 136.06 µmol/L for the High-RFI group on day -7 (P = 0.93). A significant effect of the day relative to parturition was detected (P < 0.001) (Figure 4.1, C).

4.3.2.4 Plasma NEFA Concentrations

On the day of calving, plasma NEFA concentrations were measured at 817.93 ± 85.93 mmol/L for the Low-RFI group and 738.93 ± 97.62 mmol/L for the High-RFI group, with no significant difference between the two (P = 0.81). A significant effect of the day relative to parturition was detected (P < 0.001). The lowest NEFA levels were recorded before parturition, with concentrations of 273.80 ± 83.28 mmol/L for the Low-RFI group and 273.83 ± 112.99 mmol/L for the High-RFI group on day -14 (P = 0.81). Following this period, NEFA concentrations increased in both groups, reaching a maximum 7 days after calving. The Low-RFI group had a concentration of 1146.42 ± 92.83 mmol/L, while the High-RFI group had 1126.26 ± 141.04 mmol/L, with no significant difference between them (P = 0.82). Post-calving, NEFA levels remained high in the Low-RFI group but decreased in the High-RFI

group, showing a trend towards significance on day 14 after parturition ($P = 0.10$) (Figure 4.1, D).

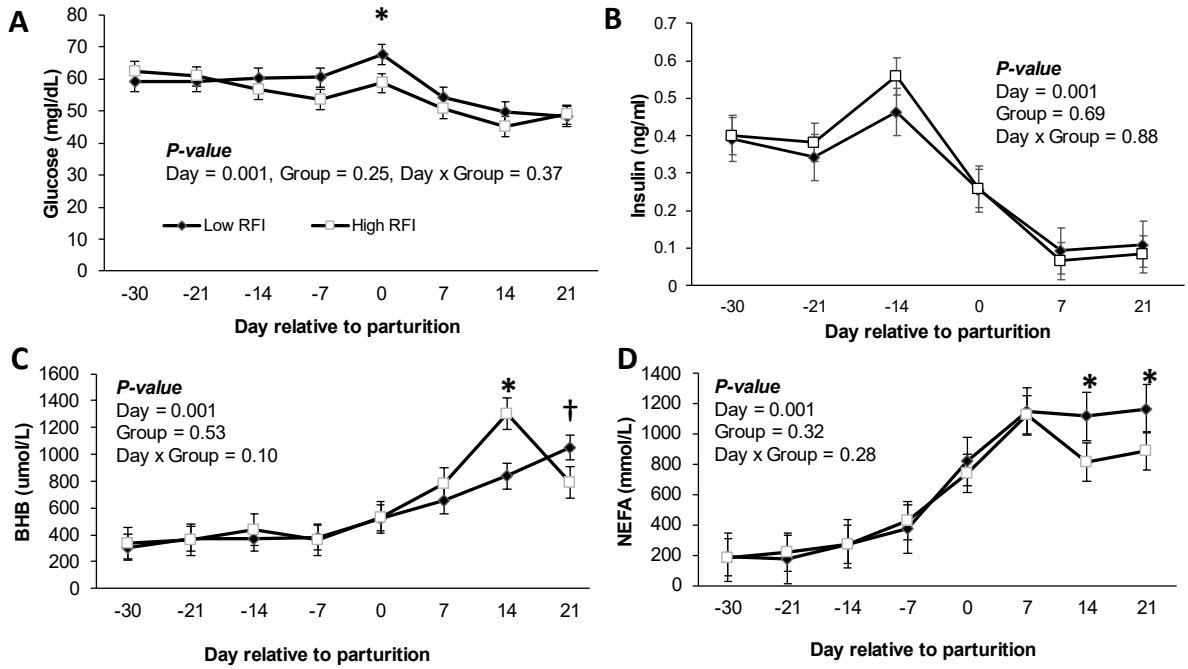

Figure 4.1. Plasma concentration of metabolic blood biomarkers in High and Low RFI dairy cows. **(A)** BHB (umol/L) **(B)** NEFA (mmol/L) **(C)** Glucose (mg/dL) **(D)** Insulin (ug/L). Data are represented as least squares means and their standard errors. *, $P < 0.05$; +, $P < 0.10$.

4.3.3 Plasma Oxidative Stress Markers

4.3.3.1 Plasma antioxidant concentrations

The Low-RFI group did not show a significant difference in plasma antioxidant concentrations compared to the High-RFI group, with values of 0.1197 ± 0.005 mM for Low-RFI and 0.1090 ± 0.006 mM for High-RFI ($P = 0.24$). However, 21 days after parturition, there was a tendency for the Low-RFI group to have higher antioxidant levels in circulation (0.1251 ± 0.008 mM for Low-RFI versus 0.1014 ± 0.010 mM for High-RFI, $P = 0.08$). A significant effect of day was detected in our analysis ($P = 0.001$), with a decrease in plasma antioxidant

concentration observed after parturition in both groups. On day -21 before parturition, plasma antioxidant concentrations were 0.1336 ± 0.008 mM for the Low-RFI group and 0.1320 ± 0.011 mM for the High-RFI group (P = 0.91). By day 7 after parturition, plasma antioxidant levels had decreased to 0.1005 ± 0.008 mM in the Low-RFI group and to 0.09348 ± 0.010 mM in the High-RFI group, with no significant difference between the treatments (P = 0.60) (Figure 4.2, A).

4.3.3.2 Plasma protein carbonyl

Plasma protein carbonyl concentrations did not show significant differences between the groups either before or after parturition, with values of 1.5823 ± 0.1368 nmol/mg for the Low-RFI group and 1.4185 ± 0.1137 nmol/mg for the High-RFI group (P = 0.36). However, a significant effect of the day relative to parturition was detected (P = 0.03). The lowest levels of plasma protein carbonyl concentrations were recorded before parturition, with 1.6382 ± 0.1320 nmol/mg for the Low-RFI group and 1.3507 ± 0.1647 nmol/mg for the High-RFI group on day -21 (P = 0.17). The highest levels were observed after parturition, with concentrations on day 7 after calving reaching 1.9095 ± 0.1426 nmol/mg for the Low-RFI group and 1.7807 ± 0.1647 nmol/mg for the High-RFI group (P = 0.55) (Figure 4.2, B).

4.3.3.3 Plasma 8-OHdG concentrations

Plasma 8-OHdG concentrations did not show significant differences between the groups either before or after parturition, with values of 10.5999 ± 0.12 ng/mL for the Low-RFI group and 10.8212 ± 0.16 ng/mL for the High-RFI group (P = 0.29). The lowest levels for the Low-RFI group were recorded before parturition, with 10.3152 ± 0.24 ng/mL on day -21 (P = 0.17). The High-RFI group's 8-OHdG levels remained stable throughout most time points, with

10.8692 ± 0.32 ng/mL recorded on day -21. For the Low-RFI group, the highest levels were observed after parturition, reaching 10.7556 ± 0.21 ng/mL on day 7 after calving. In contrast, the High-RFI group's levels remained similar to prepartum values (10.7819 ± 0.25 ng/mL, *P* = 0.93) (Figure 4.2, C).

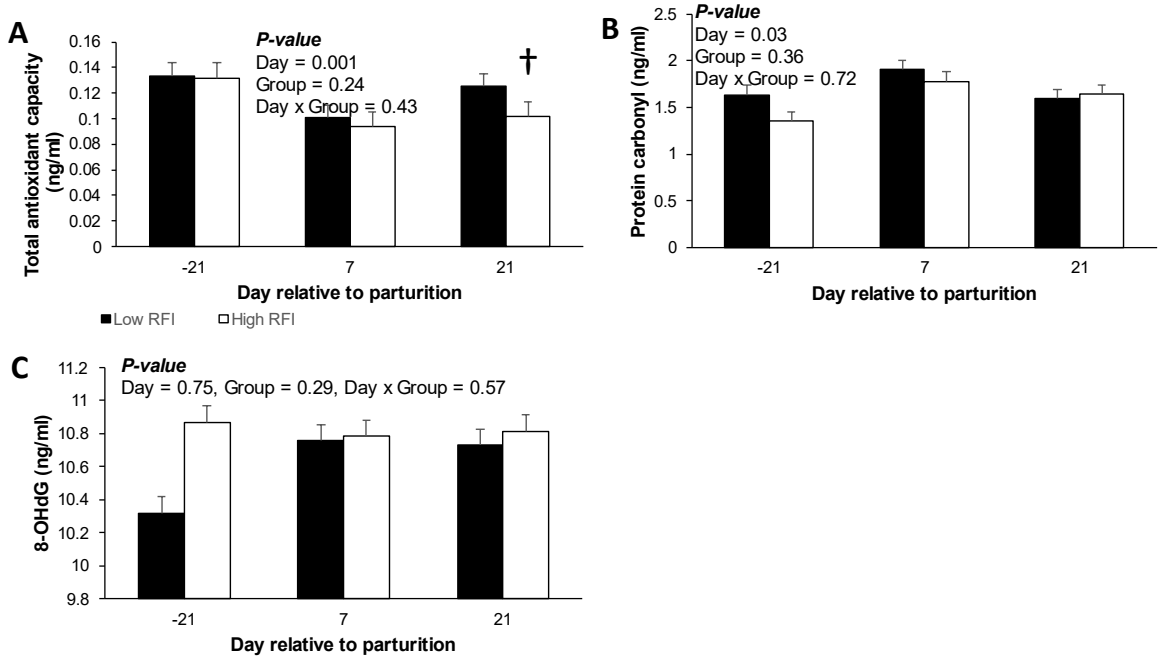

Figure 4.2. Plasma concentration of oxidative stress markers in High and Low RFI dairy cows. **(A)** Total antioxidant capacity (mM) **(B)** Protein carbonyl (nmol/mg) **(C)** 8ohDG (ng/mL). Data are represented as least squares means and their standard errors. *, $P < 0.05$; +, $P < 0.10$.

4.3.3 The NAD metabolome

4.3.3.1 Liver NAD metabolome

The Low-RFI group did not show a significant difference in liver NAD concentrations compared to the High-RFI group, with values of 2109128 ± 118004 for Low-RFI and 2187262 ± 148566 for High-RFI (*P* = 0.68). The effect of day was close to a tendency (*P* = 0.14), with a slight increase in liver NAD concentration observed after parturition in both groups. (Figure 4.3, A). Similarly, NADH levels in liver did not differ between the groups (90284 ± 20897 for

the Low-RFI group and 102473 ± 27295 for the High-RFI; P = 0.72). However, after parturition, there was a decrease in NADH concentration in both groups (68336 ± 32368 for Low-RFI and 85152 ± 41102 for High-RFI (P = 0.75) (Figure 4.3, B).

Liver NADP concentration was not significantly different between the groups before or after parturition (204770 ± 29368 for Low-RFI and 226651 ± 36159 for High-RFI; P = 0.64) A significant effect of day was detected in our analysis (P < 0.001), with an increase in liver NADP concentration observed after parturition in both groups. On day -21 before parturition, liver NADP concentrations were 127795 ± 33103 for the Low-RFI group and 143920 ± 41316 for the High-RFI group (P = 0.76). By day 7 after parturition, liver NADP levels had decreased to 281745 ± 33103 in the Low-RFI group and to 309382 ± 41316 in the High-RFI group, with no significant difference between the treatments (P = 0.60) (Figure 4.3, C). Liver NADPH followed a similar pattern, increasing after parturition in both groups (P = 0.59) (Figure 4.3, D).

Liver Nicotinic Acid did not differ between the groups and tended to not change after calving (495621 ± 24062 for the Low-RFI group and 519842 ± 29858 for the High-RFI; P = 0.53) (Figure 4.3, E). Niacinamide in liver also did not differ between the groups (1109179 ± 57178 for Low-RFI versus 1130092 ± 71291 for High-RFI, P = 0.82) and was unaffected by day (P = 0.97) (Figure 4.3, F).

Nicotinamide Riboside in liver did not differ between the groups, but a tendency was detected for a depletion after calving (P = 0.08). The levels went from 1431914 ± 120698 for the Low-RFI group and 1222045 ± 151509 for the High-RFI 21 days before parturition (P = 0.28) to 1102893 ± 120698 for the Low-RFI group and 1183656 ± 151509 for the High-RFI 7 days after parturition (P = 0.67) (Figure 4.3, G).

The liver concentration of Nicotinamide Ribotide was significantly different between the groups before parturition (P = 0.04), and this was the only component of the NAD

metabolome that was significantly affected by the RFI. The mean concentration was 168552 ± 19310 for Low-RFI and 111054 ± 22106 for High-RFI ($P = 0.06$). There was also a tendency for an effect of day relative to parturition ($P = 0.06$).

The sum of all previously described metabolites, also known as the NAD metabolome, did not differ between the groups (5200429 ± 261222 for Low-RFI versus 5291054 ± 326215 for High-RFI, $P = 0.83$) and did not seem to be influenced by day relative to parturition ($P = 0.41$) (Figure 4.3, I).

The hepatic ratio of NAD+/NADH did not differ between the groups before or after parturition (35.05 ± 5.54 for Low-RFI versus 23.30 ± 7.32 for High-RFI, $P = 0.22$), and an influence of day was not detected (P = 0.25) (Figure 4.3, J).

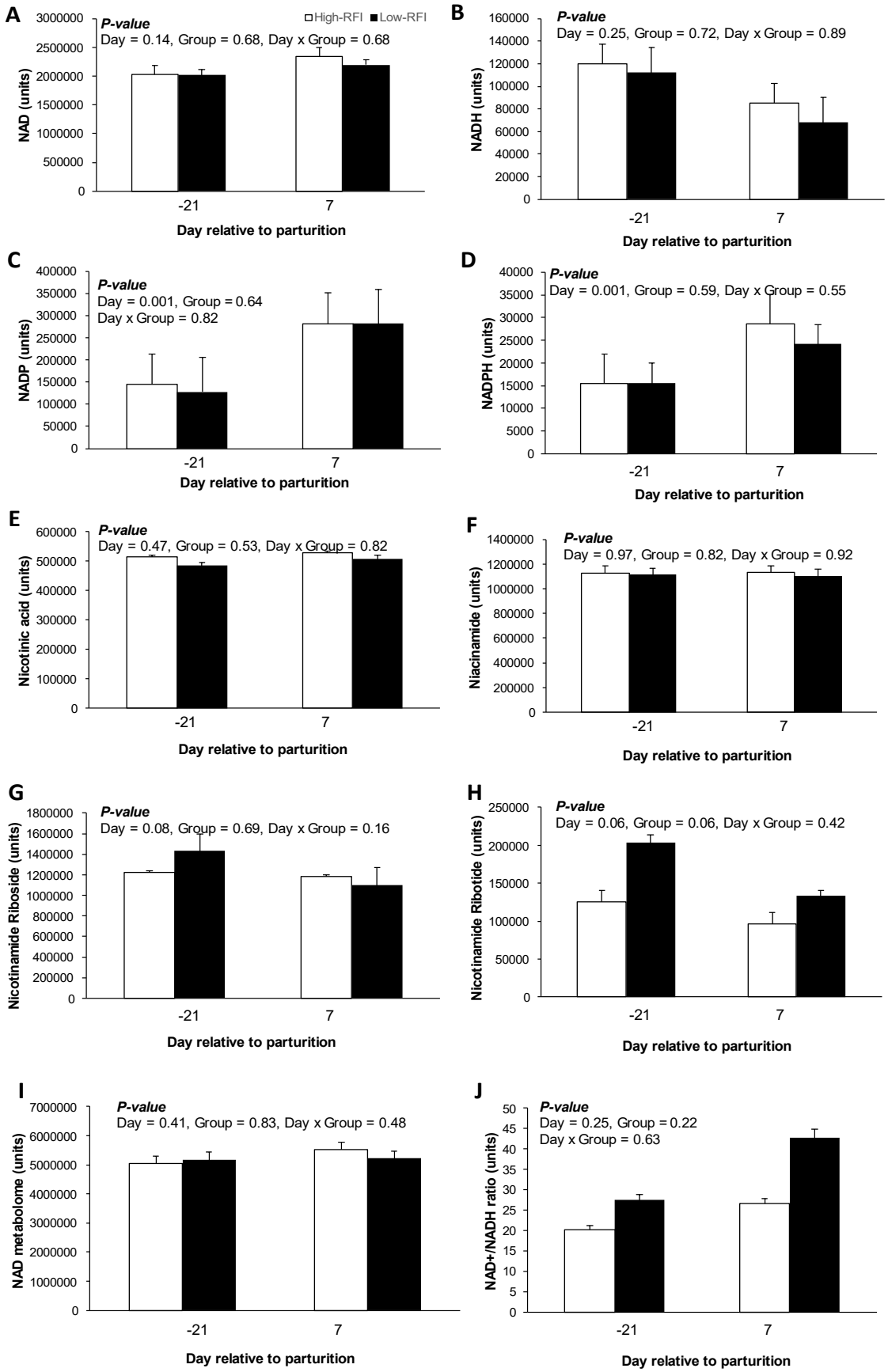

Figure 4.3. Liver NAD metabolome in High and Low RFI dairy cows. **(A)** NAD **(B)** NADH **(C)** NADP **(D)** NADPH **(E)** Nicotinic acid **(F)** Niacinamide **(G)** Nicotinamide Riboside **(H)**

Nicotinamide Ribotide **(I)** NAD metabolome **(J)** NAD+/NADH ratio. Data are represented as least squares means and their standard errors. *, $P < 0.05$; +, $P < 0.10$. The NAD metabolome comprises the sum of NAD+, NADH, NADP+, NADPH, Nicotinic acid, Nicotinamide, Nicotinamide Riboside and Nicotinamide Ribotide.

4.4 Discussion

Our results demonstrate a decrease in plasma glucose following parturition, with the lowest point 14 days after calving. This reduction is likely due to the increased glucose utilization for lactose synthesis in the mammary gland. To meet the demands of early lactation, dairy cows upregulate hepatic gluconeogenesis and decrease the expression of insulin-regulated glucose transporter GLUT4 on peripheral tissues, resulting in reduced glucose uptake (Bell & Bauman, 1997). This transient state of insulin resistance mechanistically induces lipolysis, which increases the availability of NEFA for β-oxidation in peripheral tissues and re-esterification in the mammary gland. This allows circulating glucose to be conserved for lactose synthesis, which plays a key role in osmotically regulating milk secretion. (Rico *et al.,* 2015; Drackley *et al.,* 2005; Drackley and Andersen, 2006). The highest lipolysis levels, demonstrated by circulating NEFA, were observed concurrently with the lower glucose points. In the Low-RFI group, there was an almost three-fold increase 7 days after parturition compared with 7 days before. In the High-RFI, this increase was of a two-fold magnitude.

Reactive oxygen species (ROS) represent a group of extremely reactive molecules generated by various cell types in reaction to environmental chemical and physical stimuli. These ROS are crucial for host defense as they eliminate invading pathogens. Neutrophils express high levels of NADPH oxidase (NOX) and are a great source of oxidants in mammals. Nonetheless, an excessive build-up of ROS or inadequate clearance can lead to oxidative harm, causing DNA damage, lipid peroxidation, and protein denaturation (Rahman *et al.,* 2006). Stable oxidation biomarkers, like protein side-chain oxidation products, can be quantified using

carbonyl assays. These assays allow for the precise measurement of protein oxidation, providing insights into oxidative stress levels. Additionally, the efficiency of oxidative defense mechanisms can be evaluated through total antioxidant capacity (TAC) measurements. TAC offers an antioxidant index based on circulating concentrations of antioxidants, reflecting the overall antioxidant status of the organism. One of the critical markers of oxidative DNA damage is 8-hydroxydeoxyguanosine (8-OHdG), a nucleoside product formed during the DNA repair process. Elevated levels of 8-OHdG are indicative of oxidative stress-induced DNA damage, making it a valuable biomarker for assessing the impact of oxidative stress on genetic material. In dairy cows, oxidative stress was not detected surrounding parturition either in dystocic or eutocic calvings (Yokus *et al.*, 2007).

In breeding goats, protein carbonyl (PC) levels reached its highest point on parturition day, while 8-OHdG and total antioxidant capacity (TAC) progressively increased until 21 days into lactation (Yu SiJia *et al.*, 2017). These findings differ from our results, in which the biomarkers for protein and DNA oxidation slightly increase after parturition, and TAC significantly decreases.

Treating cells with 1mM of pyruvate increases cytosolic NAD+/NADH ratio, but decreases the mitochondrial ratio. This represents the consumption of NADH by lactate dehydrogenase in the cytosol, as the ratio of pyruvate/lactate is also an indicative of the redox state, and the oxidation of pyruvate and TCA cycle, yielding NADH in mitochondria. However, incubation with glucose (20mM) decreases NAD+ both in mitochondria and cytosol, as glycolysis happens in the cytosol forming NADH and TCA in the mitochondria also favoring NADH formation. Alternative fuels, like β-hydroxybutyrate (1mM) decreased the ratio of NAD+/NADH in mitochondria, while Acetoacetic acid (1mM) increased. This is in accordance with the NAD-dependent equilibrium of β-hydroxybutyrate dehydrogenase, in which BHB drives the production of NADH and acetoacetate drives the consumption of it (Hu *et al.*, 2021).

Pires and Grummer (2007) administered Nicotinic Acid in the form of ruminal bolus in three concentrations (6, 30, or 60 mg of NA/kg of body weight) to cows under feed restriction for 48h. The lower dose was able to decrease NEFA concentrations to less than half the initial value (546 μEq/L) for 1h, but the two higher doses were able to decrease the concentrations of NEFA to less than before the feed restriction started (reaching less than 100 μEq/L) for 3 hours. However, a rebound effect was observed, and it was proportional to the dose administered. NEFA concentrations reached over 1800 μEq/L and steadily decreased after 9 hours of administration. In a second trial, they infused Nicotinic Acid hourly for 8 hours and found similar results. In 2 to 3 hours after the final infusion, the rebound effect happened elevating NEFA. Insulin concentrations also increased during the rebound, which could be explained due to the transient insulin resistance state induced by NEFA. In small ruminants, it was demonstrated that oral administration of NA was capable of elevating glucose and insulin, but it also caused a delayed decrease of glucose after an insulin shot, which is associated with impaired glucose tolerance (Thornton & Schultz, 1980).

Our findings indicate that the concentration of NADP in the liver nearly doubled after parturition, accompanied by an increase in NADPH levels. In mice, elevated cytoplasmic NADPH has hepatoprotective effects and is associated with an extended health span (Jamerson & Bradshaw, 2024). This rise in NADP(H) post-parturition might be linked to enhanced protection against oxidative stress. Nicotinamide nucleotide transhydrogenase (NNT) plays a key role in facilitating hydride transfer between NAD(H) and NADP(+), utilizing the energy from the mitochondrial proton gradient to produce high levels of NADPH (Pedersen *et al.*, 2008). This NADPH is essential for biosynthesis and free radical detoxification. NNT is vital in mitigating mitochondrial redox imbalance, and NNT knockout mice (Nnt-/-) exhibit worsened fatty liver disease when subjected to a high-fat diet (Navarro *et al.*, 2017). Although

we did not measure NNT activity or levels in our study, we hypothesize that NNT may contribute to the observed increase in NADPH levels in the liver.

Overall, our results indicate an increase in NAD metabolites and a decrease in NAD precursor concentrations in the liver. Notably, Nicotinamide Ribotide, also known as Nicotinamide Mononucleotide (NMN), was the only variable significantly impacted by Residual Feed Intake (RFI), showing lower levels in less efficient animals. NMN also showed a tendency to decrease post-calving. Similarly, Nicotinamide Riboside (NR), another NAD(P) precursor, decreased after parturition. The overall metabolome, representing the combined profile of all analyzed metabolites, remained unchanged relative to calving, likely due to a balance between variables increasing and decreasing. These findings contrast with observations in mice, where there is a depletion of the NAD metabolome and metabolites to increase their concentration in the circulation and mammary gland (Ear *et al.*, 2019).

4.5 Conclusion

In conclusion, our study reveals a dynamic alteration in the energy metabolism associated with parturition and metabolic efficiency. The observed increase in hepatic NAD metabolites coupled with a decrease in NAD precursors suggests a heightened demand for NAD biosynthesis during this period. The overall metabolome remained stable, indicating a compensatory balance between different metabolic pathways. Our findings also show a decrease in glucose and insulin levels post-parturition, while non-esterified fatty acids (NEFA) and beta-hydroxybutyrate (BHB) levels increased, reflecting a metabolic shift towards fat mobilization and ketogenesis. Interestingly, oxidative stress markers appeared unchanged by calving, although the Low-RFI group tended to exhibit higher total antioxidant capacity, suggesting potential differences in oxidative stress management related to metabolic efficiency.

Further research is needed to elucidate the underlying mechanisms and potential implications for liver function and overall health in dairy cows. Understanding these processes could lead to more precise nutritional and management strategies, optimizing dairy cow health and productivity. Exploring the relationship between metabolic efficiency and oxidative stress management may also provide insights into improving resilience and reducing disease incidence in dairy herds. Such findings could inform the development of industry practices that enhance dairy cow well-being and boost farm profitability.

5. References

Abeyta, M., Horst, E., Goetz, B., Rodriguez-Jimenez, S., Mayorga, E., Al-Qaisi, M., & Baumgard, L. (2023). Effects of hindgut acidosis on inflammation, metabolism, and productivity in lactating dairy cows fed a high-fiber diet. *Journal of Dairy Science*, *106*(4), 2879-2889. https://doi.org/10.3168/jds.2022-22680

Aditya, S., Humer, E., Pourazad, P., Khiaosa-Ard, R., & Zebeli, Q. (2018). Metabolic and stress responses in dairy cows fed a concentrate-rich diet and submitted to intramammary lipopolysaccharide challenge. *Animal*, *12*(4), 741-749.

Anderson, K. A., Madsen, A. S., Olsen, C. A., & Hirschey, M. D. (2017). Metabolic control by sirtuins and other enzymes that sense NAD+, NADH, or their ratio. *Biochimica et Biophysica Acta (BBA) - Bioenergetics*, *1858*(12), 991-998. https://doi.org/10.1016/j.bbabio.2017.09.005

Andreasen, A. S., Krabbe, K. S., Krogh-Madsen, R., Taudorf, S., Pedersen, B. K., & Møller, K. (2008). Human endotoxemia as a model of systemic inflammation. *Current medicinal chemistry*, *15*(17), 1697–1705. https://doi.org/10.2174/092986708784872393

Aschenbach, J. R., Kristensen, N. B., Donkin, S. S., Hammon, H. M., & Penner, G. B. (2010). Gluconeogenesis in dairy cows: the secret of making sweet milk from sour dough. *IUBMB life*, *62*(12), 869–877. https://doi.org/10.1002/iub.400

Balaban, R. S., Nemoto, S., & Finkel, T. (2005). Mitochondria, Oxidants, and Aging. *Cell*, *120*(4), 483-495. https://doi.org/10.1016/j.cell.2005.02.001

Barsig, J., Küsters, S., Vogt, K., Volk, D., Tiegs, G., & Wendel, A. (1995). Lipopolysaccharide-induced interleukin-10 in mice: Role of endogenous tumor necrosis factor-α. *European Journal of Immunology*, *25*(10), 2888-2893. https://doi.org/10.1002/eji.1830251027

Bauman, D. E., & Bruce Currie, W. (1980). Partitioning of Nutrients During Pregnancy and Lactation: A Review of Mechanisms Involving Homeostasis and Homeorhesis. *Journal of Dairy Science*, *63*(9), 1514-1529. https://doi.org/10.3168/jds.S0022-0302(80)83111-0

Bell, A. W., R. Slepetis, and R. A. Ehrhardt. 1995. Growth and accretion of energy and protein in the gravid uterus during late pregnancy in Holstein cows. J. Dairy Sci. 78:1954.

Bell, A. W., & Bauman, D. E. (1997). Adaptations of glucose metabolism during pregnancy and lactation. *Journal of mammary gland biology and neoplasia*, *2*(3), 265–278. https://doi.org/10.1023/a:1026336505343

Bergman E. N. (1990). Energy contributions of volatile fatty acids from the gastrointestinal tract in various species. *Physiological reviews*, *70*(2), 567–590. https://doi.org/10.1152/physrev.1990.70.2.567

Bertoldo, M. J., Listijono, D. R., Ho, W. J., Riepsamen, A. H., Goss, D. M., Richani, D., Jin,

X. L., Mahbub, S., Campbell, J. M., Habibalahi, A., Loh, W. N., Youngson, N. A., Maniam, J., Wong, A. S., Selesniemi, K., Bustamante, S., Li, C., Zhao, Y., Marinova, M. B., . . . Wu, L. E. (2020). NAD+ Repletion Rescues Female Fertility during Reproductive Aging. *Cell Reports*, *30*(6), 1670-1681.e7. https://doi.org/10.1016/j.celrep.2020.01.058

Betsinger, C. N., & Cristea, I. M. (2019). Mitochondrial function, metabolic regulation, and human disease viewed through the prism of sirtuin 4 (SIRT4) functions. *Journal of proteome research*, *18*(5), 1929-1938.

Bikman, B. T., & Summers, S. A. (2011). Ceramides as modulators of cellular and whole-body metabolism. *The Journal of clinical investigation*, *121*(11), 4222–4230. https://doi.org/10.1172/JCI57144

Billingham, L. K., & Chandel, N. S. (2019). NAD-biosynthetic pathways regulate innate immunity. *Nature Immunology*, *20*(4), 380-382. https://doi.org/10.1038/s41590-019-0353-x

Bogado Pascottini, O., & LeBlanc, S. (2020). Metabolic markers for purulent vaginal discharge and subclinical endometritis in dairy cows. *Theriogenology*, *155*, 43-48. https://doi.org/10.1016/j.theriogenology.2020.06.005

Bogado Pascottini, O., Bruinjé, T. C., Couto Serrenho, R., Mion, B., & LeBlanc, S. J. (2021). Association of metabolic markers with neutrophil function in healthy postpartum dairy cows. *Veterinary immunology and immunopathology*, *232*, 110182. https://doi.org/10.1016/j.vetimm.2020.110182

Boon, J., Hoy, A. J., Stark, R., Brown, R. D., Meex, R. C., Henstridge, D. C., Schenk, S., Meikle, P. J., Horowitz, J. F., Kingwell, B. A., Bruce, C. R., & Watt, M. J. (2013). Ceramides contained in LDL are elevated in type 2 diabetes and promote inflammation and skeletal muscle insulin resistance. *Diabetes*, *62*(2), 401–410. https://doi.org/10.2337/db12-0686

Bradford, B. J., Yuan, K., Farney, J. K., Mamedova, L. K., & Carpenter, A. J. (2015). Invited review: Inflammation during the transition to lactation: New adventures with an old flame. *Journal of dairy science*, *98*(10), 6631–6650. https://doi.org/10.3168/jds.2015-9683

Brown, G. C., Camacho, M., & Williams-Gray, C. H. (2023). The Endotoxin Hypothesis of Parkinson's Disease. *Movement disorders : official journal of the Movement Disorder Society*, *38*(7), 1143–1155. https://doi.org/10.1002/mds.29432

Bühler, S., Frahm, J., Liermann, W., Tienken, R., Kersten, S., Meyer, U., Huber, K., & Dänicke, S. (2018). Effects of energy supply and nicotinic acid supplementation on phagocytosis and ROS production of blood immune cells of periparturient primi- and pluriparous dairy cows. Research in Veterinary Science, 116, 62-71. https://doi.org/10.1016/j.rvsc.2017.09.012

Cai, H., Zeng, H., Chen, Y., Chen, X., Rong, S., Luo, H., ... & Liu, S. Ketolysis Activates T Cell Function Against Staphylococcus Aureus Infection by Fueling the Tricarboxylic Acid (TCA) Cycle and Affecting Histone Acetylation.Cell reports, 2024.

Campbell, J., Murphy, M., Christensen, R., & Overton, T. (1994). Kinetics of Niacin

Supplements in Lactating Dairy Cows. Journal of Dairy Science, 77(2), 566-575. https://doi.org/10.3168/jds.S0022-0302(94)76985-X

Carretta, M. D., Barría, Y., Borquez, K., Urra, B., Rivera, A., Alarcón, P., Hidalgo, M. A., & Burgos, R. A. (2020). β-hydroxybutyrate and hydroxycarboxylic acid receptor 2 agonists activate the AKT, ERK and AMPK pathways, which are involved in bovine neutrophil chemotaxis. *Scientific Reports*, *10*(1), 1-13. https://doi.org/10.1038/s41598-020-69500-2

Carretta, M. D., Creutzburg, P., Borquez, K., Quiroga, J., Alarcón, P., Rivera, A., & Burgos, R. A. (2023). Hydroxycarboxylic acid receptor 2 (HCA2) agonists induce NET formation and MMP-9 release from bovine polymorphonuclear leukocytes. *Developmental & Comparative Immunology*, *139*, 104562. https://doi.org/10.1016/j.dci.2022.104562

Castro, R., Kalecký, K., Huang, N. K., Petersen, K., Singh, V., Ross, A. C., ... & Bottiglieri, T. (2024). A very-low carbohydrate content in a high-fat diet modifies the plasma metabolome and impacts systemic inflammation and experimental atherosclerosis. The Journal of Nutritional Biochemistry, 126, 109562.

Cetina Biefer, H. R., Vasudevan, A., & Elkhal, A. (2017). Aspects of Tryptophan and Nicotinamide Adenine Dinucleotide in Immunity: A New Twist in an Old Tale. *International Journal of Tryptophan Research : IJTR*, *10*. https://doi.org/10.1177/1178646917713491

Chirivi, M., Rendon, C. J., Myers, M. N., Prom, C. M., Roy, S., Sen, A., Lock, A. L., & Contreras, G. A. (2022). Lipopolysaccharide induces lipolysis and insulin resistance in adipose tissue from dairy cows. *Journal of dairy science*, *105*(1), 842–855. https://doi.org/10.3168/jds.2021-20855

Creely, S. J., McTernan, P. G., Kusminski, C. M., Fisher, M., Da Silva, N. F., Khanolkar, M., Evans, M., Harte, A. L., & Kumar, S. (2007). Lipopolysaccharide activates an innate immune system response in human adipose tissue in obesity and type 2 diabetes. *American Journal of Physiology-Endocrinology and Metabolism*. https://doi.org/E-00302-2006

Connor, E. (2015). Invited review: Improving feed efficiency in dairy production: Challenges and possibilities. Animal, 9(3), 395-408. https://doi.org/10.1017/S1751731114002997

Connor, E., Hutchison, J., Van Tassell, C., & Cole, J. (2019). Defining the optimal period length and stage of growth or lactation to estimate residual feed intake in dairy cows. Journal of Dairy Science, 102(7), 6131-6143. https://doi.org/10.3168/jds.2018-15407

Dong, Z., Sun, X., Tang, Y., Luo, S., Jia, H., Xu, Q., Jiang, Q., Loor, J. J., Xu, W., & Xu, C. (2022). β-hydroxybutyrate impairs monocyte function *via* the ROS-NLR family pyrin domain-containing three inflammasome (NLRP3) pathway in ketotic cows. *Frontiers in veterinary science*, *9*, 925900. https://doi.org/10.3389/fvets.2022.925900

Drackley, J., LaCount, D., Elliott, J., Klusmeyer, T., Overton, T., Clark, J., & Blum, S. (1998). Supplemental Fat and Nicotinic Acid for Holstein Cows During an Entire Lactation. Journal of Dairy Science, 81(1), 201-214. https://doi.org/10.3168/jds.S0022-0302(98)75567-5

Drackley, J. K. (1999). Biology of Dairy Cows During the Transition Period: The Final Frontier? *Journal of Dairy Science*, *82*(11), 2259-2273. https://doi.org/10.3168/jds.S0022-0302(99)75474-3

Drackley, J. K., Overton, T. R., & Douglas, G. N. (2001). Adaptations of Glucose and Long-Chain Fatty Acid Metabolism in Liver of Dairy Cows during the Periparturient Period. *Journal of Dairy Science*, *84*, E100-E112. https://doi.org/10.3168/jds.S0022-0302(01)70204-4

Ear, P. H., Chadda, A., Gumusoglu, S. B., Schmidt, M. S., Vogeler, S., Malicoat, J., Kadel, J., Moore, M. M., Migaud, M. E., Stevens, H. E., & Brenner, C. (2019). Maternal Nicotinamide Riboside Enhances Postpartum Weight Loss, Juvenile Offspring Development, and Neurogenesis of Adult Offspring. *Cell reports*, *26*(4), 969–983.e4. https://doi.org/10.1016/j.celrep.2019.01.007

Elamin, M., Ruskin, D. N., Sacchetti, P., & Masino, S. A. (2020). A unifying mechanism of ketogenic diet action: The multiple roles of nicotinamide adenine dinucleotide. *Epilepsy research*, *167*, 106469. https://doi.org/10.1016/j.eplepsyres.2020.106469

Fan, R., Cui, J., Ren, F., Wang, Q., Huang, Y., Zhao, B., Wei, L., Qian, X., & Xiong, X. (2018). Overexpression of NRK1 ameliorates diet- and age-induced hepatic steatosis and insulin resistance. *Biochemical and biophysical research communications*, *500*(2), 476–483. https://doi.org/10.1016/j.bbrc.2018.04.107

Gansemer, E. R., McCommis, K. S., Martino, M., King-McAlpin, A. Q., Potthoff, M. J., Finck, B. N., Taylor, E. B., & Rutkowski, D. T. (2020). NADPH and Glutathione Redox Link TCA Cycle Activity to Endoplasmic Reticulum Homeostasis. *IScience*, *23*(5), 101116. https://doi.org/10.1016/j.isci.2020.101116

Goff, J., & Horst, R. (1997). Physiological Changes at Parturition and Their Relationship to Metabolic Disorders,. *Journal of Dairy Science*, *80*(7), 1260-1268. https://doi.org/10.3168/jds.S0022-0302(97)76055-7

Grant, R., Berg, J., Mestayer, R., Braidy, N., Bennett, J., Broom, S., & Watson, J. (2019). A Pilot Study Investigating Changes in the Human Plasma and Urine NAD+ Metabolome During a 6 Hour Intravenous Infusion of NAD+. *Frontiers in Aging Neuroscience*, *11*. https://doi.org/10.3389/fnagi.2019.00257

Greer, E. L., Dowlatshahi, D., Banko, M. R., Villen, J., Hoang, K., Blanchard, D., ... & Brunet, A. (2007). An AMPK-FOXO pathway mediates longevity induced by a novel method of dietary restriction in C. elegans. *Current biology*, *17*(19), 1646-1656.

Greenbaum, A. L., & Pinder, S. (1968). Changes in the activities of enzymes of the biosynthetic pathway of the nicotinamide nucleotides in rat mammary gland during the lactation cycle. *Biochemical Journal*, *107*(1), 63-67. https://doi.org/10.1042/bj1070063

Gross, J., Grossen-Rösti, L., Wall, S., Wellnitz, O., & Bruckmaier, R. (2020). Metabolic status is associated with the recovery of milk somatic cell count and milk secretion after

lipopolysaccharide-induced mastitis in dairy cows. *Journal of Dairy Science, 103*(6), 5604-5615. https://doi.org/10.3168/jds.2019-18032

Grummer, R. R., 1995: Impact of changes in organic nutrient metabolism on feeding the transition dairy cow. *Journal of Animal Science* 73, 2820–2833.

Guidry, A. J., Paape, M. J., & Pearson, R. E. (1976). Effects of parturition and lactation on blood and milk cell concentrations, corticosteroids, and neutrophil phagocytosis in the cow. *American journal of veterinary research*, *37*(10), 1195–1200.

Guo, H., Callaway, J. B., & Ting, J. P. (2015). Inflammasomes: Mechanism of action, role in disease, and therapeutics. *Nature Medicine*, *21*(7), 677-687. https://doi.org/10.1038/nm.3893

Guzmán, M., & Blázquez, C. (2001). Is there an astrocyte–neuron ketone body shuttle?. *TRENDS in Endocrinology & metabolism*, *12*(4), 169-173.

Hahn, P., & Taller, M. (1987). Ketone formation in the intestinal mucosa of infant rats. *Life Sciences*, *41*(12), 1525-1528. https://doi.org/10.1016/0024-3205(87)90718-1

Heine, H., Rietschel, E. T., & Ulmer, A. J. (2001). The biology of endotoxin. *Molecular biotechnology*, *19*, 279-296.

Hirschberger, S., Strauß, G., Effinger, D., Marstaller, X., Ferstl, A., Müller, M. B., ... & Kreth, S. (2021). Very-low-carbohydrate diet enhances human T-cell immunity through immunometabolic reprogramming. *EMBO Molecular Medicine*, *13*(8), e14323.

Hirschey, M. D., Shimazu, T., Goetzman, E., Jing, E., Schwer, B., Lombard, D. B., Grueter, C. A., Harris, C., Biddinger, S., Ilkayeva, O. R., Stevens, R. D., Li, Y., Saha, A. K., Ruderman, N. B., Bain, J. R., Newgard, C. B., Farese Jr, R. V., Alt, F. W., Kahn, C. R., . . . Verdin, E. (2010). SIRT3 regulates mitochondrial fatty-acid oxidation by reversible enzyme deacetylation. *Nature*, *464*(7285), 121-125. https://doi.org/10.1038/nature08778

Hoeben, D., Heyneman, R., & Burvenich, C. (1997). Elevated levels of beta-hydroxybutyric acid in periparturient cows and in vitro effect on respiratory burst activity of bovine neutrophils. *Veterinary immunology and immunopathology*, *58*(2), 165–170. https://doi.org/10.1016/s0165-2427(97)00031-7

Holland, W. L., & Summers, S. A. (2008). Sphingolipids, Insulin Resistance, and Metabolic Disease: New Insights from *in vivo* Manipulation of Sphingolipid Metabolism. *Endocrine Reviews*, *29*(4), 381-402. https://doi.org/10.1210/er.2007-0025

House, W. A., and A. W. Bell. 1993. Mineral accretion in the fetus and adnexa during late gestation in Holstein cows. J. Dairy Sci. 76:2999.

Hu, Q., Wu, D., Walker, M., Wang, P., Tian, R., & Wang, W. (2021). Genetically encoded biosensors for evaluating NAD+/NADH ratio in cytosolic and mitochondrial compartments. *Cell Reports Methods*, *1*(7), 100116. https://doi.org/10.1016/j.crmeth.2021.100116

Hu, Q., Wu, D., Walker, M., Wang, P., Tian, R., & Wang, W. (2021). Genetically encoded biosensors for evaluating NAD+/NADH ratio in cytosolic and mitochondrial compartments. *Cell reports methods*, *1*(7).

Hugo, S. E., Cruz-Garcia, L., Karanth, S., Anderson, R. M., Stainier, Y. R., & Schlegel, A. (2012). A monocarboxylate transporter required for hepatocyte secretion of ketone bodies during fasting. *Genes & Development*, *26*(3), 282-293. https://doi.org/10.1101/gad.180968.111

Izumi, K., Fukumori, R., Oikawa, S., & Oba, M. (2019). Short communication: Effects of butyrate supplementation on the productivity of lactating dairy cows fed diets differing in starch content. *Journal of dairy science*, *102*(12), 11051–11056. https://doi.org/10.3168/jds.2019-17113

Jamerson, L. E., & Bradshaw, P. C. (2024). The Roles of White Adipose Tissue and Liver NADPH in Dietary Restriction-Induced Longevity. *Antioxidants*, *13*(7), 820. https://doi.org/10.3390/antiox13070820

Jiang, W., Wang, S., Xiao, M., Lin, Y., Zhou, L., Lei, Q., Xiong, Y., Guan, K., & Zhao, S. (2011). Acetylation Regulates Gluconeogenesis by Promoting PEPCK1 Degradation via Recruiting the UBR5 Ubiquitin Ligase. *Molecular Cell*, *43*(1), 33-44. https://doi.org/10.1016/j.molcel.2011.04.028

Jordan, S., Tung, N., Casanova-Acebes, M., Chang, C., Cantoni, C., Zhang, D., Wirtz, T. H., Naik, S., Rose, S. A., Brocker, C. N., Gainullina, A., Hornburg, D., Horng, S., Maier, B. B., Cravedi, P., LeRoith, D., Gonzalez, F. J., Meissner, F., Ochando, J., Rahman, A., … Merad, M. (2019). Dietary Intake Regulates the Circulating Inflammatory Monocyte Pool. *Cell*, *178*(5), 1102–1114.e17. https://doi.org/10.1016/j.cell.2019.07.050

Kannan, K., & Jain, S. K. (2000). Oxidative stress and apoptosis. *Pathophysiology*, *7*(3), 153-163.

Kazuhei Kurosawa, Hideo Shibata, Norio Hayashi, Nobuhiro Sato, Takenobu Kamada, Kunio Tagawa, Kinetics of Hydroperoxide Degradation by NADP-Glutathione System in Mitochondria, *The Journal of Biochemistry*, Volume 108, Issue 1, July 1990, Pages 9–16, https://doi.org/10.1093/oxfordjournals.jbchem.a123169

Kehrli, M., Nonnecke, B., & Roth, J. (1989). Alterations in bovine neutrophil function during the periparturient period.March 1989 American Journal of Veterinary Research 50(2):207-14

Kleppe, B. B., Aiello, R. J., Grummer, R. R., & Armentano, L. E. (1988). Triglyceride accumulation and very low density lipoprotein secretion by rat and goat hepatocytes in vitro. *Journal of dairy science*, *71*(7), 1813–1822. https://doi.org/10.3168/jds.S0022-0302(88)79750-7

Knaus, W. (2009). Dairy cows trapped between performance demands and adaptability. *Journal of the Science of Food and Agriculture*, *89*(7), 1107-1114. https://doi.org/10.1002/jsfa.3575

Laffel, L. (1999). Ketone bodies: A review of physiology, pathophysiology and application of monitoring to diabetes. *Diabetes/Metabolism Research and Reviews*, *15*(6), 412-426. https://doi.org/10.1002/(SICI)1520-7560(199911/12)15:6

Larsen, M., & Kristensen, N. B. (2013). Precursors for liver gluconeogenesis in periparturient dairy cows. *Animal*, *7*(10), 1640-1650.

Lean, I. J., LeBlanc, S. J., Sheedy, D. B., Duffield, T., Santos, J. E. P., & Golder, H. M. (2023). Associations of parity with health disorders and blood metabolite concentrations in Holstein cows in different production systems. *Journal of dairy science*, *106*(1), 500–518. https://doi.org/10.3168/jds.2021-21673

LeBlanc S. J. (2020). Review: Relationships between metabolism and neutrophil function in dairy cows in the peripartum period. *Animal : an international journal of animal bioscience*, *14*(S1), s44–s54. https://doi.org/10.1017/S1751731119003227

Li, Y., Zou, S., Ding, H., Hao, N., Huang, Y., Tang, J., Cheng, J., Feng, S., Li, J., Wang, X., & Wu, J. (2020). Low Expression of Sirtuin 1 in the Dairy Cows with Mild Fatty Liver Alters Hepatic Lipid Metabolism. *Animals : an open access journal from MDPI*, *10*(4), 560. https://doi.org/10.3390/ani10040560

Liang, F., Kume, S., & Koya, D. (2009). SIRT1 and insulin resistance. *Nature Reviews Endocrinology*, *5*(7), 367-373. https://doi.org/10.1038/nrendo.2009.101

Liang, H., & Ward, W. F. (2006). PGC-1alpha: a key regulator of energy metabolism. *Advances in physiology education*, *30*(4), 145–151. https://doi.org/10.1152/advan.00052.2006

Lin, S. J., Ford, E., Haigis, M., Liszt, G., & Guarente, L. (2004). Calorie restriction extends yeast life span by lowering the level of NADH. *Genes & development*, *18*(1), 12-16.

Line Agledal, Marc Niere & Mathias Ziegler (2010) The phosphate makes a difference: cellular functions of NADP, Redox Report, 15:1, 2-10, DOI: 10.1179/174329210X12650506623122

Liu, L., Su, X., Quinn, W. J., Hui, S., Krukenberg, K., Frederick, D. W., Redpath, P., Zhan, L., Chellappa, K., White, E., Migaud, M., Mitchison, T. J., Baur, J. A., & Rabinowitz, J. D. (2018). Quantitative Analysis of NAD Synthesis-Breakdown Fluxes. *Cell Metabolism*, *27*(5), 1067-1080.e5. https://doi.org/10.1016/j.cmet.2018.03.018

Long, Y. C., & Zierath, J. R. (2006). AMP-activated protein kinase signaling in metabolic regulation. *Journal of Clinical Investigation*, *116*(7), 1776-1783. https://doi.org/10.1172/JCI29044

Luda, K. M., Longo, J., Kitchen-Goosen, S. M., Duimstra, L. R., Ma, E. H., Watson, M. J., ... & Jones, R. G. (2023). Ketolysis drives CD8+ T cell effector function through effects on histone acetylation. *Immunity*, *56*(9), 2021-2035.

Mangerich, A., & Bürkle, A. (2012). Pleiotropic Cellular Functions of PARP1 in Longevity and Aging: Genome Maintenance Meets Inflammation. *Oxidative Medicine and Cellular*

Longevity, *2012*(1), 321653. https://doi.org/10.1155/2012/321653

Manns, J. G., & Boda, J. M. (1967). Insulin release by acetate, propionate, butyrate, and glucose in lambs and adult sheep. *The American journal of physiology*, *212*(4), 747–755. https://doi.org/10.1152/ajplegacy.1967.212.4.747

McCarthy, M. M., Piepenbrink, M. S., & Overton, T. R. (2015). Associations between hepatic metabolism of propionate and palmitate in liver slices from transition dairy cows. *Journal of dairy science*, *98*(10), 7015–7024. https://doi.org/10.3168/jds.2015-9695

McDaniel, S. S., Rensing, N. R., Thio, L. L., Yamada, K. A., & Wong, M. (2011). The ketogenic diet inhibits the mammalian target of rapamycin (mTOR) pathway. *Epilepsia*, *52*(3), e7-e11.

McFadden, J., & Rico, J. (2019). Invited review: Sphingolipid biology in the dairy cow: The emerging role of ceramide. *Journal of Dairy Science*, *102*(9), 7619-7639. https://doi.org/10.3168/jds.2018-16095

McLean, P. (1958). Carbohydrate metabolism of mammary tissue II. Levels of oxidised and reduced diphosphopyridine nucleotide and triphosphopyridine nucleotide in the rat mammary gland. *Biochimica et Biophysica Acta*, *30*(2), 316-324. https://doi.org/10.1016/0006-3002(58)90056-8

McNamara J. P. (1991). Regulation of adipose tissue metabolism in support of lactation. *Journal of dairy science*, *74*(2), 706–719. https://doi.org/10.3168/jds.S0022-0302(91)78217-9

Morey, S., Mamedova, L., Anderson, D., Armendariz, C., Titgemeyer, E., & Bradford, B. (2011). Effects of encapsulated niacin on metabolism and production of periparturient dairy cows. Journal of Dairy Science, 94(10), 5090-5104. https://doi.org/10.3168/jds.2011-4304

Mysore, V., Cullere, X., Mears, J., Rosetti, F., Okubo, K., Liew, P. X., Zhang, F., Rosenbauer, F., Stone, R. M., Aster, J. C., Von Andrian, U. H., Lichtman, A. H., Raychaudhuri, S., & Mayadas, T. N. (2021). FcγR engagement reprograms neutrophils into antigen cross-presenting cells that elicit acquired anti-tumor immunity. *Nature Communications*, *12*(1), 1-23. https://doi.org/10.1038/s41467-021-24591-x

Navarro, C. D., Figueira, T. R., Francisco, A., Dal'Bó, G. A., Ronchi, J. A., Rovani, J. C., Escanhoela, C. A., Oliveira, H. C., Castilho, R. F., & Vercesi, A. E. (2017). Redox imbalance due to the loss of mitochondrial NAD(P)-transhydrogenase markedly aggravates high fat diet-induced fatty liver disease in mice. *Free Radical Biology and Medicine*, *113*, 190-202. https://doi.org/10.1016/j.freeradbiomed.2017.09.026

Navas, L. E., & Carnero, A. (2021). NAD+ metabolism, stemness, the immune response, and cancer. *Signal transduction and targeted therapy*, *6*(1), 2. https://doi.org/10.1038/s41392-020-00354-w

Neudorf, H. (2020). The Impact of Acute Ingestion of a Ketone Monoester Drink on LPS-Stimulated NLRP3 Activation in Humans with Obesity. *Nutrients*, *12*(3), 854.

https://doi.org/10.3390/nu12030854

Neudorf, H. (2020). *Examining the effect of short-term oral ketone supplementation on markers of NLRP3 inflammasome activation in individuals with obesity* (T). University of British Columbia. Retrieved from https://open.library.ubc.ca/collections/ubctheses/24/items/1.0391908

O'Neill LA, Bryant CE, Doyle SL (2009) Therapeutic targeting of Toll-like receptors for infectious and inflammatory diseases and cancer. Pharmacol Rev 61: 177–197.

Obsil, T., & Obsilova, V. (2008). Structure/function relationships underlying regulation of FOXO transcription factors. *Oncogene*, *27*(16), 2263-2275.

Okabe, K., Yaku, K., Tobe, K. *et al.* Implications of altered NAD metabolism in metabolic disorders. *J Biomed Sci* 26, 34 (2019). https://doi.org/10.1186/s12929-019-0527-8

Onizawa, Y., Katoh, T., Miura, R., Konda, K., Noguchi, T., Iwata, H., Kuwayama, T., Hamano, S., & Shirasuna, K. (2022). Acetoacetate is a trigger of NLRP3 inflammasome activation in bovine peripheral blood mononuclear cells. *Veterinary immunology and immunopathology*, *244*, 110370. https://doi.org/10.1016/j.vetimm.2021.110370

Osborne, B., Reznick, J., Wright, L. E., Sinclair, D. A., Cooney, G. J., & Turner, N. (2022). Liver-specific overexpression of SIRT3 enhances oxidative metabolism, but does not impact metabolic defects induced by high fat feeding in mice. *Biochemical and Biophysical Research Communications*, *607*, 131-137. https://doi.org/10.1016/j.bbrc.2022.03.088

Ospina, P. A., Nydam, D. V., Stokol, T., & Overton, T. R. (2010). Evaluation of nonesterified fatty acids and beta-hydroxybutyrate in transition dairy cattle in the northeastern United States: Critical thresholds for prediction of clinical diseases. *Journal of dairy science*, *93*(2), 546–554. https://doi.org/10.3168/jds.2009-2277

Pazzaglia, S., & Pioli, C. (2020). Multifaceted Role of PARP-1 in DNA Repair and Inflammation: Pathological and Therapeutic Implications in Cancer and Non-Cancer Diseases. *Cells*, *9*(1), 41. https://doi.org/10.3390/cells9010041

Pedersen, A., Karlsson, G. B., & Rydström, J. (2008). Proton-translocating transhydrogenase: an update of unsolved and controversial issues. *Journal of bioenergetics and biomembranes*, *40*, 463-473.

Petrović K, Djoković R, Cincović M, Hristovska T, Lalović M, Petrović M, Majkić M, Došenović Marinković M, Anđušić L, Devečerski G, Stojanović D, Štrbac F. Niacin Status Indicators and Their Relationship with Metabolic Parameters in Dairy Cows during Early Lactation. Animals. 2022; 12(12):1524. https://doi.org/10.3390/ani12121524

Pires, J., & Grummer, R. (2007). The Use of Nicotinic Acid to Induce Sustained Low Plasma Nonesterified Fatty Acids in Feed-Restricted Holstein Cows. Journal of Dairy Science, 90(8), 3725-3732. https://doi.org/10.3168/jds.2006-904

Park, S., Chung, M., Son, J., Yun, H. H., Park, J., Yim, J., Jung, S., Lee, S., & Jeong, K. (2021). The role of Sirtuin 2 in sustaining functional integrity of the liver. *Life Sciences, 285,* 119997. https://doi.org/10.1016/j.lfs.2021.119997

Paulik, E., Jayaram, H. N., & Weber, G. (1991). Determination of NAD pyrophosphorylase activity in biological samples. *Analytical Biochemistry*, *197*(1), 143-148. https://doi.org/10.1016/0003-2697(91)90370-9

Pierre, K., & Pellerin, L. (2005). Monocarboxylate transporters in the central nervous system: distribution, regulation and function. *Journal of neurochemistry*, *94*(1), 1–14. https://doi.org/10.1111/j.1471-4159.2005.03168.x

Pigeolet, E., Corbisier, P., Houbion, A., Lambert, D., Michiels, C., Raes, M., Zachary, M., & Remacle, J. (1990). Glutathione peroxidase, superoxide dismutase, and catalase inactivation by peroxides and oxygen derived free radicals. *Mechanisms of Ageing and Development*, *51*(3), 283-297. https://doi.org/10.1016/0047-6374(90)90078-T

Stubbs, B. J., Koutnik, A. P., Goldberg, E. L., Upadhyay, V., Turnbaugh, P. J., Verdin, E., & Newman, J. C. (2020). Investigating ketone bodies as immunometabolic countermeasures against respiratory viral infections. *Med, 1*(1), 43-65.

Plaizier, J., Khafipour, E., Li, S., Gozho, G., & Krause, D. (2012). Subacute ruminal acidosis (SARA), endotoxins and health consequences. *Animal Feed Science and Technology*, *172*(1-2), 9-21. https://doi.org/10.1016/j.anifeedsci.2011.12.004

Puchalska, P., & Crawford, P. A. (2017). Multi-dimensional Roles of Ketone Bodies in Fuel Metabolism, Signaling, and Therapeutics. *Cell metabolism*, *25*(2), 262–284. https://doi.org/10.1016/j.cmet.2016.12.022

Qiao, L., & Shao, J. (2006). SIRT1 regulates adiponectin gene expression through Foxo1-C/enhancer-binding protein alpha transcriptional complex. *The Journal of biological chemistry*, *281*(52), 39915–39924. https://doi.org/10.1074/jbc.M607215200

Rambault, M., Gilbert, F. B., Roussel, P., Tessier, A., David, V., Germon, P., Winter, N., & Remot, A. (2023). Neutrophils expressing major histocompatibility complex class II molecules circulate in blood and milk during mastitis and show high microbicidal activity. *Journal of dairy science*, *106*(6), 4245–4256. https://doi.org/10.3168/jds.2022-22728

Ratajczak, J., Joffraud, M., Trammell, S. A., Ras, R., Canela, N., Boutant, M., Kulkarni, S. S., Rodrigues, M., Redpath, P., Migaud, M. E., Auwerx, J., Yanes, O., Brenner, C., & Cantó, C. (2016). NRK1 controls nicotinamide mononucleotide and nicotinamide riboside metabolism in mammalian cells. *Nature Communications*, *7*(1), 1-12. https://doi.org/10.1038/ncomms13103

Rathbun, F. M., Pralle, R. S., Bertics, S. J., Armentano, L. E., Cho, K., Do, C., ... & White, H. M. (2017). Relationships between body condition score change, prior mid-lactation phenotypic residual feed intake, and hyperketonemia onset in transition dairy cows. *Journal of dairy*

science, *100*(5), 3685-3696.

Rardin, M. J., He, W., Nishida, Y., Newman, J. C., Carrico, C., Danielson, S. R., Guo, A., Gut, P., Sahu, A. K., Li, B., Uppala, R., Fitch, M., Riiff, T., Zhu, L., Zhou, J., Mulhern, D., Stevens, R. D., Ilkayeva, O. R., Newgard, C. B., Jacobson, M. P., … Verdin, E. (2013). SIRT5 regulates the mitochondrial lysine succinylome and metabolic networks. *Cell metabolism*, *18*(6), 920–933. https://doi.org/10.1016/j.cmet.2013.11.013

Reilly, P. E. B., & Ford, E. J. H. (1971). The effects of different dietary contents of protein on amino acid and glucose production and on the contribution of amino acids to gluconeogenesis in sheep. *British Journal of Nutrition*, *26*(2), 249–263. doi:10.1079/BJN19710032

Ringseis R, Zeitz JO, Weber A, Koch C, Eder K. Hepatic transcript profiling in early-lactation dairy cows fed rumen-protected niacin during the transition from late pregnancy to lactation. J Dairy Sci. 2019 Jan;102(1):365-376. Doi: 10.3168/jds.2018-15232. Epub 2018 Oct 24. PMID: 30487053.

Roberts, C. K., Barnard, R. J., Sindhu, R. K., Jurczak, M., Ehdaie, A., & Vaziri, N. D. (2006). Oxidative stress and dysregulation of NAD(P)H oxidase and antioxidant enzymes in diet-induced metabolic syndrome. *Metabolism*, *55*(7), 928-934. https://doi.org/10.1016/j.metabol.2006.02.022

Saxton, R. A., & Sabatini, D. M. (2017). MTOR Signaling in Growth, Metabolism, and Disease. *Cell*, *168*(6), 960. https://doi.org/10.1016/j.cell.2017.02.004

Sazanov, L., & Jackson, J. (1994). Proton-translocating transhydrogenase and NAD- and NADP-linked isocitrate dehydrogenases operate in a substrate cycle which contributes to fine regulation of the tricarboxylic acid cycle activity in mitochondria. *FEBS Letters*, *344*(2-3), 109-116. https://doi.org/10.1016/0014-5793(94)00370-X

Shi, X., Li, D., Deng, Q., Li, Y., Sun, G., Yuan, X., Song, Y., Wang, Z., Li, X., Li, X., & Liu, G. (2015). NEFAs activate the oxidative stress-mediated NF-κB signaling pathway to induce inflammatory response in calf hepatocytes. *The Journal of Steroid Biochemistry and Molecular Biology*, *145*, 103-112. https://doi.org/10.1016/j.jsbmb.2014.10.014

Shimazu, T., Hirschey, M. D., Hua, L., Dittenhafer-Reed, K. E., Schwer, B., Lombard, D. B., Li, Y., Bunkenborg, J., Alt, F. W., Denu, J. M., Jacobson, M. P., & Verdin, E. (2010). SIRT3 Deacetylates Mitochondrial 3-Hydroxy-3-Methylglutaryl CoA Synthase 2 and Regulates Ketone Body Production. *Cell Metabolism*, *12*(6), 654-661. https://doi.org/10.1016/j.cmet.2010.11.003

Sipka, A. S., Chandler, T. L., Weichhart, T., Schuberth, H., & Mann, S. (2022). Inhibition of mTOR in bovine monocyte derived macrophages and dendritic cells provides a potential mechanism for postpartum immune dysfunction in dairy cows. *Scientific Reports*, *12*(1), 1-16. https://doi.org/10.1038/s41598-022-19295-1

Sjöholm A. (1995). Ceramide inhibits pancreatic beta-cell insulin production and mitogenesis

and mimics the actions of interleukin-1 beta. *FEBS letters*, *367*(3), 283–286. https://doi.org/10.1016/0014-5793(95)00470-t

Song, Y., Wang, K., Loor, J. J., Jiang, Q., Yang, Y., Jiang, S., Liu, S., He, J., Feng, X., Du, X., Lei, L., Gao, W., Liu, G., & Li, X. (2022). β-Hydroxybutyrate inhibits apoptosis in bovine neutrophils through activating ERK1/2 and AKT signaling pathways. *Journal of Dairy Science*, *105*(4), 3477-3489. https://doi.org/10.3168/jds.2021-21259

Song, Y., Yang, Y., Zeng, W., Loor, J. J., Jiang, Q., Peng, Z., Li, Y., Jiang, S., Feng, X., Du, X., Li, X., & Liu, G. (2022). β-Hydroxybutyrate impairs neutrophil migration distance through activation of a protein kinase C and myosin light chain 2 signaling pathway in ketotic cows. *Journal of Dairy Science*, *105*(1), 761-771. https://doi.org/10.3168/jds.2021-20875

Ster, C., Loiselle, M., & Lacasse, P. (2012). Effect of postcalving serum nonesterified fatty acids concentration on the functionality of bovine immune cells. *Journal of Dairy Science*, *95*(2), 708-717. https://doi.org/10.3168/jds.2011-4695

Stubbs, B. J., Koutnik, A. P., Goldberg, E. L., Upadhyay, V., Turnbaugh, P. J., Verdin, E., & Newman, J. C. (2020). Investigating ketone bodies as immunometabolic countermeasures against respiratory viral infections. *Med*, *1*(1), 43-65.

Sun, X., Tang, Y., Jiang, C., Luo, S., Jia, H., Xu, Q., Zhao, C., Liang, Y., Cao, Z., Shao, G., Loor, J. J., & Xu, C. (2021). Oxidative stress, NF-κB signaling, NLRP3 inflammasome, and caspase apoptotic pathways are activated in mammary gland of ketotic Holstein cows. *Journal of Dairy Science*, *104*(1), 849-861. https://doi.org/10.3168/jds.2020-18788

Sundrum, A. (2015). Metabolic Disorders in the Transition Period Indicate that the Dairy Cows' Ability to Adapt is Overstressed. *Animals*, *5*(4), 978-1020. https://doi.org/10.3390/ani5040395

Suriyasathaporn, W., Daemen, A. J., Noordhuizen-Stassen, E. N., Dieleman, S. J., Nielen, M., & Schukken, Y. H. (1999). Beta-hydroxybutyrate levels in peripheral blood and ketone bodies supplemented in culture media affect the in vitro chemotaxis of bovine leukocytes. *Veterinary immunology and immunopathology*, *68*(2-4), 177–186. https://doi.org/10.1016/s0165-2427(99)00017-3

Talley, J. T., & Mohiuddin, S. S. (2020). Biochemistry, fatty acid oxidation. In: StatPearls. StatPearls Publishing, Treasure Island (FL); 2023. PMID: 32310462.

Tennen, R. I., & Chua, K. F. (2011). Chromatin regulation and genome maintenance by mammalian SIRT6. *Trends in biochemical sciences*, *36*(1), 39–46. https://doi.org/10.1016/j.tibs.2010.07.009

Theys, C., Lauwers, D., Perez-Novo, C., & Berghe, W. V. (2022). PPARα in the Epigenetic Driver Seat of NAFLD: New Therapeutic Opportunities for Epigenetic Drugs? *Biomedicines*, *10*(12). https://doi.org/10.3390/biomedicines10123041

Thornton, J., & Schultz, L. (1980). Effects of Administration of Nicotinic Acid on Glucose,

Insulin, and Glucose Tolerance in Ruminants. Journal of Dairy Science, 63(2), 262-268. https://doi.org/10.3168/jds.S0022-0302(80)82923-7

Titov, D. V., Cracan, V., Goodman, R. P., Peng, J., Grabarek, Z., & Mootha, V. K. (2016). Complementation of mitochondrial electron transport chain by manipulation of the NAD+/NADH ratio. *Science*. https://doi.org/aad4017

Trammell, S. A., Yu, L., Redpath, P., Migaud, M. E., & Brenner, C. (2016). Nicotinamide Riboside Is a Major NAD+ Precursor Vitamin in Cow Milk. *The Journal of Nutrition*, *146*(5), 957-963. https://doi.org/10.3945/jn.116.230078

Tyagi, S., Gupta, P., Saini, A. S., Kaushal, C., & Sharma, S. (2011). The peroxisome proliferator-activated receptor: A family of nuclear receptors role in various diseases. *Journal of Advanced Pharmaceutical Technology & Research*, *2*(4), 236-240. https://doi.org/10.4103/2231-4040.90879

Vanholder, T., Papen, J., Bemers, R., Vertenten, G., & Berge, A. C. (2015). Risk factors for subclinical and clinical ketosis and association with production parameters in dairy cows in the Netherlands. *Journal of dairy science*, *98*(2), 880–888. https://doi.org/10.3168/jds.2014-8362

Vazquez, B. N., Thackray, J. K., Simonet, N. G., Kane-Goldsmith, N., Martinez-Redondo, P., Nguyen, T., ... & Serrano, L. (2016). SIRT 7 promotes genome integrity and modulates non-homologous end joining DNA repair. *The EMBO journal*, *35*(14), 1488-1503.

Vestergaard, E. T., Zubanovic, N. B., Rittig, N., Møller, N., Kuhre, R. E., Holst, J. J., ... & Thomsen, H. H. (2021). Acute ketosis inhibits appetite and decreases plasma concentrations of acyl ghrelin in healthy young men. *Diabetes, Obesity and Metabolism*, *23*(8), 1834-1842.

Walesky, C., & Apte, U. (2015). Role of Hepatocyte Nuclear Factor 4α (HNF4α) in Cell Proliferation and Cancer. *Gene Expression*, *16*(3), 101-108. https://doi.org/10.3727/105221615X14181438356292

Watt, M. J., Barnett, A. C., Bruce, C. R., Schenk, S., Horowitz, J. F., & Hoy, A. J. (2012). Regulation of plasma ceramide levels with fatty acid oversupply: evidence that the liver detects and secretes de novo synthesised ceramide. *Diabetologia*, *55*(10), 2741–2746. https://doi.org/10.1007/s00125-012-2649-3

Wei, X., Cai, C., He, J., Yu, C., Mitloehner, F., Liu, B., Yao, J., & Cao, Y. (2018). Effects of biotin and nicotinamide supplementation on glucose and lipid metabolism and milk production of transition dairy cows. *Animal Feed Science and Technology*, *237*, 106-117. https://doi.org/10.1016/j.anifeedsci.2018.01.012

Wilk, A., Hayat, F., Cunningham, R., Li, J., Garavaglia, S., Zamani, L., Ferraris, D. M., Sykora, P., Andrews, J., Clark, J., Davis, A., Chaloin, L., Rizzi, M., Migaud, M., & Sobol, R. W. (2020). Extracellular NAD+ enhances PARP-dependent DNA repair capacity independently of CD73 activity. *Scientific Reports*, *10*(1), 1-21. https://doi.org/10.1038/s41598-020-57506-9

Wiltrout, D., & Satter, L. (1972). Contribution of Propionate to Glucose Synthesis in the

Lactating and Nonlactating Cow. *Journal of Dairy Science*, *55*(3), 307-317. https://doi.org/10.3168/jds.S0022-0302(72)85487-0

Xin, L., Ipek, Ö., Beaumont, M., Shevlyakova, M., Christinat, N., Masoodi, M., Greenberg, N., Gruetter, R., & Cuenoud, B. (2018). Nutritional Ketosis Increases NAD+/NADH Ratio in Healthy Human Brain: An *in vivo* Study by 31P-MRS. *Frontiers in Nutrition*, *5*. https://doi.org/10.3389/fnut.2018.00062

Yang, Y., & Sauve, A. A. (2016). NAD(+) metabolism: Bioenergetics, signaling and manipulation for therapy. *Biochimica et biophysica acta*, *1864*(12), 1787–1800. https://doi.org/10.1016/j.bbapap.2016.06.014

Yokus, B., Bademkiran, S., & Cakir, D. U. (2007). Total anti-oxidant capacity and oxidative stress in dairy cattle and their associations with dystocia. *Medycyna Wet*, *63*(2), 167-170.

Yoshizaki, T., Milne, J. C., Imamura, T., Schenk, S., Sonoda, N., Babendure, J. L., ... & Olefsky, J. M. (2009). SIRT1 exerts anti-inflammatory effects and improves insulin sensitivity in adipocytes. *Molecular and cellular biology*, *29*(5), 1363-1374. https://doi.org/10.1128/MCB.00705-08

Youm, Y. H., Nguyen, K. Y., Grant, R. W., Goldberg, E. L., Bodogai, M., Kim, D., D'Agostino, D., Planavsky, N., Lupfer, C., Kanneganti, T. D., Kang, S., Horvath, T. L., Fahmy, T. M., Crawford, P. A., Biragyn, A., Alnemri, E., & Dixit, V. D. (2015). The ketone metabolite β-hydroxybutyrate blocks NLRP3 inflammasome-mediated inflammatory disease. *Nature medicine*, *21*(3), 263–269. https://doi.org/10.1038/nm.3804

Yuan, K., Shaver, R., Bertics, S., Espineira, M., & Grummer, R. (2012). Effect of rumen-protected niacin on lipid metabolism, oxidative stress, and performance of transition dairy cows. Journal of Dairy Science, 95(5), 2673-2679. https://doi.org/10.3168/jds.2011-5096

Yu SiJia, Y. S., Shi DongHui, S. D., Zhu Yong, Z. Y., Xu JianXiong, X. J., Xu WeiNa, X. W., & Zhang Jing, Z. J. (2017). A research in oxidative stress and damage of breeding goats. Chinese Journal of Animal Nutrition, 29 (3), 814-823 ref. 22

Zarrin, M., Grossen-Rösti, L., Bruckmaier, R., & Gross, J. (2017). Elevation of blood β-hydroxybutyrate concentration affects glucose metabolism in dairy cows before and after parturition. *Journal of Dairy Science*, *100*(3), 2323-2333. https://doi.org/10.3168/jds.2016-11714

Zebeli, Q., Sivaraman, S., Dunn, S., & Ametaj, B. (2011). Intermittent parenteral administration of endotoxin triggers metabolic and immunological alterations typically associated with displaced abomasum and retained placenta in periparturient dairy cows. *Journal of Dairy Science*, *94*(10), 4968-4983. https://doi.org/10.3168/jds.2011-4194

Zhang, D., Yang, H., Kong, X., Wang, K., Mao, X., Yan, X., Wang, Y., Liu, S., Zhang, X., Li, J., Chen, L., Wu, J., Wei, M., Yang, J., & Guan, Y. (2011). Proteomics analysis reveals diabetic

kidney as a ketogenic organ in type 2 diabetes. *American Journal of Physiology-Endocrinology and Metabolism*. https://doi.org/E-00308-2010

Zhang, X., Jiang, L., & Liu, H. (2021). Forkhead Box Protein O1: Functional Diversity and Post-Translational Modification, a New Therapeutic Target? *Drug Design, Development and Therapy*, *15*, 1851-1860. https://doi.org/10.2147/DDDT.S305016

Zhang, Y., Li, X., Zhang, H., Zhao, Z., Peng, Z., Wang, Z., Liu, G., & Li, X. (2018). Non-Esterified Fatty Acids Over-Activate the TLR2/4-NF-Kb Signaling Pathway to Increase Inflammatory Cytokine Synthesis in Neutrophils from Ketotic Cows. *Cellular physiology and biochemistry : international journal of experimental cellular physiology, biochemistry, and pharmacology*, *48*(2), 827–837. https://doi.org/10.1159/000491913

Zhao, C., Hu, X., Bao, L., Wu, K., Zhao, Y., Xiang, K., ... & Fu, Y. (2022). Gut dysbiosis induces the development of mastitis through a reduction in host anti-inflammatory enzyme activity by endotoxemia. *Microbiome*, *10*(1), 205.

Zhu, X. H., Lu, M., Lee, B. Y., Ugurbil, K., & Chen, W. (2015). *In vivo* NAD assay reveals the intracellular NAD contents and redox state in healthy human brain and their age dependences. *Proceedings of the national academy of sciences*, *112*(9), 2876-2881.

Ziegler, M., Monné, M., Nikiforov, A., Agrimi, G., Heiland, I., & Palmieri, F. (2021). Welcome to the Family: Identification of the NAD+ Transporter of Animal Mitochondria as Member of the Solute Carrier Family SLC25. *Biomolecules*, *11*(6), 880. https://doi.org/10.3390/biom11060880

Zinicola, M., & Bicalho, R. C. (2019). Association of peripartum plasma insulin concentration with milk production, colostrum insulin levels, and plasma metabolites of Holstein cows. *Journal of dairy science*, *102*(2), 1473–1482. https://doi.org/10.3168/jds.2017-14029\